UNIVERSIDAD POLITÉCNICA DE CARTAGENA

DEPARTAMENTO DE MINERÍA, GEOLOGÍA Y CARTOGRAFÍA

OPTIMIZACIÓN DE PARÁMETROS PARA LA EXTRACCIÓN DE ELEMENTOS DESDE MINERALES EN MEDIOS ÁCIDOS

OPTIMIZATION OF PARAMETERS FOR THE EXTRACTION OF ELEMENTS FROM MINERALS IN ACID MEDIA

Memoria presentada por Norman Rodrigo Toro Villarroel, Ingeniero Civil Metalúrgico, Magister en Ingeniería Industrial, para optar al grado de Doctor por la Universidad Politécnica de Cartagena

Directores:
Manuel Cánovas Vidal
Emilio Trigueros Tornero

Cartagena, 2020

Tesis por publicaciones:

Esta memoria se presenta en la modalidad de compendio de publicaciones.

Los artículos que constituyen la tesis son los siguientes:

- **Publicación 1: N. Toro***, M. Saldaña, E. Gálvez, M. Cánovas, E. Trigueros, J. Castillo and P. Hernández. "Optimization of Parameters for the Dissolution of Mn from Manganese Nodules with the Use of Tailings in an Acid Medium" Q2 ISI WoS. Minerals, 2019; https://doi.org/10.3390/min9070387

- **Publicación 2: N. Toro***, W. Briceño, K. Pérez, M. Cánovas, E. Trigueros, R. Sepúlveda and P. Hernández. "Leaching of Pure Chalcocite in a Chloride Media Using Sea Water and Waste Water" Q1 ISI WoS. Metals, 2019; https://doi.org/10.3390/met9070780

- **Publicación 3:** M. Saldaña, **N. Toro***, J. Castillo, P. Hernández, E. Trigueros, and A. Navarra. **"**Development of an Analytical Model for the Extraction of Manganese from Marine Nodules" Q1 ISI WoS. Metals, 2019 https://doi.org/10.3390/met9080903

- **Publicación 4: N. Toro***, K. Pérez, M. Saldaña, R. I. Jeldres, M. Jeldres and M. Cánovas. "Dissolution of pure chalcopyrite with manganese nodules and waste water" Q1 ISI WoS. Journal of Materials Research and Technology, 2019 https://doi.org/10.1016/j.jmrt.2019.11.020

- **Publicación 5 (En Revisión): N. Toro***, W. Briceño, A. Navarra, K. Pérez, M. Cánovas and E. Trigueros. "Statistical and kinetic study for leaching of covellite in a chloride media" Q1 ISI WoS. Journal of Materials Research and Technology.

Agradecimientos

Primero, quiero agradecer a mis padres por brindarme cariño, confianza y apoyo a lo largo de mi carrera universitaria. Me dio la oportunidad de luchar por el sueño de convertirme en profesional.

Para mi pareja Pamela Flores y amigos que han hecho de este camino algo grato de recorrer, por estar conmigo en todo momento, por aportar buenos momentos y brindar su apoyo de forma constante.

A Manuel Cánovas y Emilio Trigueros por ser mis guías y responsables de este proyecto. Por darme apoyo y a la vez aconsejarme en temas no solamente académicos, sino laborales, que me han ayudado a entender mejor mi entorno y mis capacidades.

A mi equipo de investigación, Manuel Saldaña y Kevin Pérez del laboratorio "Nuevas Líneas de Investigación", a quienes tuve la oportunidad y fortuna de formar como investigadores, con quienes trabajé a la par en todo este proceso, y logramos metas conjuntas.

También, agradecer la contribución de la Unidad de Equipo Científico - MAINI de la Universidad Católica del Norte por ayudar a generar datos mediante microscopía electrónica automatizada QEMSCAN®, y por facilitar el análisis químico de las soluciones, en todas las investigaciones realizadas.

Resumen

Actualmente, la gran minería del cobre chilena se encuentra frente a nuevos problemas y desafíos a superar. El principal problema, es de carácter medio ambiental, debido a que la mayor parte de la producción es por procesos de flotación, lo que implica aumentar la generación de relaves, ocasionando drenajes ácidos que generan la movilidad de elementos pesados al medio ambiente. Otro desafío importante, es diversificar las extracciones de otros elementos (como ocurre actualmente con el molibdeno) para impulsar la exportación de productos básicos y aumentar el empleo. Además, se deben tratar recursos que hoy en día no se están aprovechando a escala industrial, un ejemplo son los minerales de cobre negro, estos recursos generalmente no se incorporan en las pilas de lixiviación. Estos minerales exóticos tienen cantidades considerables de Mn (aproximadamente 29%), lo que representa un atractivo comercial.

Para abordar este desafío, se realizaron investigaciones a nivel laboratorio, de extracción de cobre y manganeso desde cobres negros mediante procesos de lixiviación. Se evaluaron diferentes aditivos y concentraciones de estos mediante la aplicación de modelos estadísticos de regresión cuadrática, evaluando efectos lineales, interacciones y curvaturas. Además, se diseñaron y probaron con éxito nuevos procesos de extracción.

Finalmente, se pudo demostrar que para la disolución de Mn ya sea desde nódulos marinos o cobres negros, se obtienen resultados positivos al adicionar Fe en el sistema, siendo un parámetro óptimo de trabajo una razón de MnO_2/Fe de 1/2, logrando extracciones sobre el 70% en tiempos de 20 min. Para la disolución de Cu desde sulfuros secundarios, se puede concluir que los mejores resultados se obtienen al trabajar a elevadas concentraciones de cloruro, siendo poco relevante la concentración de H_2SO_4. Por otra parte, para la disolución de calcopirita, trabajar en un medio clorurado incorporando altas concentraciones de MnO_2 (razones de $MnO_2/CuFeS_2$ de 5/1) favorece el mantener un alto valor de potencial en el sistema, superando la pasivación de este mineral.

Abstract

Currently, the great copper mining is facing new problems and challenges to overcome. The main problem is environmental, because most of the production is due to flotation processes, which implies increasing the generation of tailings, causing acid drains that generate the mobility of heavy elements to the environment. Another important challenge is to diversify the extractions of other elements (as is currently the case with molybdenum) to boost the export of basic products and increase employment. In addition, resources that are not currently being used on an industrial scale should be treated, an example is black copper ores, these resources are generally not incorporated into the extraction circuits or are not treated, whether in stocks, platforms leaching or waste. These exotic minerals have considerable amounts of Mn (approximately 29%), which represents a commercial appeal.

To address this challenge, research was carried out at the laboratory level, for the extraction of copper and manganese from minerals through leaching processes. Evaluating different additives and concentrations thereof, applying the use of statistical models of quadratic regression, evaluating linear effects, interactions and curvatures. And in other cases, creating new extraction processes.

Finally, it was discovered that for the dissolution of Mn either from marine nodules or black copper, very positive results are obtained by adding Fe in the system, an optimal working parameter being a ratio of MnO_2/Fe of 1/2, achieving extractions above 70% in times of 20 min. For the dissolution of Cu from secondary sulphides, it was found that the best results are obtained when working at high concentrations of chloride, the concentration of H_2SO_4 being insignificant. On the other hand, for the dissolution of chalcopyrite, working in a chlorinated medium incorporating high concentrations of $MnO2$ (ratios of $MnO_2 / CuFeS_2$ of 5/1) favors maintaining a high potential value in the system, overcoming the passivation of this mineral.

Tabla de contenidos

Lista de Figuras

1. Introducción

Chile es el principal productor de cobre a nivel mundial con un 27,9% de participación [1] y con un 29% de las reservas de este commodity [2]. Dentro del territorio nacional existen 3.817 depósitos de minerales de cobre [1], en donde la explotación de los mismos representa un 92% de las exportaciones por el mercado minero [3]. Actualmente, parte de la estrategia a nivel país es lograr pasar de 5,78 millones de toneladas de cobre fino a alrededor de 6,2 millones de toneladas en 2027, aumentando en un 1,7% [4]. Sin embargo, pese a estas cifras positivas presentadas, en los últimos años los yacimientos de cobre han presentado un descenso en sus leyes, bajando desde un 1% en el año 2004 a 0,65% en 2016 [3]. Por este motivo, en los últimos años se están buscando nuevas alternativas para mejorar esta problemática en el país. Una opción interesante es la extracción de otros elementos, ya sea como subproductos de menas de cobre, residuos generados por la industria o incluso explotar recursos submarinos debido a la ausencia de menas de alta ley en la superficie. Otra alternativa es optimizar los parámetros operacionales de los procesos ya existentes con el fin de aumentar las extracciones y a la vez disminuir los costos y tiempos de trabajo.

Actualmente, los dos procesos más utilizados para extraer elementos en Chile (principalmente cobre) son los procesos de lixiviación y flotación. Sin embargo, los procesos de flotación generan problemas medio ambientales, debido a la gran cantidad de relaves que generan y los drenajes ácidos generados por la oxidación de pirita en tranques de relaves, lo cual se ve reflejado en la movilidad de elementos pesados al medio ambiente [5]. Por este motivo, existe la necesidad de generar un nuevo impulso que supere cierto estancamiento en la capacidad de crecimiento de la industria minera. Esto genera la obligación de desarrollar investigaciones que propongan nuevos mecanismos de extracción, nuevos aditivos a los procesos y/o la optimización de parámetros de trabajo, que deben estar en línea con las necesidades medio ambientales actuales.

Para solucionar lo anteriormente expuesto, se propone realizar una lixiviación a nivel laboratorio de minerales y concentrados en estado puro en medios ácidos, evaluando parámetros de dosificación de reactivos con el objetivo de encontrar un modelo cuadrático que permita predecir la extracción del elemento de interés, determinando las condiciones necesarias para mejorar la cinética de disolución y

analizar los efectos de estos parámetros en la extracción.

La lixiviación ha demostrado ser un método eficiente para tratar menas de leyes bajas y medias a escala industrial. Se ha trabajado históricamente en la minería a través de pilas de lixiviación, logrando buenos resultados [6]. En los últimos años, las lixiviaciones agitadas (reactores) se han incorporado a los procesos industriales, debido a las nuevas exigencias que se generan por minerales más refractarios, además de la aparición de impurezas complejas de eliminar por procesos convencionales. Los estudios de minerales que están en un estado puro (o casi totalmente), y que además abarcan modelos estadísticos para optimizar parámetros, no suelen ser comunes en el área de investigación de la lixiviación debido a la dificultad de encontrar minerales de alta ley que se encuentren de forma homogénea. Además, el hecho de que son trabajos interdisciplinarios que comprenden tópicos de ingeniería metalúrgica e ingeniería industrial ha limitado su desarrollo. Este tipo de estudios permite sensibilizar parámetros y generar propuestas que agilicen futuros trabajos de investigación.

El presente trabajo de investigación contribuye en el campo de la metalurgia e ingeniería industrial, específicamente las áreas de lixiviación y estadística. Este trabajo se ha realizado en el contexto de 5 estudios de extracción de elementos (Cu y Mn), en donde cada uno de estos propone novedosos métodos para aplicar en la industria minera, y, además, optimizar los resultados actuales en las pilas de lixiviación.

Para cumplir este objetivo, se utilizará la metodología de optimización de la superficie para evaluar el efecto de X variables independientes para la disolución de un elemento. Con un análisis ANOVA se obtendrán los parámetros (lineales, interacciones y curvatura), eliminando todo valor sesgado ($p > 0,05$), lo cual permitirá aumentar la representatividad del modelo (R^2), del cual se propondrá una ecuación de extracción.

Finalmente se realizarán pruebas de lixiviación, para los parámetros de mayor impacto en el modelo y se evaluarán diferentes concentraciones de aditivos. Esto permitirá concluir el mecanismo de trabajo más apropiado para la disolución del elemento deseado, desde un mineral o concentrado.

1.1 Metodología de trabajo

Todas las pruebas experimentales se realizaron en el laboratorio "Nuevas líneas de investigación" perteneciente al Departamento de Ingeniería Metalúrgica y Minas, de la Universidad Católica del Norte. La metodología experimental se llevó a cabo en 2 etapas, las cuales se detallan a continuación:

1.1.1 Preparación del mineral

En los 5 estudios realizados para este trabajo de investigación, se trabajó con nódulos de manganeso, cobres negros, sulfuros secundarios (calcosina y covelina) y sulfuro primario (calcopirita).

Era fundamental que los minerales a utilizar estuvieran lo más puros posibles, para disminuir las desviaciones en los resultados. Por este motivo fueron reducidos de tamaño con el uso de un mortero para evitar contaminación debido a las impurezas y polvo que están presentes en un chancador.

La reducción de tamaño del mineral se realiza hasta que el 100% esté a una granulometría -10#. Luego se procede a homogenizar el mineral, y se toman 2 muestras representativas de 1 g cada una, para ser enviadas a análisis químico y mineralógico.

Los análisis químicos fueron determinados por espectrometría de emisión atómica de plasma acoplado inductivamente (ICP-AES), mientras que la mineralogía de las muestras se determinó de dos formas: un análisis QEMSCAN, que es un microscopio electrónico de exploración que se modificó tanto en hardware como en software, y/o utilizando un difractómetro de rayos X de la marca Bruker, modelo automático e informatizado de D8.

Para la clasificación de tamaños en los diferentes estudios, el material fue molido en el mortero cuidadosamente, y clasificado a través de mallas tamices, hasta llegar a los rangos deseados.

1.1.2 Proceso de lixiviación

El ácido sulfúrico utilizado para todas las pruebas de lixiviación fue de grado P.A., con una pureza del 95-97%, una densidad de 1,84 kg/L y un peso molecular de 98,80 g/mol.

Las pruebas de lixiviación se llevaron a cabo en un circuito de reactores de vidrio de 50 mL con una relación sólido / líquido de 0,01. Se mantuvo en suspensión un total de 200 mg de mineral del mineral a procesar con el uso de un agitador magnético de cinco posiciones (IKA ROS, CEP 13087-534, Campinas, Brasil) a una velocidad de 600 rpm. Las pruebas se realizaron a una temperatura ambiente de 25 °C, mientras que para otras se varío la temperatura (de 25 a 90 °C) evitando la evaporación de agua con el uso de un refrigerante de vidrio conectado a la parte superior de los reactores. Los refrigerantes son alimentados por una manguera conectada a la llave de agua potable, de este modo al pasar el chorro de agua a temperatura ambiente y hacer contacto con el gas caliente que sale del reactor hace que éste se condense y vuelva al mismo (ver Figura 1). Las pruebas se realizaron por duplicado y las mediciones (o análisis) se realizaron en muestras de 5 mL sin diluir utilizando espectrometría de absorción atómica con un coeficiente de variación ≤ 5% y un error relativo entre 5 y 10%. Las mediciones del pH y el potencial de oxidación-reducción (ORP) de las soluciones de lixiviación se realizaron con un medidor de pH-ORP (HANNA HI-4222 (instrumentos HANNA, Woonsocket, Rhode Island, EE. UU.)). La solución ORP se midió en una celda de electrodo de combinación ORP compuesta de un electrodo de trabajo de platino y un electrodo de referencia de Ag/AgCl saturado.

Figura 1 Circuito de reactores en serie (Fuente: Autor)

1.1.3 Modelamiento matemático y diseño de experimentos

El diseño de experimentos (DOE) ayuda a investigar los efectos de las variables de entrada (factores) sobre una o más variables de salida (respuesta) [7]. El diseño de experimentos consiste en una serie de pruebas en las que se realizan cambios o perturbaciones de forma intencional en las variables de entrada [8], recolectando los datos de la salida para su posterior análisis [9]. Se desarrolló un diseño factorial, de manera de estudiar el efecto del Tiempo, Concentración de H_2SO_4 y la relación MnO_2/Fe_2O_3 en la recuperación de manganeso, donde la variable respuesta fue expresada basada tanto en los efectos lineales, las interacciones y la curvatura de las variables independientes, tal como se muestra en la ecuación 1.

$$\text{Element Extraction (\%)} = \alpha + \sum_{i=1}^{n} \beta_i x_i + \sum_{i=1}^{n} \sum_{j=1}^{n} \beta_{ij} x_i x_j \tag{1}$$

Donde α es la constante general, x_i son las n variable independientes y β son los coeficientes de los diferentes efectos de las variables independientes. Posterior al ajuste del modelo de regresión múltiple, previa linealización de los factores de orden dos o superior, se procede a la optimización de la respuesta, identificando el nivel de los factores que maximizan la recuperación de manganeso o cobre para el conjunto de valores muestreados, tal como se desarrolló en Toro et al. [9].

Posterior al ajuste y optimización mediante el diseño de un modelo factorial, se extiende el diseño experimental, de manera de incluir las variables independientes tamaño de partícula, temperatura y velocidad de agitación de los reactores al modelo analítico, replanteándolo como un sistema de ecuaciones de primer orden, tal como se presenta en el trabajo desarrollado por Saldaña et al. [10], en donde se ajustan los modelos analítico para la lixiviación mediante los modelos analíticos desarrollados anteriormente por Mellado et al. [11-13], en donde se considera que el comportamiento de la lixiviación podría ser modelado usando un sistema de ecuaciones como el mostrado en la Ecuación 2.

$$\frac{\partial y}{\partial \tau} = -k_\tau y^{n_\tau} \tag{2}$$

Donde y representa la recuperación (R_t), k_τ es la constante cinética y n_τ es el orden de la reacción. El subíndice τ representa una escala de tiempo que depende del

fenómeno a modelar. Para resolver la Ecuación (2) una condición inicial es requerida, introduciéndose un retraso (ω). Luego, la solución general es conocida y su solución está dada por la Ecuación 3.

$$R_\tau = R_\tau^\infty\left(1 - e^{-k_\tau(\tau-\omega)}\right) \tag{3}$$

R_τ^∞ es la máxima recuperación esperada en condiciones operacionales. Dixon y Hendrix [14-15] consideraron que el fenómeno ocurre en diferentes escalas de tamaño (relacionado a la altura de la pila de lixiviación) y tiempo, sin embargo, este supuesto solo aplica para el análisis del proceso a escala industrial. Luego, modificando la ecuación para ajustar un modelo al diseño experimental, se tiene que es posible explicar la recuperación del elemento valioso desde el mineral según la Ecuación 4.

$$R(X) = R^\infty\left(1 - e^{-g(X)}\right) \tag{4}$$

Donde $R^\infty = 100\%$ es la máxima recuperación esperada de mineral bajo las condiciones experimentales (condiciones de laboratorio), mientras que $g(X)$ es una ecuación polinómica, explicada por las variables muestreadas indicadas anteriormente.

2 Estado del arte

2.1 Minerales de manganeso

El manganeso, es un metal de transición de color gris plateado, similar al hierro. Este elemento pertenece al grupo 7 y periodo 4 de la tabla periódica con numero atómico 25, su masa atómica es de 54,94 g/mol, es un metal duro y muy frágil [16]. El manganeso tiene una densidad de 7,3 g/cm^3, con un punto de fusión y ebullición de 1246 y 2061 °C respectivamente [17].

El Mn está entre los 12 elementos con mayor abundancia en la corteza terrestre [18], este metal, ampliamente distribuido en rocas, constituye aproximadamente el 0,1% de la corteza terrestre; su ocurrencia no está asociada a la forma metálica libre, sino a diversas formas compuestas, siendo los más abundantes óxidos, sulfuros, carbonatos y silicatos [19]. El manganeso también se puede encontrar en las profundidades oceánicas, en forma de nódulos, micro concreciones, recubrimientos y costras, se estima que ocupan hasta 30% del pacífico [17].

La disolución de Mn desde nódulos marinos o cobres negros es un proceso de lixiviación en el que se trabaja a bajos valores de potencial. Para lograr extraer el Mn y otros metales de interés desde estos recursos, es necesario el uso de un agente reductor [20].

2.1.1 Nódulos marinos

Los nódulos de manganeso, también conocidos como nódulos polimetálicos, desde su descubrimiento en los años 1873-76 durante la afamada expedición Challenger, han sido objeto de gran interés y especulación [21]. Estos nódulos de Mn son concreciones conformadas principalmente de minerales de óxido de hierro y manganeso hidratados (Ver Figura 2), aunque también se encuentran cantidades menores de níquel, cobre, cobalto, molibdeno y elementos de tierras raras [22].

Estas concreciones rocosas se encuentran diseminadas en los fondos marinos de los océanos Atlántico, Indico y Pacífico Norte, principalmente, a profundidades de 4.000-5.000 m. Tienen una forma casi esférica de color entre marrón y negro [23]. Los nódulos, generalmente, tienen un tamaño promedio de entre 1-12 cm, pero su diámetro puede variar desde milímetros (micronódulos) hasta 20 cm [21].

Figura 2 Nódulos de manganeso [21]

2.1.2 Cobres negros

Chile posee los yacimientos porfídicos más inmensos del planeta, que son esencialmente depósitos de baja ley, pero de gran tonelaje. Si bien, estos depósitos pueden no tener gran atractivo económico en su fase hipógena, el panorama cambia cuando el pórfido ha desarrollado procesos supérgenos. Dichos procesos pueden ser, enriquecimiento secundario y/o mineralización de cobre exótico. La mineralización primaria del pórfido está compuesta por un protolito de sulfuros de hierro y cobre, hospedada por distintas asociaciones mineralógicas alteradas. El mineral precursor de estos yacimientos metalíferos es la pirita. Ésta al reaccionar con el agua, genera ácido sulfúrico, promoviendo la movilidad de metales, como el cobre, que, bajo ciertas condiciones de potencial y pH, pueden ser transportadas logrando precipitar aguas abajo y formando yacimientos denominados exóticos [24-25].

La mineralización existente en estos yacimientos comprende distintas especies de minerales de cobre tales como, crisocola, atacamita, copper pitch y copper wad [24, 26]. Estos últimos, definidos como mineraloides, debido a que cristalizan de manera amorfa (Ver Figura 3) [27]. También son denominados silicatoides rico en Si-Fe-Cu-Mn [28]

Figura 3 Mineral de cobre negro [29]

2.2 Minerales de cobre

La mayor parte de los minerales de cobre en el planeta corresponden a minerales sulfurados y una menor cantidad a minerales oxidados [30]. La mayor parte de la producción de cobre en el mundo se realiza mediante el procesamiento de minerales sulfurados (75%) por procesos de flotación y fundición [31], mientras que el resto (25%) se trabaja por la vía hidrometalúrgica [32]. Sin embargo, pese a la alta producción

mundial por la vía pirometalúrgica, existe una preocupación por la contaminación del aire y las emisiones de dióxido de azufre generados por procesos de fundición convencionales [33]. Por este motivo científicos e ingenieros han planteado la hidrometalurgia como una mejor alternativa para el tratamiento de calcopirita, ya que es un proceso más amigable con el medio ambiente [34].

2.2.1 Calcosina

La calcosina es el mineral sulfurado de cobre más abundante después de la calcopirita [35] y es el que tiene un tratamiento más fácil por vía hidrometalúrgica [36]. Es un sulfuro secundario en la zona oxidada de los depósitos de cobre o cercana a ella. Cristaliza en el sistema por encima de 105 °C (Ver Figura 4) y se confunde fácilmente con djurleita [37].

Figura 4 Estructura cristalina de la calcosina [37]

2.2.2 Covelina

La covelina no es un mineral abundante, pero se halla en muchos depósitos de cobre como mineral supergénico, normalmente como recubrimiento en la zona de enriquecimiento de sulfuros. Está asociada a otros minerales principalmente calcosina, calcopirita, bornita y enargita, de los que deriva por alteración [38]. La covelina presenta un interés para el proceso hidrometalúrgico debido al porcentaje encontrado en menas de óxidos, además de ser un producto intermedio de las conversiones de fase de calcopirita [39] y transformación de digenita a covelina en un medio oxigenado [40-41]. En la Figura 5 se presenta un mineral de covelina cristalizado.

Figura 5 Cristales de covelina [42]

2.2.3 Calcopirita

La calcopirita es el mineral de cobre más abundante en el planeta [43], además, uno de los minerales más refractarios en los procesos de hidrometalurgia [44]. Es un sulfuro de hierro y cobre cuya fórmula química es $CuFeS_2$, con una composición de 34,6% de cobre, 30,5% de hierro y 34,9% de azufre. Este mineral tiene una dureza 3,5 – 4, raya negra verdosa, color amarillo latón con reflejos verdes y posee brillo metálico. La estructura cristalina consiste en una red relativamente simple tetragonal, cerca de cúbico [45], con cada ión de azufre rodeado por cuatro iones metálicos de cobre y hierro situados en ángulos tetraedros y en un cierto orden en cada plano [46]. En la Figura 6 se presenta un mineral de calcopirita.

Figura 6 Cristales de calcopirita sobre matriz de cuarzo [46]

2.3 Lixiviación agitada

Generalmente la lixiviación por agitación involucra que el mineral esté sometido a altas presiones y temperaturas, dado que bajo estas condiciones se consiguen cinéticas de extracción aceptables que no son posibles bajo condiciones moderadas [47].

La lixiviación por agitación permite tener un mayor control del proceso de lixiviación. Además, la velocidad de extracción del metal es mucho mayor que la lograda mediante el proceso de lixiviación en pilas o en bateas. Sin embargo, es un proceso de mayor costo, ya que incluye los costos de la molienda del mineral, separación sólido-líquido, entre otros [48].

La ley del mineral y el tamaño de partícula tienen una importante influencia en la selección del proceso para la lixiviación de minerales, como se muestra en la Figura 7.
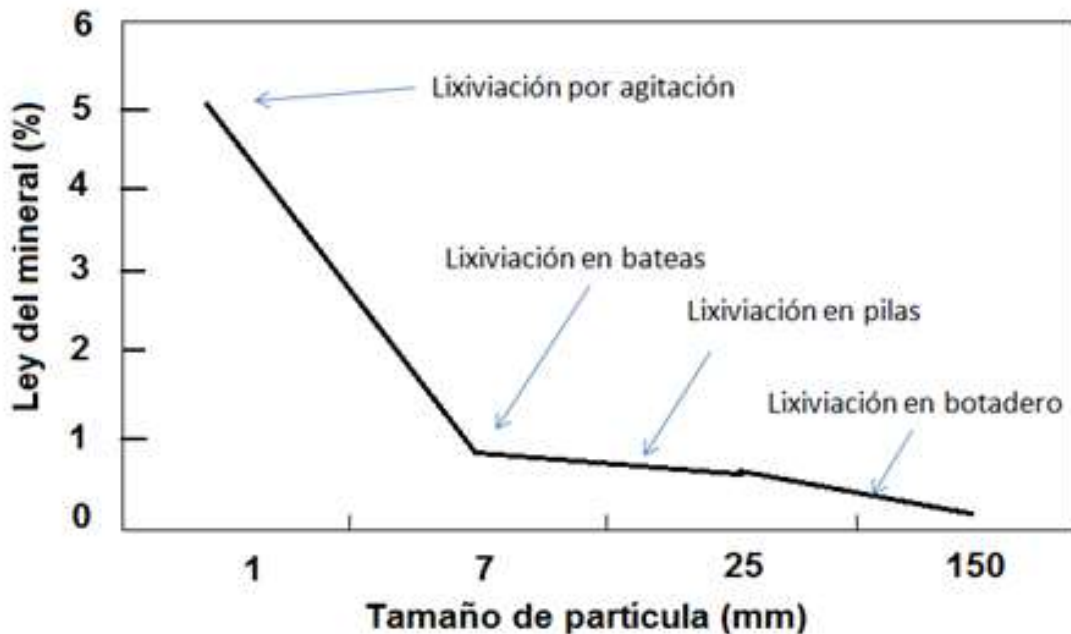

Figura 7. Relación entre la ley de cobre y tamaño de partícula del mineral para distintos métodos de lixiviación [49]

3. Optimization of Parameters for the Dissolution of Mn from Manganese Nodules with the Use of Tailings in an Acid Medium

Optimization of Parameters for the Dissolution of Mn from Manganese Nodules with the Use of Tailings in An Acid Medium

Norman Toro [1,2,*], Manuel Saldaña [3], Edelmira Gálvez [1], Manuel Cánovas [1] , Emilio Trigueros [2], Jonathan Castillo [4] and Pía C. Hernández [5]

[1] Departamento de Ingeniería en Metalurgia y Minas, Universidad Católica del Norte, Av. Angamos 610, Antofagasta 1270709, Chile

[2] Departamento de Ingeniería Minera y Civil. Universidad Politécnica de Cartagena, Paseo Alfonso Xlll N°52, 30203 Cartagena, Spain

[3] Departamento de Ingeniería Industrial, Universidad Católica del Norte, Av. Angamos 610, Antofagasta 1270709, Chile

[4] Departamento de Ingeniería en Metalurgia, Universidad de Atacama, Av. Copayapu 485, Copiapó 1531772, Chile

[5] Departamento de Ingeniería Química y Procesos de Minerales, Universidad de Antofagasta, Avda. Angamos 601, Antofagasta 1240000, Chile

* Correspondence: ntoro@ucn.cl; Tel.: +56-552651021

Abstract: Manganese nodules are an attractive source of base metals and critical and rare elements and are required to meet a high demand of today's industry. In previous studies, it has been shown that high concentrations of reducing agent (Fe) in the system are beneficial for the rapid extraction of manganese. However, it is necessary to optimize the operational parameters in order to maximize Mn recovery. In this study, a statistical analysis was carried out using factorial experimental design for the main parameters, including time, MnO_2/Fe_2O_3 ratio, and H_2SO_4 concentration. After this, Mn recovery tests were carried out over time at different ratios of MnO_2/Fe_2O_3 and H_2SO_4 concentrations, where the potential and pH of the system were measured. Finally, it is concluded that high concentrations of $FeSO_4$ in the system allow operating in potential and pH ranges (-0.2 to 1.2 V and -1.8 to 0.1) that favor the formation of Fe^{2+} and Fe^{3+}, which enable high extractions of Mn (73%) in short periods of time (5 to 20 min) operating with an optimum MnO_2/Fe_2O_3 ratio of 1:3 and a concentration of 0.1 mol/L of H_2SO_4.

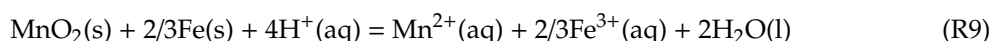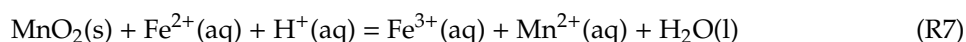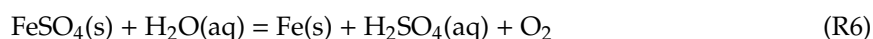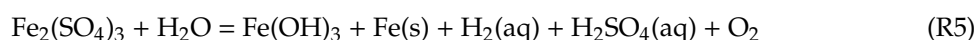**Keywords:** leaching; manganese nodules; optimization of parameters; tailings
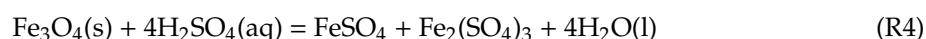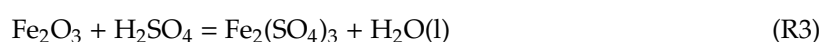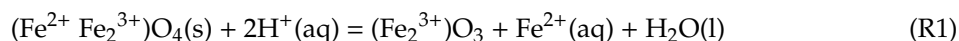
1. Introduction

The oxides of Fe and Mn are formed by direct precipitation in ambient seawater and are mainly deposited on the flat parts and the flanks of seamounts, where ocean currents prevent sedimentation [1,2]. These deposits are found in the oceans around the world [3] and among these are the manganese nodules [4].

The economic interest in ferromanganese (Fe-Mn) nodules is due to high grades of base, critical, and rare metals [5]. These metals that provide mineral deposits on the seabed are necessary for the rapid development of high technology application. They also support the growth and quality of life of the middle class in densely populated countries with expanding markets and economies [6]. Manganese is the most abundant marine nodule metal, with an average content of around 24% [7].

In order to dissolve Mn present in marine nodules in acidic media, it is necessary to use a reducing agent [8]. Studies have reported that the acid leaching of manganese nodules with the use of Fe as the

reducing agent is efficient at room temperature [8–11]. In a study conducted by Zakeri et al. [8], ferrous ions were added for the reductive dissolution of manganese nodules. The authors indicated that in a molar H_2SO_4/MnO_2 ratio of 2:1 and a molar Fe^{2+}/MnO_2 ratio of 3:1, it was possible to dissolve 90% of Mn in 20 min at 20 °C. Bafgui et al. [9] performed acid leaching of manganese nodules by adding Fe, comparing their results with those previously obtained by Zakeri et al. [8]. The authors concluded that when operating with high Fe/MnO_2 ratios, Fe^0 is a more efficient reducing agent compared to Fe^{2+} because it maintains high activity in the system through the regeneration of ferrous ions.

For the acidic leaching of marine nodules with the use of residues (tailings and slags) containing Fe_2O_3, only two studies have been presented [10,11]. In the studies carried out by Toro et al. [10] and Toro et al. [11], it was shown that variables, such as particle size and agitation speed, do not majorly influence the dissolution of MnO_2 and that the most important variable is the Fe_2O_3 concentration in the system. In the study carried out by Toro et al. [10] with the use of smelter slag, extraction of 70% of Mn was achieved in 40 min when operating at a MnO_2/Fe_2O_3 ratio of 1:2, a particle size of $-47 + 38$ μm, and a H_2SO_4 concentration of 1 mol/L. In the later study carried out by Toro et al. [11], involving the use of tailings, it was demonstrated that under the same operating conditions as in Toro et al. [10], greater extraction of Mn (77%) was achieved because tailings are more amenable to leaching. In both studies, the following Reactions (R1)–(R9) involving the use of Fe_2O_3 were proposed.

$$(Fe^{2+} Fe_2^{3+})O_4(s) + 2H^+(aq) = (Fe_2^{3+})O_3 + Fe^{2+}(aq) + H_2O(l) \tag{R1}$$

$$3(Fe^{2+} Ti)O_3(s) + 6H^+(aq) = 3TiO_2 + 3Fe^{2+}(aq) + 3H_2O(l) \tag{R2}$$

$$Fe_2O_3 + H_2SO_4 = Fe_2(SO_4)_3 + H_2O(l) \tag{R3}$$

$$Fe_3O_4(s) + 4H_2SO_4(aq) = FeSO_4 + Fe_2(SO_4)_3 + 4H_2O(l) \tag{R4}$$

$$Fe_2(SO_4)_3 + H_2O = Fe(OH)_3 + Fe(s) + H_2(aq) + H_2SO_4(aq) + O_2 \tag{R5}$$

$$FeSO_4(s) + H_2O(aq) = Fe(s) + H_2SO_4(aq) + O_2 \tag{R6}$$

$$MnO_2(s) + Fe^{2+}(aq) + H^+(aq) = Fe^{3+}(aq) + Mn^{2+}(aq) + H_2O(l) \tag{R7}$$

$$MnO_2(s) + Fe(s) + 8H^+(aq) = 2Fe^{3+}(aq) + Mn^{2+}(aq) + 2H_2O(l) + 2H_2(g) \tag{R8}$$

$$MnO_2(s) + 2/3Fe(s) + 4H^+(aq) = Mn^{2+}(aq) + 2/3Fe^{3+}(aq) + 2H_2O(l) \tag{R9}$$

However, in previous studies [8,9], thermodynamic aspects were not considered.

Table 1 reports the statistical information of the reactions of interest with iron as a reducing agent and its transformations during manganese leaching. It is emphasized that, unlike previous investigations [11], under these conditions, elemental iron (Fe^0) was not formed, since this reaction is not spontaneous (G = 744.22 kJ) and requires a lot of energy. On the other hand, the main reducing agent is ferrous sulfate ($FeSO_4$), which is produced from the reaction between magnetite (Fe_3O_4, mostly present in tailings) and sulfuric acid (Equation (2)). With this reducing agent, it is possible to reduce manganese present in pyrolusite (Mn^{4+}), obtaining a manganese sulphate (Mn^{2+}), as observed in Equation (5).

Table 1. Thermodynamic information of the reactions (based on HSC Chemistry 5.1).

Reaction	Equation	Reaction Coefficient (K) 25 °C	$\Delta G°$ (kJ) 25 °C
$Fe_2O_{3(s)} + 3 H_2SO_{4(aq)} = Fe_2(SO_4)_{3(s)} + 3 H_2O_{(l)}$	(1)	4.21×10^{28}	$-163,37$
$Fe_3O_{4(s)} + 4H_2SO_{4(l)} = FeSO_{4(aq)} + Fe_2(SO_4)_{3(s)} + 4 H_2O_{(l)}$	(2)	6.06×10^{45}	$-261,30$
$Fe_2(SO_4)_{3(s)} + 6 H_2O_{(l)} = 2 Fe(OH)_{3(s)} + 3 H_2SO_{4(l)}$	(3)	2.14×10^{-35}	$197,87$
$2 FeSO_{4(aq)} + 2 H_2O_{(l)} = 2 Fe_{(s)} + 2 H_2SO_{4(l)} + O_{2(g)}$	(4)	4.02×10^{-131}	$744,22$
$2 FeSO_{4(aq)} + 2 H_2SO_{4(aq)} + MnO_{2(s)} = Fe_2(SO_4)_{3(s)} + 2 H_2O_{(l)} + MnSO_{4(aq)}$	(5)	9.06×10^{34}	$-199,52$

The smelting slag is one of the main solid wastes of the copper industry and the produced volume increases day by day [12]. In Chile, the smelters produce 163 tons of slag per day [13] and companies such as Altonorte perform slag flotation for the recovery of Cu. During flotation for each ton of Cu obtained, 151 tons of tailings are generated [14], which are mainly disposed of in tailing dams and represent the most significant environmental liability according to their size and risk of a mining site [15]. Another example is what happened in Lavrio, Greece, due to the intensive mining and metallurgical activities in the last century. This generated huge amount of waste, including acid-generating sulfidic tailings, carbonaceous tailings, and slags. Quantification of the human health risks indicated that direct ingestion of contaminated particles is the most important exposure route for the intake of contaminants by humans [16]. Komnitsas et al. [17] conducted research on waste generated by intensive mining and mineral processing activities in Navodari and Baia, on the Romanian Black Sea coast. Analyzing the experimental results and the associated risks, the authors conclude that it is necessary to rehabilitate the affected areas through removal of toxic and heavy elements from sulphidic tailings and leachates with biosorption and biosolubilisation techniques and development of a vegetative cover on phosphogypsnm stacks and sulphidic tailings dumps. For this reason, it is important to highlight the importance of studying options to reuse waste generated from metallurgical processes.

In Chile, ocean mining is not regulated and is also under-exploited for security reasons [18]. Due to this, it is not possible to carry out a cost-effectiveness study on the extraction of nodules from sea depths. Mining technologies have been developed in the world for the extraction of polymetallic nodules [19]. However, there is no study indicating cost differences between the different methods available on the market. In spite of this, it is necessary to continue investigating processes for the extraction of elements from marine nodules, because technologies are being developed to collect minerals from sea beds and, in the near future, they could be considered as viable alternatives to meet the high demand for metals.

In this investigation, the use of Fe_2O_3, which is present in tailings, to facilitate reductive leaching of MnO_2 from marine nodules for the recovery of Mn is evaluated. The objective is to minimize these environmental liabilities and optimize the most important process variables (time, acid concentration, and MnO_2/Fe_2O_3 ratio).

2. Materials and Methods

2.1. Manganese Nodule Sample

The marine nodules used in this work were the same as those previously used in Toro et al. [11]. They were analyzed by means of atomic emission spectrometry by induction-coupled plasma (ICP-AES), developed in the applied geochemistry laboratory of the department of geological sciences of the Catholic University of the North. They contained 15.96% Mn and 0.45% Fe; Mn was present as MnO_2 (29.85%) and Fe as Fe_2O_3 (26.02%).

2.2. Tailings

The tailings used for the present investigation were the same as those used in Toro et al. [11]. The methods used to determine their chemical and mineralogical composition are the same as those used for the analysis of the manganese nodules. Figure 1 shows the chemical species determined by QEMSCAN. There were several phases that contained iron (mainly magnetite (58.52%) and hematite (4.47%), while the content of Fe was estimated at 41.90%.
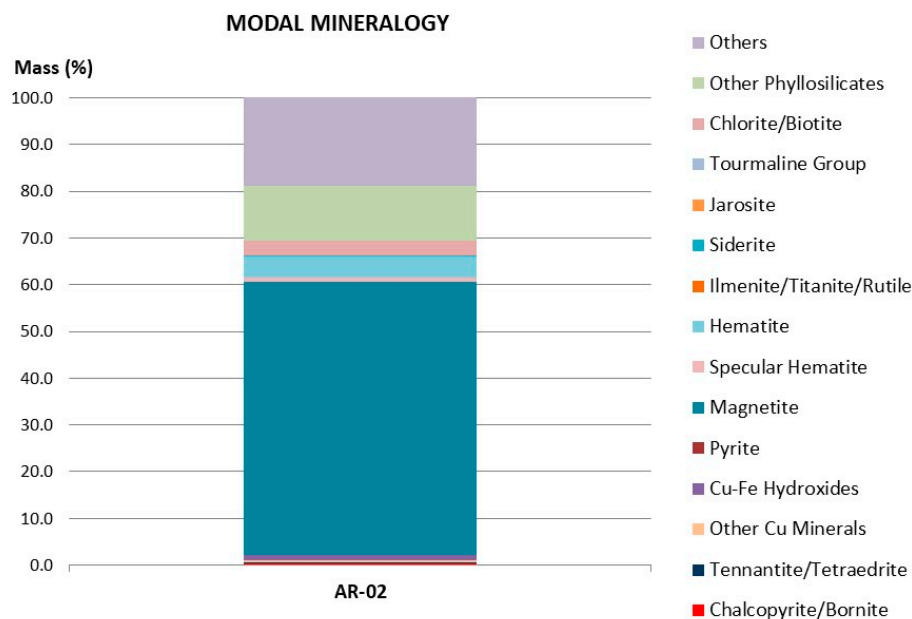
Figure 1. Detailed modal mineralogy.

2.3. Reagents Used—Leaching Parameters

The sulfuric acid used for the leaching tests was grade PA, with 95–97% purity, a density of 1.84 kg/L, and a molecular weight of 98.80 g/mol. The leaching tests were carried out in a 50 mL glass reactor with a 0.01 solid:liquid ratio. A total of 200 mg of Mn nodules were maintained in suspension with the use of a 5 position magnetic stirrer (IKA ROS, CEP 13087-534, Campinas, Brazil) at a speed of 600 rpm. The tests were conducted at a room temperature of 25 °C, while the studied variables were additives, particle size, and leaching time. Also, the tests were performed in duplicate and measurements (or analyses) were carried out on 5 mL undiluted samples using atomic absorption spectrometry with a coefficient of variation ≤5% and a relative error between 5% and 10%. Measurements of pH and oxidation-reduction potential (ORP) of leach solutions were made using a pH-ORP meter (HANNA HI-4222). The ORP solution was measured using a combination of an ORP electrode cell composed of a platinum operating electrode and a saturated Ag/AgCl reference electrode. The solid waste obtained was analyzed by XRD with the use of a Bruker brand diffractometer; the patterns of the main crystalline phases were obtained using Eva software.

2.4. Estimation of Linear and Interaction Coefficients for Complete Factorial Designs of Experiments of 3^3

In previous studies [8–11], in which the dissolution of Mn from marine nodules was investigated with the use of Fe as a reducing agent, it was demonstrated that for high concentrations of Fe in the system (ratios of Fe/MnO_2 greater than 1), quite high extractions were obtained (over 70%) in short periods of time (5 to 30 min). The studies conducted by Bafghi et al. [9] and Toro et al. [10] indicated that the concentration of Fe in the system is the most important variable in order to shorten MnO_2 dissolution times; it was also found that the concentration of H_2SO_4 is not an important parameter. However, in these studies, it was not possible to indicate an optimum MnO_2/Fe ratio and H_2SO_4 concentration in relation to time. In order to overcome this and elucidate Mn extraction from marine nodules, three independent variables were selected for the factorial design of 3^3 experiments, namely time, sulfuric acid concentration, and MnO_2/Fe_2O_3 ratio. This approach allows the determination of the effect of the most relevant factors, as well as their levels, and the development of an experimental model that allows through the determination of coefficients the optimization of the response variable [20–22]. A factorial design was applied involving three factors, each one having three levels; thus, 27 experimental tests were carried out. Minitab 18 software was used for the experimental design and development of a multiple regression equation [23].

Then, the response variable was expressed based on the linear effect of the variables of interest and considering the effects of interaction and curvature, as shown in Equation (6).

$$\text{Mn Extraction (\%)} = \alpha + \beta_1 \times x_1 + \beta_2 \times x_2 + \beta_3 \times x_3 + \beta_{12} \times x_1 \times x_2 + \beta_{13} \times x_1 \times x_3 + \beta_{23} \times x_2 \times x_3 + \beta_{11} \times x_1^2 + \beta_{22} \times x_2^2 + \beta_{33} \times x_3^2, \tag{6}$$

where α is an overall constant, x_i is the value of the level "i" of the factor x, β_i is the coefficient of the linear factor x_i, β_{ij} is the coefficient of the interactions $x_i \times x_j$, n is the level of the factor, and Mn extraction is the dependent variable.

Table 2 shows the values of the levels for each factor, while Table 3 shows the recovery obtained for each configuration.

Table 2. Experimental conditions.

Parameters/Values	Low	Medium	High
Time (min)	10	20	30
MnO_2/Fe_2O_3	2/1	1/1	1/2
H_2SO_4 (mol/L)	0.1	0.5	1
Codifications	−1	0	1

Table 3. Experimental configuration and Mn extraction.

Exp. No.	Time (min)	MnO_2/Fe_2O_3 Ratio	Sulfuric Acid Conc. (mol/L)	Mn Extraction (%)
1	10	1/1	0.1	48.42
2	20	2/1	0.5	38.78
3	20	1/1	1	57.32
4	30	2/1	1	42.55
5	10	1/2	0.5	70.24
6	20	2/1	0.1	38.10
7	30	1/1	1	72.96
8	30	1/2	0.1	74.20
9	10	2/1	0.5	33.23
10	10	2/1	1	33.33
11	20	1/1	0.5	56.80
12	30	2/1	0.1	42.30
13	20	1/1	0.1	55.95
14	10	2/1	0.1	32.83
15	10	1/1	1	50.23
16	10	1/2	0.1	70.21
17	20	1/2	0.1	73.20
18	20	1/2	0.5	73.20
19	30	1/1	0.1	71.96
20	30	1/1	0.5	72.33
21	10	1/2	1	70.90
22	20	1/2	1	73.40
23	20	2/1	1	39.22
24	30	1/2	0.5	74.90
25	10	1/1	0.5	48.91
26	30	1/2	1	75.21
27	30	2/1	0.5	42.00

3. Results and Discussion

3.1. Effect of Variables

From the principal components analysis, it is seen that there is no main effect of the sulfuric acid concentration factor, which means that the average response is the same across all levels of the factor, while the time and MnO_2/Fe_2O_3 ratio factors have a main effect since the variation between

the different levels affects the response differently, as shown in main effects plot for Mn extraction of Figure 2. Developing the ANOVA test and the multiple linear regression adjustment, the recovery according to the predictive variables of time and MnO_2/Fe_2O_3 ratio is given by Equation (7).

$$\text{Mn Extraction (\%)} = 53.90 + 6.12 \times x_1 - 17.40 \times x_2 - 4.00 \times x_2^2, \tag{7}$$

where x_1 represents the time factor and x_2 represents the MnO_2/Fe_2O_3 ratio (previous coding). Then, it is seen that the double and triple interaction factors, together with the curvature of time and H_2SO_4 concentration factors, do not contribute to the explanation of the variability of the model.

A gradient analysis of manganese extraction, ∇Mn Extraction $(x_1, x_2) = (6.12, -23.40)$, indicates an increase in the positive direction of the predictor variables. The response decreases faster with respect to the variable x_2 than with respect to the variable x_1, as shown in Figure 3.
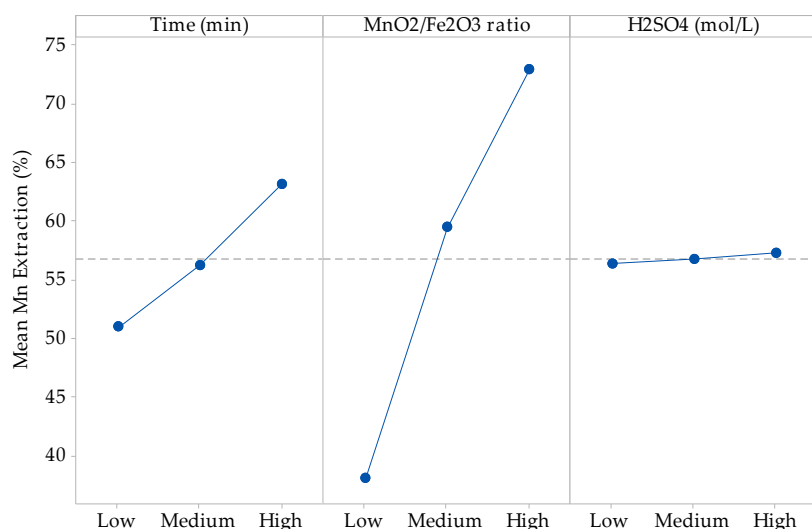
Figure 2. Linear effect plot for Mn extraction (%).
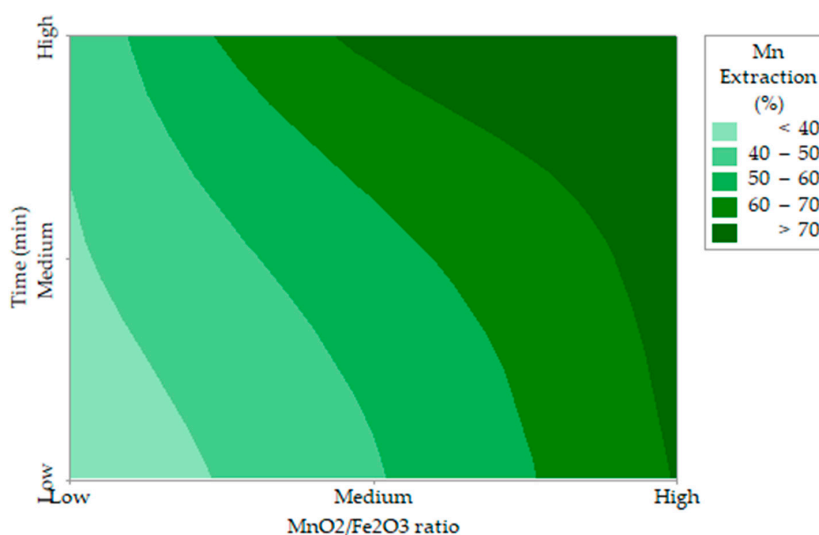
Figure 3. Contour plot of Mn extraction (%) versus MnO_2/Fe_2O_3, time (min).

The ANOVA test indicates that the model adequately represents manganese extraction for the set of sampled values. Also, the model does not require additional adjustments and is validated by the following goodness-of-fit statistics. The p-value of the model ($p < 0.05$) indicates that it is statistically significant. The value of the R^2 statistic is 94.94%, which indicates that approximately 95% of the total variability is explained by the model, while the predictive R^2 is 92.79%, indicating that the model can

adequately predict the response to new observations. The F test indicates the significance of the model, given that $F_{Regression}(143.89) >> (F_{Table} = F_{3,23}(3.03))$, while the residual normality test indicates that these are distributed with media -7.41×10^{-7}, with a standard deviation of 3.5. The p-value of the Kolmogorov-Smirnov test is greater than the level of significance, so it is not possible to reject the assumption of the regression model, which is that the residuals are normally distributed.

3.2. Effect on Acid Concentration and MnO$_2$/Fe$_2$O$_3$ Ratio

In Figure 4, it can be seen that the largest extractions of Mn from marine nodules are obtained when operating at MnO_2/Fe_2O_3 ratios less than 1:1, which agrees with the theories proposed by Kanungo et al. [24], Zakeri et al. [8], Bafghi et al. [9], and Toro et al. [10], which mentioned that the presence of more Fe than MnO_2 in the system improved Mn dissolution in short periods of time. The highest Mn dissolution (76.10%) was obtained by operating at a MnO_2/Fe_2O_3 ratio of 1:3 with a H_2SO_4 concentration of 1 mol/L at 30 min. However, this extraction is not far from that obtained when operating at a MnO_2/Fe_2O_3 ratio of 1:2 (75.50%) at the same acid concentration. For the MnO_2/Fe_2O_3 ratios described in Figure 4b–d, it can be seen that, for leaching times of 30 min, very similar values are obtained, but much higher dissolution kinetics are seen in 1:2 and 1:3 ratios where higher than 65% recoveries of Mn are obtained after 5 min. For a MnO_2/Fe_2O_3 ratio of 2:1 (Figure 4a), much lower dissolution is obtained compared to the other cases under the same operating conditions; the maximum dissolution achieved is 48.30% after 30 min when the H_2SO_4 concentration is 1 mol/L.

The concentration of H_2SO_4 in the system is not significant when MnO_2/Fe_2O_3 ratios are 1:2 and 1:3; this finding agrees with those of Toro et al. [10], who mention that high concentrations of Fe_2O_3 in the system are independent of the acid concentration. However, it can be observed that this factor has a greater impact as long as there is a lower concentration of reducing agent ($FeSO_4$) in the system. For a MnO_2/Fe_2O_3 ratio of 2:1, there is a difference of 3.30% between 0.1 and 1 mol/L of H_2SO_4.

For these two variables analyzed under the exposed operational parameters, it can be observed that when operating at a MnO_2/Fe_2O_3 ratio of 1:2, at a concentration of H_2SO_4 of 0.5 mol/L at 20 min, similar results like those obtained when operating in a MnO_2/Fe_2O_3 ratio of 1:3 (73.50% approximately) are obtained. This is consistent with what was proposed by Toro et al. [11], who indicated that, when operating at high concentrations of Fe_2O_3 in the system, the dissolution kinetics of MnO_2 were drastically increased and significant differences were only observed in short periods of time (5 to 10 min). However, for the second case mentioned in Figure 4d, better results are obtained at low acid concentrations (0.1 mol/L). For this reason, it can be concluded that it is more convenient to operate at MnO_2/Fe_2O_3 ratios of 1:3 and low concentrations of acid (0.1 mol/L) at 20 min. This is because the tailings are wastes that do not have a commercial value and their reuse is beneficial, while the increase of the acid concentration in the system results in a direct increase in the cost of the process.
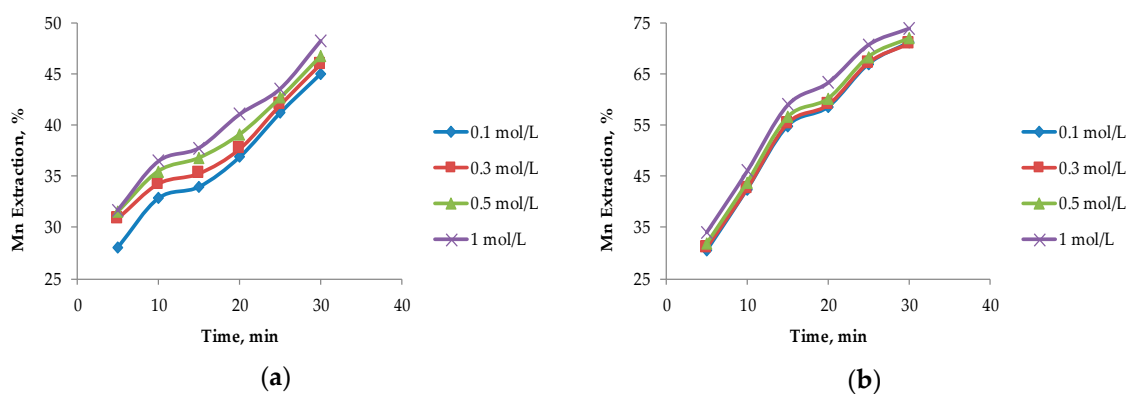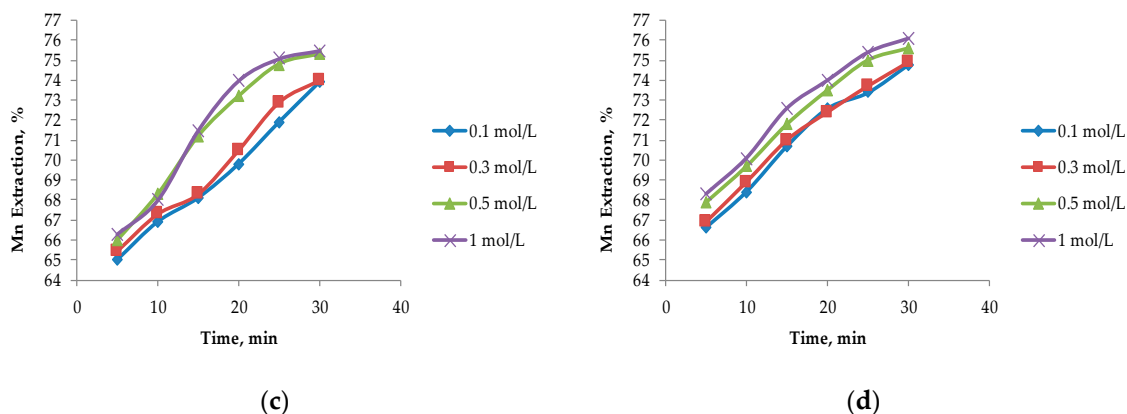

Figure 4. *Cont*.

(c)

(d)

Figure 4. Effect on the acid concentration at different ratios of MnO_2/Fe_2O_3: (**a**) Ratio 2:1; (**b**) ratio 1:1; (**c**) ratio 1:2; and (**d**) ratio 1:3 (25 °C, 600 rpm, −75 + 53 µm).

Based on the results presented in Figure 4, Figure 5 shows that an optimum MnO_2/Fe_2O_3 ratio can be determined. It can be seen that there is no difference in manganese extractions when operating at 1:3 and 1:4 ratios. For short periods of time (5 to 20 min), it can be observed that there are greater extractions for ratios higher than 1:2, achieving dissolutions of Mn over 70% at 15 min. However, it can be seen that at 30 min the results converge in extractions of approximately 75%. Finally, it can be indicated that for times between 15 to 25 min, it is convenient to operate at a MnO_2/Fe_2O_3 ratio of 1:3, while at 30 min, the optimum ratio is 1:2. Figure 6 shows the potential and pH values obtained in the tests presented in Figure 5, which vary between (−0.2 V to 1.2 V) and (−1.8 to 0.1), respectively.
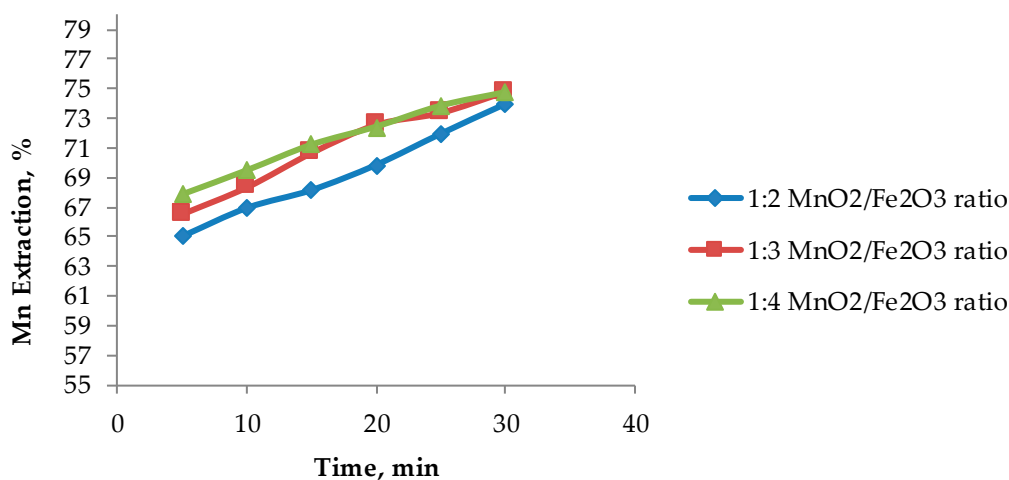

Figure 5. Effect of the MnO_2/Fe_2O_3 ratio on manganese extraction (25 °C, 600 rpm, −75 + 53 µm, acid concentration of 0.1 mol/L).
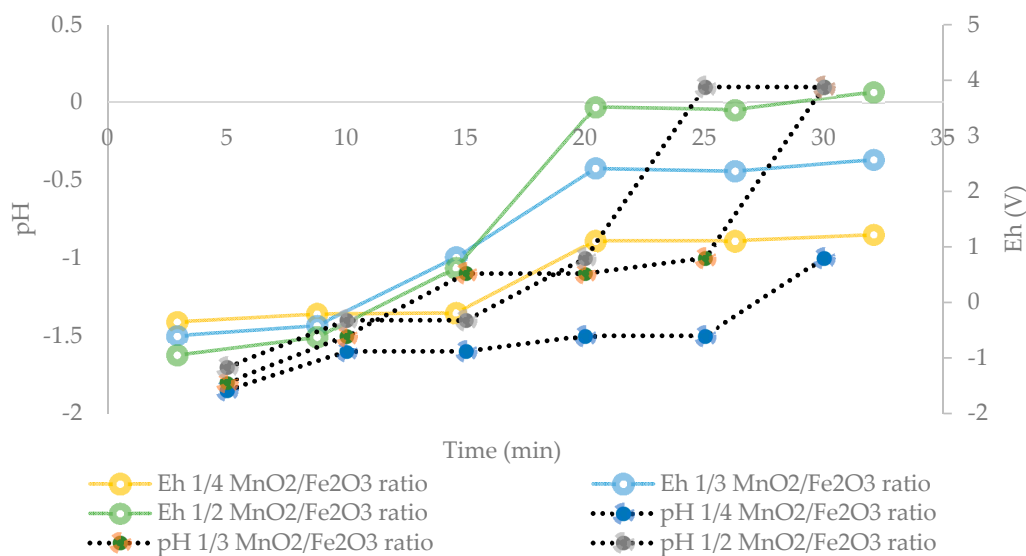
Figure 6. Effect of the potential and pH in solution at different MnO_2/Fe_2O_3 ratios (25 °C, 600 rpm, −75 + 53 μm, acid concentration of 0.1 mol/L).

Senanayake [25] stated that during reductive leaching of MnO_2 with the use of $FeSO_4$ as a reducing agent, the values of potential and pH must be in the range of −0.4 to 1.4 V and −2 to 0.1 in order to dissolve Mn. In addition, it is indicated that the divalent Fe (II), produced by the partial acid dissolution of Fe_3O_4, acts as a reducing agent for MnO_2. Under these conditions, Mn ions remain in solution and do not precipitate through oxidation-reduction reactions by the presence of Fe^{2+} and Fe^{3+} ions [26]. This can be seen in Figure 7, when analyzing the residues of the present study by XRD analysis and mainly the presence of fayalite ($Fe_2^{+2} SiO_4$), magnetite (Fe_3O_4), and gypsum ($CaSO_4 \cdot 2H_2O$) is observed. It is concluded that, in these residues, no Fe precipitates were generated from the solution when tailings were added. In future studies, it may be interesting to perform a kinetic study to elucidate the effect of temperature in order to determine the Mn dissolution mechanisms from marine nodules in very short periods of time (5 min).
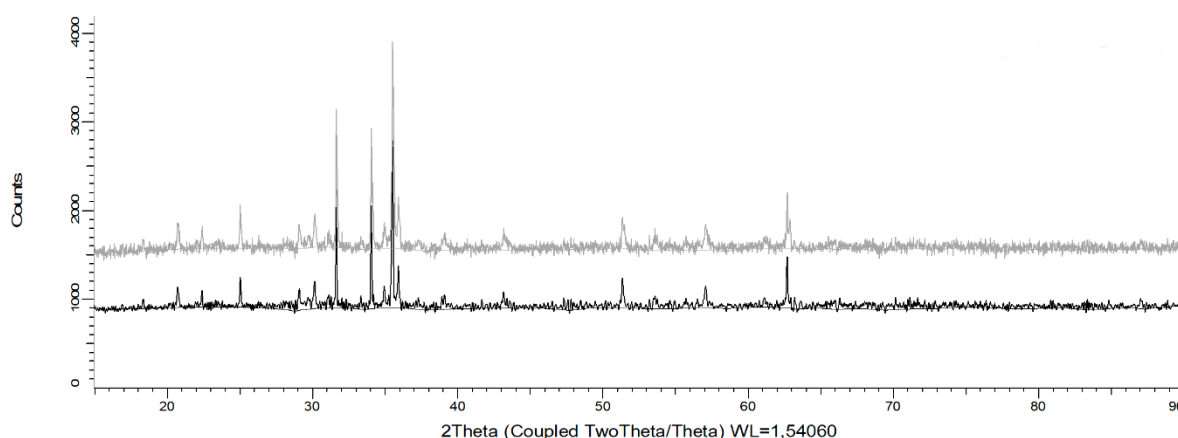

Figure 7. X-ray diffractogram of solid waste after leaching for 30 min at 25 °C using a MnO_2/Fe_2O_3 ratio of 1:2, 600 rpm, −75 + 53 μm, and an acid concentration of 0.1 mol/L.

4. Conclusions

The present study shows results by means of a statistical model as well as extraction curves versus time to investigate the extraction of Mn from MnO_2 present in manganese nodules using tailings obtained from slag flotation when operating in an acid medium and a room temperature of 25 °C.

$FeSO_4$ proves to be a good reducing agent, shortening the dissolution time of MnO_2. The main findings are the following:

1. At 30 min, the optimum MnO_2/Fe_2O_3 ratio is 1:2, with a H_2SO_4 concentration of 0.1 mol/L, achieving a Mn extraction of 74%.
2. For short periods of time (5 to 20 min), the optimum MnO_2/Fe_2O_3 ratio is 1:3, with a H_2SO_4 concentration of 0.1 mol/L, achieving a Mn extraction between 68% and 73%.
3. When operating at MnO_2/Fe_2O_3 ratios lower than 1:1, the concentration of acid in the system is not an important factor.
4. High concentrations of $FeSO_4$ in the system allow the operation in potential and pH ranges, which favor the generation of Fe^{2+} and Fe^{3+}; thus, the formation of Fe precipitates is avoided.

The reductive leaching of marine nodules in an acidic medium with the addition of tailings is an attractive and cost efficient alternative and results in high extraction of Mn in short periods of time with the use of low concentrations of acid. In the future, a study should be carried out to improve the economic viability of the process.

References

1. Konstantinova, N.; Cherkashov, G.; Hein, J.R.; Mirão, J.; Dias, L.; Madureira, P.; Kuznetsov, V.; Maksimov, F. Composition and characteristics of the ferromanganese crusts from the western Arctic Ocean. *Ore Geol. Rev.* **2017**, *87*, 88–99. [CrossRef]
2. Hein, J.R.; Koschinsky, A. Deep-Ocean Ferromanganese Crusts and Nodules. In *Treatise on Geochemistry*; Elsevier: Amsterdam, The Netherlands, 2014; Volume 13, pp. 273–291.
3. Marino, E.; González, F.J.; Somoza, L.; Lunar, R.; Ortega, L.; Vázquez, J.T.; Reyes, J.; Bellido, E. Strategic and rare elements in Cretaceous-Cenozoic cobalt-rich ferromanganese crusts from seamounts in the Canary Island Seamount Province (northeastern tropical Atlantic). *Ore Geol. Rev.* **2017**, *87*, 41–61. [CrossRef]
4. Josso, P.; Pelleter, E.; Pourret, O.; Fouquet, Y.; Etoubleau, J.; Cheron, S.; Bollinger, C. A new discrimination scheme for oceanic ferromanganese deposits using high fi eld strength and rare earth elements. *Ore Geol. Rev.* **2017**, *87*, 3–15. [CrossRef]
5. Cronan, D.S. Cobalt-rich ferromanganese crusts in the Pacific. In *Handbook of Marine Mineral Deposits*; CRC Press: Boca Raton, FL, USA, 2000; pp. 239–279.
6. Hein, J.R.; Cherkashov, G.A. Preface for Ore Geology Reviews Special Issue: Marine Mineral Deposits: New resources for base, precious, and critical metals. *Ore Geol. Rev.* **2017**. [CrossRef]
7. Sharma, R. Environmental Issues of Deep-Sea Mining. *Procedia Earth Planet. Sci.* **2015**, *11*, 204–211. [CrossRef]
8. Zakeri, A.; Bafghi, M.S.; Shahriari, S.; Das, S.C.; Sahoo, P.K.; Rao, P.K. Dissolution kinetics of manganese dioxide ore in sulfuric acid in the presence of ferrous ion. *Hydrometallurgy* **2007**, *8*, 22–27.
9. Bafghi, M.S.; Zakeri, A.; Ghasemi, Z.; Adeli, M. Reductive dissolution of manganese ore in sulfuric acid in the presence of iron metal. *Hydrometallurgy* **2008**, *90*, 207–212. [CrossRef]
10. Toro, N.; Herrera, N.; Castillo, J.; Torres, M.C.; Sepúlveda, R.S. Initial Investigation into the Leaching of Manganese from Nodules at Room Temperature with the Use of Sulfuric Acid and the Addition of Foundry Slag—Part I. *Minerals* **2018**, *8*, 565. [CrossRef]

11. Toro, N.; Saldaña, M.; Castillo, J.; Higuera, F.; Acosta, R. Leaching of Manganese from Marine Nodules at Room Temperature with the Use of Sulfuric Acid and the Addition of Tailings. *Minerals* **2019**, *9*, 289. [CrossRef]

12. Alejandra, C.; Estay, S. *Utilización de Escorias de Fundición para la Producción de Compuestos de Hierro*; Universidad de Chile: Santiago, Chile, 2006.

13. Vásquez, M. En Chile Diariamente se Desecha Cobre Avaluado en una Cifra Cercana a Los 450 Mil dólares. 2019. Available online: https://www.pucv.cl/uuaa/vriea/noticias/nuestros-investigadores/en-chile-diariamente-se-desecha-cobre-avaluado-en-una-cifra-cercana-a/2016-08-05/124009.html (accessed on 7 April 2019).

14. COCHILCO. *Sulfuros primarios: Desafíos y oportunidades I Comisión Chilena del Cobre*; COCHILCO: San Diego, Chile, 2017.

15. Medvinsky-Roa, G.; Caroca, V.; Vallejo, J. Informe sobre la situación de los Relaves Mineros en Chile para ser presentado en el cuarto informe periódico de Chile para el Comité de Derechos Económicos, Sociales y Culturales, perteneciente al consejo Económico Social de la Naciones Unidas. Providencia. 2015. Available online: https://tbinternet.ohchr.org/Treaties/CESCR/SharedDocuments/CHL/INT_CESCR_CSS_CHL_20605_S.pdf (accessed on 7 April 2019).

16. Xenidis, A.; Papassiopi, N.; Komnitsas, K. Carbonate-rich mining tailings in Lavrion: Risk assessment and proposed rehabilitation schemes. *Adv. Environ. Res.* **2003**, *7*, 207–222. [CrossRef]

17. Komnitsas, K.; Kontopoulos, A.; Lazar, I.; Cambridge, M. Risk assessment and proposed remedial actions in coastal tailings disposal sites in Romania. *Miner. Eng.* **1998**, *11*, 1179–1190. [CrossRef]

18. SERNAGEOMIN. *Anuario de la Mineria de Chile 2017*; SERNAGEOMIN: San Diego, Chile, 2017.

19. ISA. *Polymetallic Nodule Mining Technology: Current Trends and Challenges Ahead*; ISA: Chennai, India, 2008; p. 276.

20. Douglas, C. *Montgomery: Design and Analysis of Experiments*, 8th ed.; John Wiley & Sons: New York, NY, USA, 2012.

21. Ghosh, M.K.; Barik, S.P.; Anand, S. Sulphuric acid leaching of polymetallic nodules using paper as a reductant. *Trans. Indian Inst. Met* **2008**, *61*, 477–481. [CrossRef]

22. Mitić, M.; Tošić, S.; Pavlović, A.; Mašković, P.; Kostić, D.; Mitić, J.; Stevanović, V. Optimization of the extraction process of minerals from Salvia officinalis L. using factorial design methodology. *Microchem. J.* **2019**, *145*, 1224–1230. [CrossRef]

23. Mathews, P.G.; William, A. *Design of Experiments with MINITAB*; William A. Tony: Milwaukee, WI, USA, 2005.

24. Kanungo, S.B. Rate process of the reduction leaching of manganese nodules in dilute HCl in presence of pyrite. Part I. Dissolution behaviour of iron and sulphur species during leaching. *Hydrometallurgy* **1999**, *52*, 313–330. [CrossRef]

25. Senanayake, G. Acid leaching of metals from deep-sea manganese nodules—A critical review of fundamentals and applications. *Miner. Eng.* **2011**, *24*, 1379–1396. [CrossRef]

26. Komnitsas, K.; Bazdanis, G.; Bartzas, G.; Sahinkaya, E.; Zaharaki, D. Removal of heavy metals from leachates using organic/inorganic permeable reactive barriers. *Desalin. Water Treat.* **2013**, *51*, 3052–3059. [CrossRef]

4. Leaching of Pure Chalcocite in a Chloride Media Using Sea Water and Waste Water

Leaching of Pure Chalcocite in a Chloride Media Using Sea Water and Waste Water

Norman Toro [1,2,*], Williams Briceño [3], Kevin Pérez [1] , Manuel Cánovas [1] , Emilio Trigueros [2], Rossana Sepúlveda [4] and Pía Hernández [5]

[1] Departamento de Ingeniería en Metalurgia y Minas, Universidad Católica del Norte, Av. Angamos 610, Antofagasta 1270709, Chile

[2] Department of Mining, Geological and Cartographic Department, Universidad Politécnica de Cartagena, Paseo Alfonso Xlll N°52, 30203 Cartagena, Spain

[3] Departamento de Ingeniería Industrial, Universidad Católica del Norte, Av. Angamos 610, Antofagasta 1270709, Chile

[4] Departamento de Ingeniería en Metalurgia, Universidad de Atacama, Av. Copayapu 485, Copiapó 1531772, Chile

[5] Departamento de Ingeniería Química y Procesos de Minerales, Universidad de Antofagasta, Avda. Angamos 601, Antofagasta 1240000, Chile

* Correspondence: ntoro@ucn.cl; Tel.: +56-552651021

Abstract: Chalcocite is the most important and abundant secondary copper ore in the world with a rapid dissolution of copper in an acid-chloride environment. In this investigation, the methodology of surface optimization will be applied to evaluate the effect of three independent variables (time, concentration of sulfuric acid and chloride concentration) in the leaching of pure chalcocite to extract the copper with the objective of obtaining a quadratic model that allows us to predict the extraction of copper. The kinetics of copper dissolution in regard to the function of temperature is also analyzed. An ANOVA indicates that the linear variables with the greatest influence are time and the chloride concentration. Also, the concentration of chloride-time exerts a significant synergic effect in the quadratic model. The ANOVA indicates that the quadratic model is representative and the R^2 value of 0.92 is valid. The highest copper extraction (67.75%) was obtained at 48 h leaching under conditions of 2 mol/L H_2SO_4 and 100 g/L chloride. The XRD analysis shows the formation of a stable and non-polluting residue; such as elemental sulfur (S^0). This residue was obtained in a leaching time of 4 h at room temperature under conditions of 0.5 mol/L H_2SO_4 and 50 g/L Cl^-.

Keywords: chalcocite; sulphide leaching; copper; reusing water; desalination residue; ecological treatment

1. Introduction

Most of the copper minerals on the planet correspond to sulfur minerals and a smaller amount of oxidized minerals. A report by COCHILCO [1] mentions that the world copper production is currently 19.7 million tons. Seventy-five percent of this total comes from the pyrometallurgical processing of copper sulfide minerals processed in smelting plants [2], and 25% by the hydrometallurgical route [3].

There is a need to generate a new momentum that overcomes a certain stagnation in the growth capacity of the mining industry. Even in its role as a surplus generator, large-scale mining faces great challenges. These include an increase in costs due to various factors; such as the deterioration of laws and other elements associated with the aging of deposits and input costs to be compatible with sustainable development demands [4].

Sulfur minerals have been treated for decades with flotation and pyrometallurgical processes [5], which result in major environmental problems; such as tailings dams and the generation of acid drainage (sulfuric acid and oxides of iron) by the oxidation of sulfur minerals with a high presence of pyrite. This sulfide is one of the most common and abundant minerals in the world and is associated with hydrothermal mineralization [6]. On the other hand, foundries produce large emissions of sulfur dioxide (SO_2), which together, with NO_x and CO_2, can cause large problems; such as acid rain and increasing local pollution, therefore, the abatement of waste gases is an important task for the protection of the environment [7–9]. As a result, new hydrometallurgical alternatives are being developed in the mining industry, because they are more ecological and economic processes to recover copper [10,11].

Chalcocite is the most abundant copper sulfide mineral after chalcopyrite [5,12], and it is the copper sulfide the most easily treated by hydrometallurgical routes [13]. Several investigations have been carried out for the leaching of this mineral with the use of multiple additives and in different media such as; bioleaching [14–18], ferric sulfate solution [19], chloride media [20–23], pressure leaching for chalcocite [24] and synthetic chalcocite (white metal) [25].

When operating in sulphated or chloride media, the oxidative dissolution of the chalcocite occurs in two stages [13,19,20,23,25].

$$Cu_2S + 2Fe^{3+} = Cu^{2+} + 2Fe^{2+} + CuS \qquad (1)$$

$$CuS + 2Fe^{3+} = Cu^{2+} + 2Fe^{2+} + S^0 \qquad (2)$$
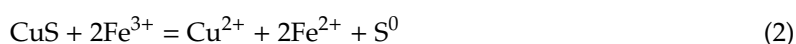
The first stage of leaching of the chalcocite is much faster than the second stage. This is controlled by diffusion of the oxidant on the surface of the ore at low values of activation energy (4–25 kJ mol^{-1}) [19]. The second stage is slower and can be accelerated depending on the temperature [13,26].

The investigations shown in Table 1 were obtained as a result of high extractions (90%), but these results were obtained with the application of high temperatures and/or with the addition of ferric or cupric ions as an oxidizing agent. In addition, the previous investigations were made with mixtures of copper sulfides, with the presence of gangue or with the use of synthetic chalcocite. It is emphasized that the present investigation will include a leaching of pure chalcocite in a chlorinated medium, without the addition of oxidizing agents (Fe^{3+}, Cu^{2+}, etc.) and at room temperature.
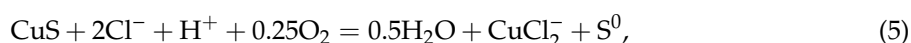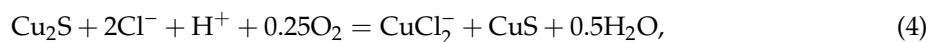
Table 1. Comparison of previous investigations of chalcocite with the use of Cl^-.

Investigation	Leaching Agent	Parameters Evaluated	Reference	Cu Ext (%)
The kinetics of leaching chalcocite (synthetic) in acidic oxygenated sulphate-chloride solutions	NaCl, H_2SO_4, HCl, HNO_3 and Fe^{3+}	Oxygen flow, stirring speed, temperature, sulfuric acid concentration, ferric ions concentration, chloride concentration and particle size.	[20]	97
The kinetics of dissolution of synthetic covellite, chalcocite and digenite in dilute chloride solutions at ambient temperatures	HCl, Cu^{2+} and Fe^{3+}	Potential effect, chloride concentration, acid concentration, temperature, dissolved oxygen and pyrite effect.	[13]	98
Leaching kinetics of digenite concentrate in oxygenated chloride media at ambient pressure	$CuCl_2$, HCl and NaCl	Effect of stirring speed, oxygen flow, cupric ion concentration, chloride concentration, acid concentration and temperature effect.	[27]	95
Leaching of sulfide copper ore in a NaCl–H_2SO_4–O_2 media with acid pre-treatment	NaCl and H_2SO_4	Chloride concentration, effect of agitation with compressed air, percentage of solids and particle size.	[22]	78

A chalcocite leaching is performed with the injection of O_2 at ambient pressure in a H_2SO_4-NaCl solution, where the leaching agents are Cu^{2+}, $CuCl^+$, $CuCl_2$ and $CuCl_3^-$, which are generated during leaching in a Cu^{2+}/Cl^- system. The general reaction of chalcocite leaching is as follows:

$$Cu_2S + 0.5O_2 + 2H^+ + 4Cl^- = 2CuCl_2^- + H_2O + S^0, \tag{3}$$
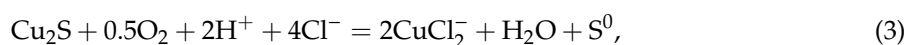
While the chalcocite leaching reactions occur in two stages, guiding us to Equation (3), the following occurs:

$$Cu_2S + 2Cl^- + H^+ + 0.25O_2 = CuCl_2^- + CuS + 0.5H_2O, \tag{4}$$

$$CuS + 2Cl^- + H^+ + 0.25O_2 = 0.5H_2O + CuCl_2^- + S^0, \tag{5}$$

The resulting products expected from this chalcocite leaching should be soluble copper; such as $CuCl_2^-$ and a solid residue of elemental sulfur (S^0) with covellite residues or copper polysulfides (CuS_2) that still contain valuable metals.

The $CuCl_2^-$ is the predominant soluble specie due to the complexation of Cu (I) with the presence of Cl^- at room temperature, in a system of high concentrations of chloride (greater than 1 M). This $CuCl_2^-$ is stable in a range of potentials between 0–500 mV and pH < 6–7 (depending on the chloride concentration in the system) [20,28].

The shortage of fresh water in arid areas is an economic, environmental and social problem [29]. The use of sea water has become increasingly important for mining in Chile, not only because of its positive effects on leaching processes due to its chloride content, but also as a strategic and indispensable resource. For example, some metallic and non-metallic mining companies in the north of Chile have deposits rich in copper, gold, silver, iron and minerals from salt lakes, which are found in hyper-arid zones and at high altitudes, which emphasizes the necessity of this resource [30]. In addition, it is important to mention that the Chilean authorities have indicated that large-scale mining projects involving the use of water from aquifers will not be authorized [31]. An attractive alternative is the use of waste water from desalination plants. These companies produce drinking water for the population, however, their disposal product pollutes the oceans, for this reason, it is necessary to think of possible alternatives to recycle this resource and at the same time optimize extraction processes in local mining.

In the present investigation, a statistical analysis will be carried out using the methodology of surface optimization (design of the central composite face) to sensitize independent parameters (time, sulfuric acid concentration and chloride concentration) in the leaching of a pure mineral of chalcocite in chlorinated media. In addition, the effect on chloride concentration in the system will be evaluated when operating with potable water, seawater and reusing waste water.

2. Materials and Methods

2.1. Chalcocite

The pure chalcocite mineral used for the present investigation was collected manually directly from the veins by expert geologists from Mina Atómica, located in the region of Antofagasta, Chile.

The pure chalcocite samples were checked by X-ray diffraction (XRD) analysis, using an automatic and computerized X-ray diffractometer Bruker model Advance D8 (Bruker, Billerica, MA, USA). Figure 1 shows the results of the XRD analysis, indicating the presence of 99.9% chalcocite. The chemical analysis was performed by atomic emission spectrometry via induction-coupled plasma (ICP-AES), the sample of chalcocite was digested using aqua regia and HF. Table 2 shows the chemical composition of the samples. The samples for XRD and ICP-OES were ground in a porcelain mortar to reach a size range between −147 + 104 μm. The procedures described were performed in the applied geochemistry laboratory of the department of geological sciences of the Universidad Católica del Norte.
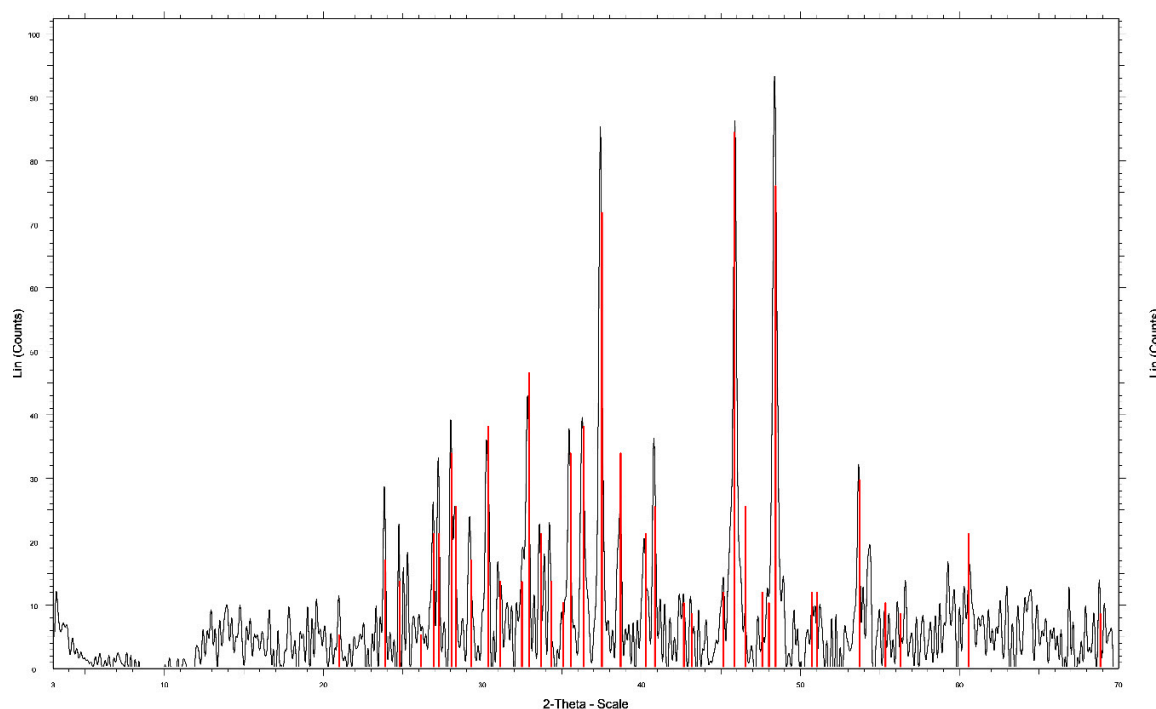
Figure 1. X-ray diffractogram for the chalcocite mineral.

Table 2. Chemical analysis of the chalcocite ore.

Component	Cu	S^0
Mass (%)	79.83	20.17

2.2. Leaching and Leaching Tests

The sulfuric acid used for the leaching tests was grade P.A., Merck brand, purity 95–97%, density 1.84 kg/L and molecular weight of 98.08 g/mol, though the tests also work with the use of sea water and waste water from the "Aguas Antofagasta" Desalination Plant. Table 3 shows the chemical composition of waste water.

Table 3. Chemical analysis of waste water.

Compound	Concentration (g/L)
Fluorine (F^-)	0.01
Calcium (Ca^{2+})	0.80
Magnesium (Mg^{2+})	2.65
Bicarbonate (HCO_3^-)	1.10
Chloride (Cl^-)	39.16
Calcium carbonate ($CaCO_3$)	13.00

Leaching tests were carried out in a 50 mL glass reactor with a 0.01 S/L ratio. A total of 200 mg of chalcocite ore in a size range between $-147 + 104$ μm and the addition of NaCl at different concentrations were maintained in agitation and suspension with the use of a 5-position magnetic stirrer (IKA ROS, CEP 13087-534, Campinas, Brazil) at a speed of 600 rpm and the temperature was controlled using an oil-heated circulator (Julabo, St. Louis, MO, USA). The temperature range tested in the experiments was 25 °C. Also, the tests were performed in duplicate and measurements (or analyzes) were carried out on 5 mL aliquot and diluted to a range of dilutions using atomic absorption spectrometry with a coefficient of variation ≤5% and a relative error between 5 to 10%. Measurements of pH and oxidation-reduction potential (ORP) of leach solutions were made using a pH-ORP meter (HANNA HI-4222, St. Louis, MO,

USA). The ORP solution was measured in a combination ORP electrode cell of a platinum working electrode and a saturated Ag/AgCl reference electrode.

2.3. Experimental Design

The effects of independent variables on Cu extraction rates from leaching of chalcocite were studied using the response surface optimization method [32–35]. The central composite face (CCF) design and a quadratic model were applied to the experimental design for Cu_2S leaching.

Twenty-seven experimental tests were carried out to study the effects of time, chloride and H_2SO_4 concentration as independent variables. Minitab 18 software (version 18, Pennsylvania State University, State College, PA, USA) was used for modeling and experimental design, which allowed the study of the linear and quadratic effects of the independent variables. The experimental data were fitted by multiple linear regression analysis to a quadratic model, considering only those factors that helped to explain the variability of the model. The empirical model contains coefficients of linear, quadratic, and two-factor interaction effects.

The general form of the experimental model is represented by:

$$Y = (overall\ constant) + (linear\ effects) + (interaction\ effects) + (curvature\ effects), \tag{6}$$

$$Y = b_0 + b_1x_1 + b_2x_2 + b_3x_3 + b_{12}x_1x_2 + b_{13}x_1x_3 + b_{23}x_2x_3 + b_{11}x_1^2 + b_{22}x_2^2 + b_{33}x_3^2, \tag{7}$$

Where, x_1 is time, x_2 is Chloride, x_3 is H_2SO_4 concentration, and b is the variable coefficients.

Table 4 presents the ranges of parameter values used in the experimental model. The variable values are codified in the model. The following Equation (8) is used for transforming a real value (Z_i) into a code value (X_i) according to the experimental design:

$$X_i = \frac{Z_i - \frac{Z_{high} + Z_{low}}{2}}{\frac{Z_{high} - Z_{low}}{2}}, \tag{8}$$

Z_{high} and Z_{low} are the highest and lowest levels of a variable, respectively [36].

Table 4. Experimental parameters for the central design of the composite face.

Experimental Parameters	Low	Medium	High
Time (h)	4	8	12
Concentration Cl^- (g/L)	20	50	100
Concentration H_2SO_4 (mol/L)	0.5	1	2
Codifications	−1	0	1

A factorial design was applied involving three factors, each one having three levels thus 27 experimental tests were carried out in Table 5, evaluating the effect of time and H_2SO_4 and chloride concentration.

The statistical R^2, R^2_{adj}, p-values and Mallows's Cp indicate whether the model obtained is adequate to describe Cu extraction under a given domain. The R^2 coefficient is a measure of the goodness of fit, which measures the proportion of total variability of the dependent variable with respect to its mean, which is explained by the regression model. The p-values represent statistical significance, which indicates whether there is a statistically significant association between the response variable and the terms. The predicted R^2 was used to determine how well the model predicts the response for new observations. Finally, Mallows's Cp is a precise measure in the model, estimating the true parameter regression [36].

Table 5. Experimental configuration and Cu extraction.

Exp. No.	Time (h)	Cl$^-$ (g/L)	H$_2$SO$_4$ (mol/L)	Cu Ext. (%)
1	4	20	0.5	31.63
2	4	20	1	33.25
3	4	20	2	37.00
4	4	50	0.5	32.25
5	4	50	1	33.38
6	4	50	2	38.00
7	4	100	0.5	44.75
8	4	100	1	44.88
9	4	100	2	46.19
10	8	20	0.5	35.75
11	8	20	1	38.75
12	8	20	2	43.00
13	8	50	0.5	48.13
14	8	50	1	49.50
15	8	50	2	50.63
16	8	100	0.5	51.50
17	8	100	1	53.00
18	8	100	2	54.88
19	12	20	0.5	52.25
20	12	20	1	52.75
21	12	20	2	52.63
22	12	50	0.5	53.13
23	12	50	1	53.13
24	12	50	2	53.00
25	12	100	0.5	53.25
26	12	100	1	53.88
27	12	100	2	55.63

3. Results

3.1. ANOVA

An ANOVA analysis (Table 6) showed F-value and p-value for the model.

Table 6. ANOVA (analysis of variance) Cu extraction.

Source	F-Value	p-Value
Regression	22.73	0
Time	123.15	0
Cl$^-$	45.25	0
H$_2$SO$_4$	5.44	0.03
Time $\times$ Time	2.06	0.17
Cl$^-$ $\times$ Cl$^-$	0.13	0.72
H$_2$SO$_4$ $\times$ H$_2$SO$_4$	0.00	0.97
Time $\times$ Cl$^-$	10.27	0.01
Time $\times$ H$_2$SO$_4$	1.18	0.29
Cl$^-$ $\times$ H$_2$SO$_4$	0.31	0.59

In the contour plot in Figure 2, it is observed that Cu extraction increases at long times, high chloride concentration, and high H$_2$SO$_4$ concentration.
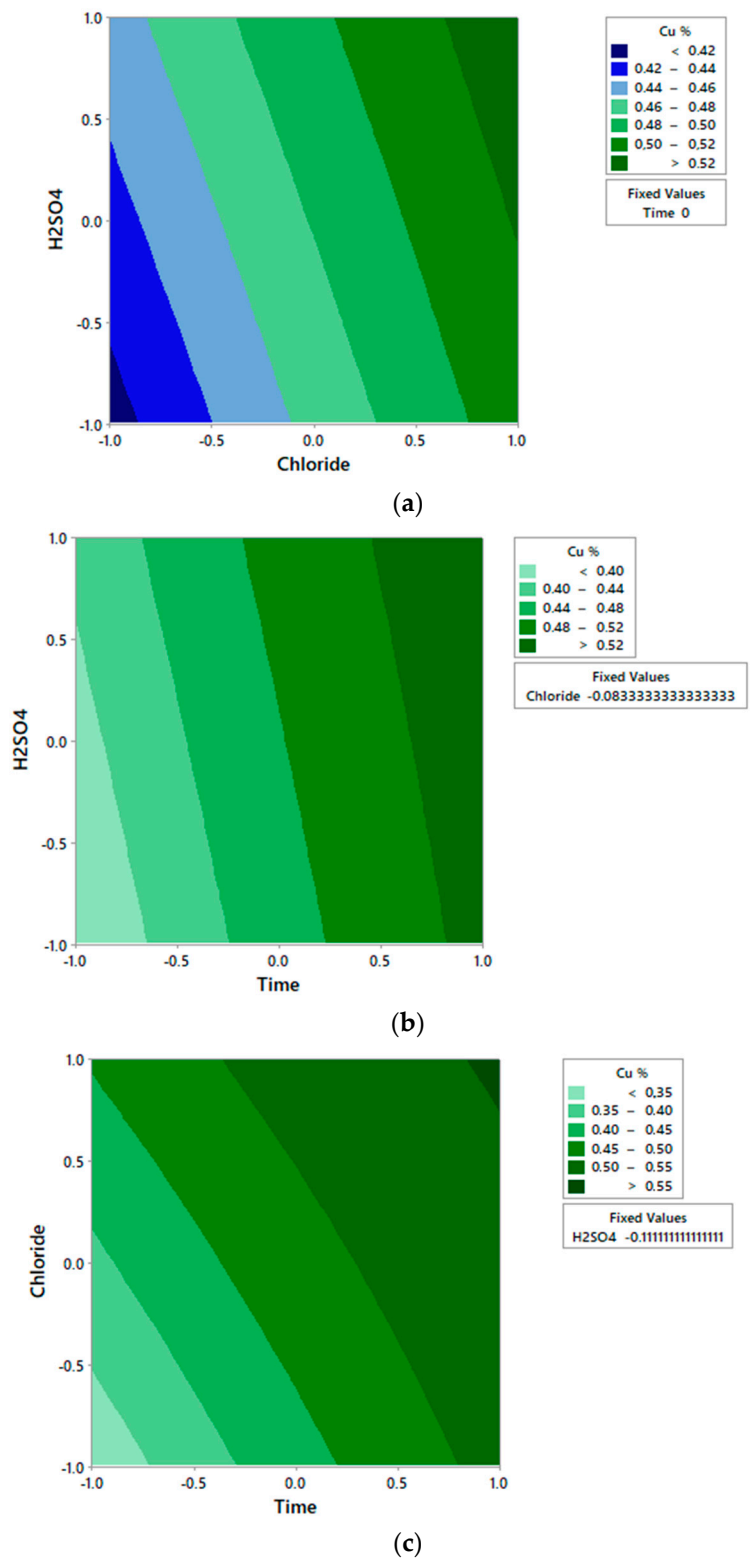
(a)

(b)

(c)

Figure 2. Experimental contour plot of independent variables of Chloride and H_2SO_4 concentration (**a**); Time and H_2SO_4 concentration (**b**); and Time and Chloride concentration (**c**) on the dependent variable Cu extraction.

Table 6 shows ANOVA analysis. There is no significant effect ($p > 0.05$) of the interactions concentration of chloride concentration of H_2SO_4 and time-concentration of H_2SO_4 in copper extraction, complying with the theory that the increase in sulfuric acid concentration does not have a great influence

on the leaching of chalcocite above 0.02 mol/L [19,22]. Rather, it is only the time-concentration interaction of chloride that must be considered in the model. Additionally, the effects of curvature of the variable chloride concentration and H_2SO_4 concentration do not contribute significantly to explaining the variability of the model. On the other hand, the linear effects of chloride time and concentration contribute to explaining the experimental model, as shown in the contour plot of Figure 2.

Figures 3 and 4 show that time, chloride and H_2SO_4 concentration, as well as the interaction of time-H_2SO_4 and Cl-H_2SO_4 affected Cu extraction.
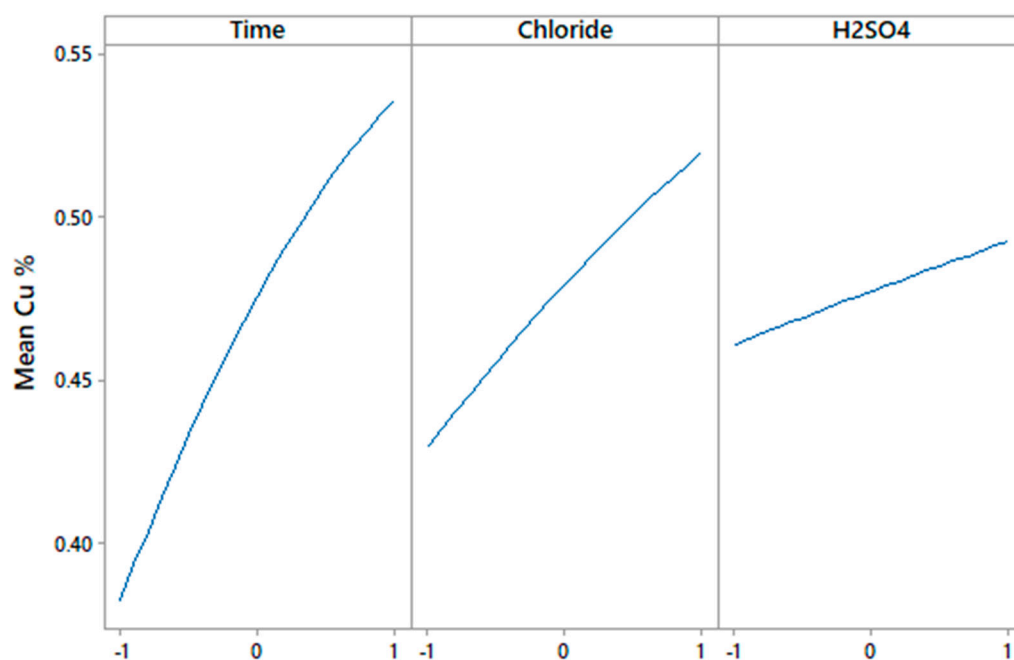
Figure 3. Linear effect plot for Cu extraction.

In Figure 3, the linear effects demonstrate what has been said by several authors [13,20,37], with respect to the effect of the concentration of chloride present in the leaching media and the effect of sulfuric acid concentration. The concentration of chloride has a great impact on the dissolution of copper from a sulfide; such as chalcocite. According to Velásquez-Yévenes et al. [38], the chloride ions present in the media increase the rate of oxidation of cuprous ions, while Cheng and Lawson [20,39] proposed that the effect of chloride ions promotes the formation of long sulfide crystals that allow the reactants to penetrate the sulfide layer, since in their tests they noticed that, in the absence of chloride ions, the kinetics of dissolution decreased considerably and that covellite did not dissolve. This with time was supported in the research of Nicol and Basson [37], without the presence of chloride ions or with a very low concentration of ions, the potential needed to dissolve covellite is very high.

Figure 4 shows the mean Cu extraction at different combinations of factor levels. In the interaction time-chloride, the lines are not parallel, and the plot indicates that there is an interaction between the factors. On the other hand, the interaction between time-H_2SO_4 and chloride-H_2SO_4 is low.

Equation (9) presents the Cu extraction model over the range of experimental conditions after eliminating the non-significant coefficients.

$$\% \text{ Extraction} = 0.47782 + 0.07472\, x_1 + 0.04462\, x_2 + 0.01568\, x_3 - 0.0163\, x_1^2 - 0.02546\, x_1 x_2, \quad (9)$$

Where x_1, x_2 and x_3 are codified variables that respectively represent time, chloride and H_2SO_4 concentration.
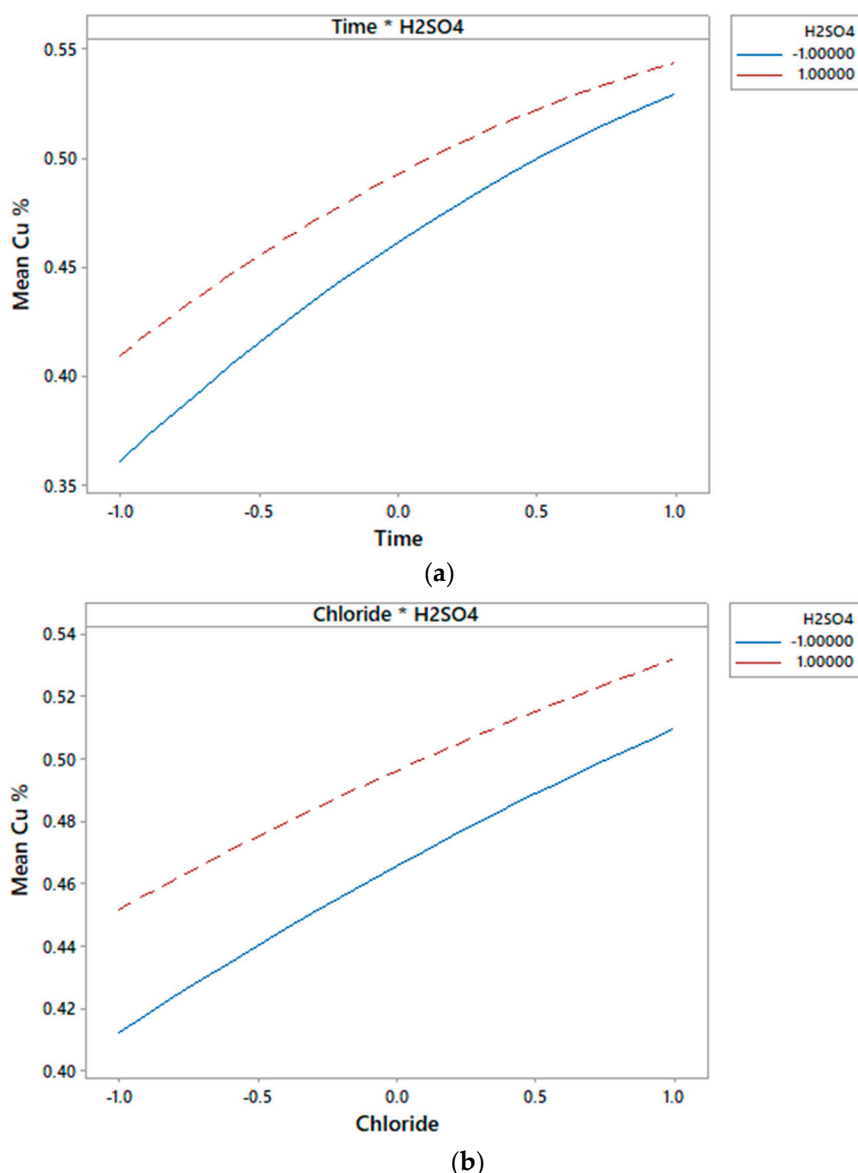
(a)

(b)

Figure 4. Interaction effect plot of independent variables Time and H2SO4 concentration (**a**); and Chloride and H2SO4 concentration (**b**) on the dependent variable Cu extraction.

An ANOVA test indicated that the quadratic model adequately represented Cu extraction from Cu_2S under the established parameter ranges. The model did not require adjustment and it was validated by the R^2 value (0.92) and R^2_{adj} value (0.90). The ANOVA analysis showed that the factors indicated influence Cu extraction from Cu_2S ($F_{Regression}$ (22.73) > $F_{T,95\%\ confidence\ level}$ = $F_{5,21}$ (2.68)). On the other hand, the p-value of the model (Equation (9)) is lower than 0.05, indicating that the model is statistically significant.

The Mallows's Cp = 3.62 (constant + 5 predictors) indicated that the model was accurate and did not present bias in estimating the true regression coefficients. This value of Cp of Mallows allows comparison with other models and establishes that the model found is the one that is most adjustable, due to the Cp closest to the number of constants and predictors.

In addition, all variance inflation factors (VIF) values are close to one, which ensures that there is no multicollinearity.

It also allows for prediction with an acceptable future forecast margin of error of R^2_{pred} = 0.8684.

Finally, from the adjustment of the ANOVA analysis, it was found that the factors considered, after analysis of the main components, explained the variation in the response. The difference between

the R^2 and R^2_{pred} of the model was minimal, thus reducing the risk that the model was over adjusted. That means, the probability that the model fits only in the sample data is lower. The ANOVA analysis indicated that time, chloride concentration, H_2SO_4 concentration and the interaction of time-chloride are the factors that explain to a greater extent the behavior of the system for the sampled data set.

Table 5 shows that the increase in sulfuric acid concentration does not affect copper dissolution, obtaining similar results under similar conditions of leaching, only a minimum amount of sulfuric acid is needed in the leaching system. This result is consistent with other investigations, since according to Cheng and Lawson [20], a concentration of sulfuric acid of 0.02 mol/L, is sufficient to perform a leaching of chalcocite and its subsequent phases as it is the djurleite, digenite ore [22]. After this value its effect is null.

On the other hand, it is shown that at a leaching time of 12 h, the values of copper extraction do not vary regardless of the concentration of chloride and sulfuric acid. This could be explained with Equations (4) and (5); Equation (4) is the rapid reaction of the transformation of chalcocite to covellite, in which a low activation energy is required to achieve its transformation [13]. When covellite is formed (Equation (5)), it needs more energy (about 72 kJ approximately) to achieve its dissolution and later become a copper polysulfide (CuS_2), what it requires is even more demanding conditions to achieve its complete dissolution [37].

3.2. Effect on the Chloride Concentration

It has been known since the 1970s that it is beneficial to work with chloride ions in the leaching of sulfide minerals [23,40]. In Figure 5a, when operating at higher chloride concentrations, higher copper recoveries are obtained. When operating with the highest chloride concentrations (100 g/L), the highest recovery (68.82%) is obtained at 48 h. However, a large difference in copper recoveries cannot be seen when operating at chloride concentrations between 20 and 50 g/L. At 48 h and 20 g/L, a recovery of 63.58% of Cu was obtained and for chloride concentrations of 50 g/L, 65.45% was obtained. On the other hand, in Figure 5b it is observed that with the use of waste water (39.16 g/L of Cl^-), results similar to those presented in Figure 5a were obtained in a Cl^- concentration of 50 g/L, so it is noted that the presence of calcium ions, fluorine, magnesium and calcium carbonate did not affect the dissolution of copper from the chalcocite. In the tests carried out with seawater, which has approximately a concentration of 20 g/L Cl^-, obtained copper extractions of up to 63.4% at 48 h with a concentration of 0.5 mol/L of sulfuric acid. In previous investigations [13,20], it has been determined that leaching is independent of a chloride concentration between 0.5 and 2 mol/L, but a greater kinetic of dissolution is observed in the first minutes and then the difference decreases as a function of time and behavior similar to that of Figure 5.

Figure 6 shows a residue analysis performed under the conditions of 50 g/L Cl^- and 0.5 mol/L H_2SO_4, in a leaching time of 4 h. The result of this XRD is useful to understand the behavior of the chalcocite in a short time and in low reagent conditions, and to observe which mineralogical species are forming. The results show a high formation of synthetic covellite (77.34 wt %), early formation of elemental sulfur (20.20 wt %) and a remaining chalcocite (4.46 wt %), which still does not dissolve. From this, it follows that the transformation of chalcocite to covellite is faster than the transformation of covellite to elemental sulfur, which is similar to that observed in Equations (4) and (5), also, according to Figure 5, the slope of the curve is decreasing slowly, which means less kinetics of copper dissolution as a function of time. In the investigation of Senanayake [28], it is reported that the dissolution of chalcocite in a chloride-iron-water system at 25 °C occurs at potentials greater than 500 mV with a pH < 4, while in the research of Miki et al. [13] it is reported that the chalcocite dissolution occurs rapidly at a potential of 500 mV but stops when it reaches 50% copper extraction. When the potential increases to 550 mV, this extraction increases again because once it reaches 50% copper extraction, the mineral present is mainly covellite, which has a dissolution kinetics lower than the chalcocite and that needs potentials greater than 600 mV to dissolve.
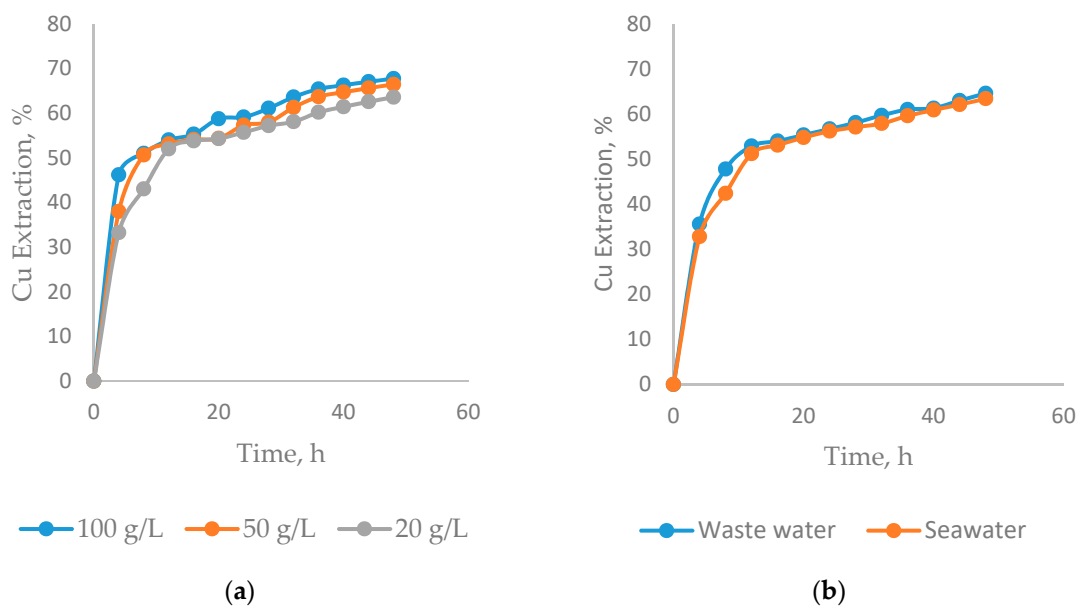
Figure 5. Effect of chloride concentration on Cu extraction from chalcocite ($T = 25°C$. $H_2SO_4 = 0.5$ mol/L); (**a**) Cl^- added by NaCl; (**b**) Cl^- added by waste water and seawater.

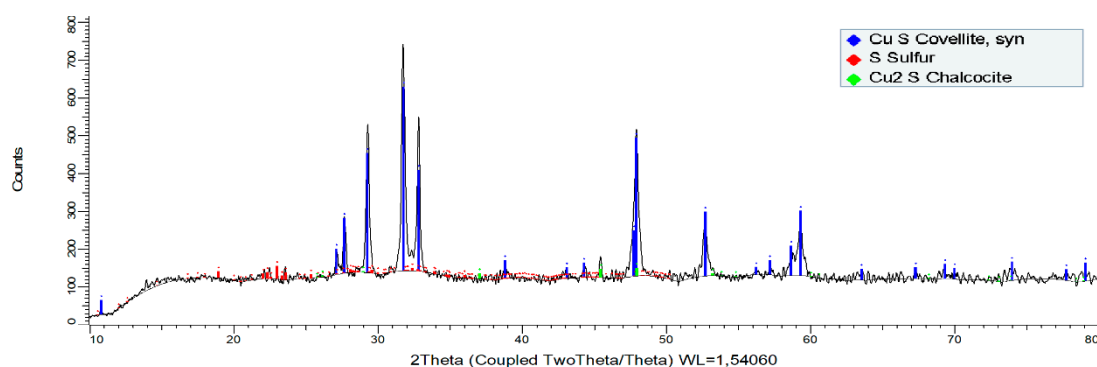**Figure 6.** X-ray diffractogram for solid residues (chalcocite mineral) after being leached at 25 °C in a time of 4 h with 0.5 mol/L H_2SO_4 and 50 g/L Cl^-.

4. Conclusions

The present investigation shows the experimental results necessary to dissolve Cu from a chalcocite mineral in chloride media. The findings of this study were:

1. The linear variables with the greatest influence in the model are: time, chloride concentration and sulfuric acid concentration, respectively.
2. Under normal pressure and temperature conditions, only the chloride-time concentration exerts a significant synergistic effect on the extraction of copper from a chalcocite mineral.
3. The ANOVA analysis indicates that the presented quadratic model is adequate to represent the copper extractions and the value of R^2 (0.92) validates it.
4. The highest copper extraction is achieved under conditions of low concentration of sulfuric acid (0.5 mol/L), high concentrations of chloride (100 g/L) and a prolonged leaching time (48 h) to obtain an extraction of 67.75% copper.
5. The XRD analysis shows the formation of a stable and non-polluting residue; such as elemental sulfur (S^0). This residue was obtained in a leaching time of 4 h at room temperature under conditions of 0.5 mol/L H_2SO_4 and 50 g/L Cl^-.

References

1. Comisión Chilena del Cobre. Sulfuros Primarios: Desafíos y Oportunidades. Registro Propiedad Intelectual N° 2833439. 2017. Available online: https://www.cochilco.cl/ListadoTemtico/sulfurosprimarios_desafíosyoportunidades.pdf (accessed on 25 April 2019).

2. Navarra, A.; Oyarzun, F.; Parra, R.; Marambio, H.; Mucciardi, F. System dynamics and discrete event simulation of copper smelters. *Miner. Metall. Process.* **2017**, *34*, 96–106. [CrossRef]

3. International Copper Study Group. *The World Copper Factbook 2017*; International Copper Study Group: Lisbon, Portugal, 2017.

4. CESCO. La Minería como plataforma para el desarrollo: Hacia una relación integral y sustentable de la industria minera en Chile. Available online: http://www.cesco.cl/wp-content/uploads/2018/06/Resumen-Position-Paper.pdf (accessed on 12 July 2019).

5. Schlesinger, M.E.; King, M.J.; Sole, K.C.; Davenport, W.G. *Extractive Metallurgy of Copper*, 5th ed.; Elsevier: Amsterdam, Netherlands, 2011.

6. Oyarzún, R.; Oyarzún, J.; Lillo, J.; Maturana, H.; Higueras, P. Mineral deposits and Cu-Zn-As dispersion-contamination in stream sediments from the semiarid Coquimbo Region, Chile. *Environ. Geol.* **2007**, *53*, 283–294. [CrossRef]

7. Dijksira, R.; Senyard, B.; Shah, U.; Lee, H. Economical abatement of high-strength SO2off-gas from a smelter. *J. South. African Inst. Min. Metall.* **2017**, *117*, 1003–1007. [CrossRef]

8. Serbula, S.M.; Milosavljevic, J.S.; Radojevic, A.A.; Kalinovic, J.V.; Kalinovic, T.S. Extreme air pollution with contaminants originating from the mining—Metallurgical processes. *Sci. Total Environ.* **2017**, *586*, 1066–1075. [CrossRef] [PubMed]

9. Zagoruiko, A.N.; Vanag, S.V. Reverse-flow reactor concept for combined SO2 and co-oxidation in smelter off-gases. *Chem. Eng. J.* **2014**, *238*, 86–92. [CrossRef]

10. Baba, A.A.; Balogun, A.F.; Olaoluwa, D.T.; Bale, R.B.; Adekola, F.A.; Alabi, A.G.F. Leaching kinetics of a Nigerian complex covellite ore by the ammonia-ammonium sulfate solution. *Korean J. Chem. Eng.* **2017**, *34*, 1133–1140. [CrossRef]

11. Pradhan, N.; Nathsarma, K.C.; Rao, K.S.; Sukla, L.B.; Mishra, B.K. Heap bioleaching of chalcopyrite: A review. *Miner. Eng.* **2008**, *21*, 355–365. [CrossRef]

12. Mindat. Copper: The mineralogy of Copper. Available online: https://www.mindat.org/element/Copper (accessed on 8 July 2019).

13. Miki, H.; Nicol, M.; Velásquez-Yévenes, L. The kinetics of dissolution of synthetic covellite, chalcocite and digenite in dilute chloride solutions at ambient temperatures. *Hydrometallurgy* **2011**, *105*, 321–327. [CrossRef]

14. Leahy, M.J.; Davidson, M.R.; Schwarz, M.P. A model for heap bioleaching of chalcocite with heat balance: Mesophiles and moderate thermophiles. *Hydrometallurgy* **2007**, *85*, 24–41. [CrossRef]

15. Lee, J.; Acar, S.; Doerr, D.L.; Brierley, J.A. Comparative bioleaching and mineralogy of composited sulfide ores containing enargite, covellite and chalcocite by mesophilic and thermophilic microorganisms. *Hydrometallurgy* **2011**, *105*, 213–221. [CrossRef]

16. Palencia, I.; Romero, R.; Mazuelos, A.; Carranza, F. Treatment of secondary copper sulphides (chalcocite and covellite) by the BRISA process. *Hydrometallurgy* **2002**, *66*, 85–93. [CrossRef]

17. Xingyu, L.; Biao, W.; Bowei, C.; Jiankang, W.; Renman, R.; Guocheng, Y.; Dianzuo, W. Bioleaching of chalcocite started at different pH: Response of the microbial community to environmental stress and leaching kinetics. *Hydrometallurgy* **2010**, *103*, 1–6. [CrossRef]

18. Ruan, R.; Zhou, E.; Liu, X.; Wu, B.; Zhou, G.; Wen, J. Comparison on the leaching kinetics of chalcocite and pyrite with or without bacteria. *Rare Met.* **2010**, *29*, 552–556. [CrossRef]

19. Niu, X.; Ruan, R.; Tan, Q.; Jia, Y.; Sun, H. Study on the second stage of chalcocite leaching in column with redox potential control and its implications. *Hydrometallurgy* **2015**, *155*, 141–152. [CrossRef]

20. Cheng, C.Y.; Lawson, F. The kinetics of leaching chalcocite in acidic oxygenated sulphate-chloride solutions. *Hydrometallurgy* **1991**, *27*, 249–268. [CrossRef]

21. Herreros, O.; Quiroz, R.; Viñals, J. Dissolution kinetics of copper, white metal and natural chalcocite in Cl2/Cl⁻ media. *Hydrometallurgy* **1999**, *51*, 345–357. [CrossRef]

22. Herreros, O.; Viñals, J. Leaching of sulfide copper ore in a NaCl-H2SO4-O2 media with acid pre-treatment. *Hydrometallurgy* **2007**, *89*, 260–268. [CrossRef]

23. Senanayake, G. Chloride assisted leaching of chalcocite by oxygenated sulphuric acid via Cu(II)-OH-Cl. *Miner. Eng.* **2007**, *20*, 1075–1088. [CrossRef]

24. Muszer, A.; Wódka, J.; Chmielewski, T.; Matuska, S. Covellinisation of copper sulphide minerals under pressure leaching conditions. *Hydrometallurgy* **2013**, *137*, 1–7. [CrossRef]

25. Ruiz, M.C.; Abarzúa, E.; Padilla, R. Oxygen pressure leaching of white metal. *Hydrometallurgy* **2007**, *86*, 131–139. [CrossRef]

26. Petersen, J.; Dixon, D. Principles, mechanisms and dynamics of chalcocite heap bioleaching. In *Microbial Processing of Metal Sulfides*; Springer: Dordrecht, The Netherlands, 2007; pp. 193–218.

27. Ruiz, M.C.; Honores, S.; Padilla, R. Leaching kinetics of digenite concentrate in oxygenated chloride media at ambient pressure. *Metall. Mater. Trans. B Process Metall. Mater. Process. Sci.* **1998**, *29*, 961–969. [CrossRef]

28. Senanayake, G. A review of chloride assisted copper sulfide leaching by oxygenated sulfuric acid and mechanistic considerations. *Hydrometallurgy* **2009**, *98*, 21–32. [CrossRef]

29. Tundisi, J.G. Water resources in the future: problems and solutions. *Estud. Avançados* **2008**, *22*, 7–16. [CrossRef]

30. Cisternas, L.A.; Gálvez, E.D. The use of seawater in mining. *Miner. Process. Extr. Metall. Rev.* **2018**, *39*, 18–33. [CrossRef]

31. MCH. Agua en la Minería. Agua en la Minería. 2018. Available online: https://www.mch.cl/columnas/agua-la-mineria/# (accessed on 3 June 2019).

32. Aguirre, C.L.; Toro, N.; Carvajal, N.; Watling, H.; Aguirre, C. Leaching of chalcopyrite (CuFeS2) with an imidazolium-based ionic liquid in the presence of chloride. *Miner. Eng.* **2016**, *99*, 60–66. [CrossRef]

33. Bezerra, M.A.; Santelli, R.E.; Oliveira, E.P.; Villar, L.S.; Escaleira, L.A. Response surface methodology (RSM) as a tool for optimization in analytical chemistry. *Talanta* **2008**, *76*, 965–977. [CrossRef]

34. Dean, A.; Voss, D.; Draguljic, D. Response Surface Methodology. In *Design and Analysis of Experiments*; Springer Texts in Statistics: Cham, Switzerland, 2017; pp. 565–614.

35. Toro, N.; Herrera, N.; Castillo, J.; Torres, C.; Sepúlveda, R. Initial Investigation into the Leaching of Manganese from Nodules at Room Temperature with the Use of Sulfuric Acid and the Addition of Foundry Slag—Part I. *Minerals* **2018**, *8*, 565. [CrossRef]

36. Montgomery, D.C. Cap. 3, 6, 7 and 10. In *Design and Analysis of Experiments*, 8th ed.; Wiley: New York, NY, USA, 2012.

37. Nicol, M.; Basson, P. The anodic behaviour of covellite in chloride solutions. *Hydrometallurgy* **2017**, *172*, 60–68. [CrossRef]

38. Velásquez-Yévenes, L.; Nicol, M.; Miki, H. The dissolution of chalcopyrite in chloride solutions: Part 1. The effect of solution potential. *Hydrometallurgy* **2010**, *103*, 108–113. [CrossRef]

39. Cheng, C.Y.; Lawson, F. The kinetics of leaching covellite in acidic oxygenated sulphate-chloride solutions. *Hydrometallurgy* **1991**, *27*, 269–284. [CrossRef]

40. Dutrizac, J.E. The leaching of sulphide minerals in chloride media. *Hydrometallurgy* **1992**, *29*, 1–45. [CrossRef]

5. Development of an Analytical Model for the Extraction of Manganese from Marine Nodules

Development of an Analytical Model for the Extraction of Manganese from Marine Nodules

Manuel Saldaña [1],*[ID]**, Norman Toro** [2,3],*, **Jonathan Castillo** [4][ID]**, Pía Hernández** [5][ID]**,
Emilio Trigueros** [3] **and Alessandro Navarra** [6]

[1] Departamento de Ingeniería Industrial, Universidad Católica del Norte, Av. Angamos 0610,
   Antofagasta 1270709, Chile
[2] Departamento de Ingeniería en Metalurgia y Minas, Universidad Católica del Norte, Av. Angamos 0610,
   Antofagasta 1270709, Chile
[3] Departamento de Ingeniería Minera y Civil, Universidad Politécnica de Cartagena, Paseo Alfonso Xlll N°52,
   Cartagena 30203, Spain
[4] Departamento de Ingeniería en Metalurgia, Universidad de Atacama, Copiapó 1531772, Chile
[5] Departamento de Ingeniería Química y Procesos de Minerales, Universidad de Antofagasta,
   Av. Angamos 601, Antofagasta 1270300, Chile
[6] Department of Mining and Materials Engineering, McGill University, 3610 University Street,
   Montreal, QC H3A 0C5, Canada
*   Correspondence: manuel.saldana@ucn.cl (M.S.); ntoro@ucn.cl (N.T.); Tel.: +56-552651021 (M.S. & N.T.)

check for updates

Abstract: Multivariable analytical models provide a descriptive (albeit approximate) mathematical relationship between a set of independent variables and one or more dependent variables. The current work develops an analytical model that extends a design of experiments for the leaching of manganese from marine nodules, using sulfuric acid (H_2SO_4) in the presence of iron-containing tailings, which are both by-products of conventional copper extraction. The experiments are configured to address the effect of time, particle size, acid concentration, Fe_2O_3/MnO_2 ratio, stirring speed and temperature, under typical industrial conditions. The recovery of manganese has been modeled using a first order differential equation that accurately fits experimental results, noting that Fe_2O_3/MnO_2 and temperature are the most critical independent variables, while the particle size is the least influential (under typical conditions). This study obtains representative fitting parameters, that can be used to explore the incorporation of Mn recovery from marine nodules, as part of the extended value chain of copper sulfide processing.

Keywords: Manganese extraction; marine nodules; acid leaching; design of experiments; ordinary differential equations; mathematical modelling
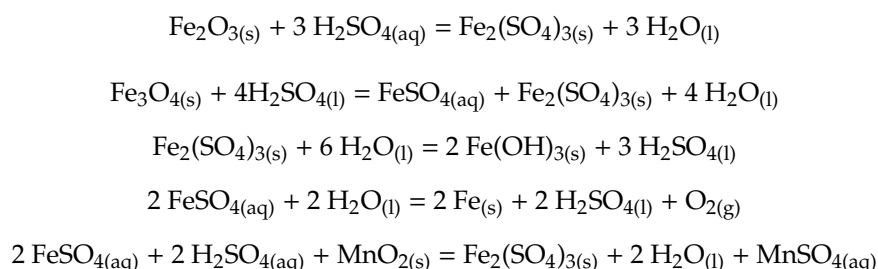
1. Introduction

Deposits of ferromanganese (Fe–Mn) are present in all of the world's oceans, on marine ridges and plateaus, where currents have released sediments for ages [1]. They originate from the accumulation of iron and manganese oxides, deposited over volcanic and sedimentary rocks that act as substrates [2]. These deposits were discovered for the first time in the Arctic Ocean of Siberia in 1968 [3]. They form concentric layers of oxide and intermetallic compounds scattered in the sedimentary zone of the seabed [4]. They are located in the Pacific, Atlantic and Indian Oceans, at depths of 4,500 m, reaching reserves that range between 1 and 3 billion tons [5].

There is generally a shortage of high-grade sources of manganese on the planet's surface [4,6], which has driven the search for alternatives. The marine nodules represent an alternative that has

economic potential [7], having an average Mn grade of approximately 24% [8]. The nodules may be further processed so that the resulting manganese may to be incorporated into steel alloys [9].

In addition, the nodules represent large reserves of other metals, such as Cu, Ni, Co and Fe, along with potentially high concentrations of Te, Ti, Pt and rare earth elements [10].

For the dissolution of MnO_2 in acidic media, it is necessary to maintain the system in potential and pH ranges of −0.4 to 1.4 V and −2 to 0.1, respectively [9]. This indicates that the use of a reducing agent is necessary to extract Mn from marine nodules [11]. Due to its low cost, abundance and good results in previous studies [4,12–17], Fe is an attractive additive for the reductive leaching of manganese nodules. Toro et al. [4] performed leaching tests of marine nodules at the laboratory level by adding smelting slags with high Fe_2O_3 contents, where it was discovered that Fe_2O_3, when reacting with H_2SO_4, forms $FeSO_4$, which is a good reducing agent of MnO_2, achieving extractions of 68% of the manganese in 5 min. In addition, in the same study previously mentioned, it was concluded that an MnO_2/Fe_2O_3 ratio of 1/2 is suitable for dissolving MnO_2 in an acidic medium. Later, Toro et al. [16] conducted tests using the Fe_2O_3 present in tailings, obtaining even better results than with the slag, as the tailings were observed to be even more reactive. When exposed to H_2SO_4, Fe_2O_3 generates ferrous sulfate ($FeSO_4$), that acts as a reducing agent for MnO_2, as described by the following reactions:

$$Fe_2O_{3(s)} + 3\ H_2SO_{4(aq)} = Fe_2(SO_4)_{3(s)} + 3\ H_2O_{(l)}$$

$$Fe_3O_{4(s)} + 4H_2SO_{4(l)} = FeSO_{4(aq)} + Fe_2(SO_4)_{3(s)} + 4\ H_2O_{(l)}$$

$$Fe_2(SO_4)_{3(s)} + 6\ H_2O_{(l)} = 2\ Fe(OH)_{3(s)} + 3\ H_2SO_{4(l)}$$

$$2\ FeSO_{4(aq)} + 2\ H_2O_{(l)} = 2\ Fe_{(s)} + 2\ H_2SO_{4(l)} + O_{2(g)}$$

$$2\ FeSO_{4(aq)} + 2\ H_2SO_{4(aq)} + MnO_{2(s)} = Fe_2(SO_4)_{3(s)} + 2\ H_2O_{(l)} + MnSO_{4(aq)}$$

The leaching process has been modeled by many authors. However, the validation, verification and implementation of these models are difficult, since there is uncertainty about the operating conditions and parameters of the leaching model [18]. Mellado et al. [19] developed analytical models that describe leaching, and are based upon the Bernoulli Equation, using constitutive equations for different levels, particles and heaps, over different scales of operation. Further work by Mellado et al. [20] extends beyond heap leaching. These more recent models are based on first-order ordinary differential equations in time, incorporating constitutive relationships derived from a combination of ordinary and partial differential equations and other relations, in combination with empirical observations. The resulting models are nonetheless simple (elegant), and are thus especially well-suited for the analysis, design, control and optimization of leaching processes [21]. Another way to describe the mechanisms that govern the leaching process was developed by Yaghobi et al. [22] through non-linear differential equations. Alternatively, Hernández et al. used a non-linear mixed-integer programming approach [23].

Other leaching studies have used the multilevel factorial design (MFD) of experiments, generating a predictive quadratic exponential regression model [24]. Liu et al. developed a leaching experiment in the laboratory, and presented an analytical model of the concentration of the leaching solution [25] using a neural network; they established a prediction model of the concentration of the leaching solution, whose maximum error was less than 2%. Other works studied the recovery of nickel and the dissolution of iron using the response surface methodology [26] to find the optimal leaching conditions for nickel laterite ores [27]. In similar work, Botane et al. [28] used linear regression to generate analytical models of continuous bioleaching in stirred tank reactors. Simulation experiments of the leaching process were carried out by Mellado et al. [29], based on analytical models and Monte Carlo simulation, concluding that there is a significant influence of the uncertainty in the input variables.

The analytical models have the advantage of being tractable, featuring algebraic parameters that can be readily fit to operational data, and extrapolated to apply them to similar operational situations. These mathematical models can be applied with enough reliability in order to technically

and economically evaluate initial projects of small and medium-scale mining, where economic resources are scarce, and mineralogical knowledge is limited.

Only a few studies have tested the reduction of manganese nodules within a sulfuric acid medium, in the presence of iron-containing tailings or slag [4,16,17]. Toro et al. [16] related Mn recovery to the MnO_2/Fe_2O_3 ratio and the sulfuric acid concentration, but only under time-independent (static) conditions. This approach involved a three-level factorial design, ignoring the potential impact of particle size distribution and agitation velocity, which are likely to have a dynamic effect upon Mn recovery. Interestingly, iron-containing tailings have been observed to be more reactive than smelter slags within the context of leaching [30]. Moreover, the previous work of Toro et al. [4,16,17] considered neither temperature, nor its interactions with other critical variables that control the effect of iron-containing reducing agents on the leaching of Mn from MnO_2 [12–15].

Finally, the objective of this work is to demonstrate the development of an analytical model based on a first order differential equation, which represents the extraction of manganese from marine nodules, under the set of parameters sampled, together with a factorial design of experiments and a multiple regression model. This approach is indeed capable of representing complex systems through relatively simple analytical models.

2. Materials and Methods

2.1. Manganese Nodule Samples

The marine nodules used in this work were the same as those previously used in Toro et al. [16]. The sample was analyzed by means of atomic emission spectrometry by induction-coupled plasma (ICP-AES), developed in the applied geochemistry laboratory of the Department of Geological Sciences of the Universidad Católica del Norte (Chile). They were composed of 15.96% Mn and 0.45% Fe, where the Mn presented in the nodules has been found to be 29.85% MnO_2.

2.2. Tailings Samples

The tailings used for the present investigation were the same as those used in Toro et al. [16]. The methods used to determine its chemical and mineralogical composition are the same as those used with the manganese nodule. Table 1 shows the chemical species determined by QEMSCAN (Quantitative Evaluation of Minerals by SCANning). There were several phases that contained iron (mainly magnetite (58.52%) and hematite (4.47%)), while the content of Fe was estimated at 41.90%.

2.3. Reagents and Leaching Parameters

The sulfuric acid used for the leaching tests was obtained from Sigma-Aldrich Chemie, GmbH (Schnelldorf, Germany), with 95–97% purity, and a density of 1.84 kg/L. The leaching tests were carried out in a 50 mL glass reactor with a 0.01 solid/liquid ratio. A total of 200 mg of Mn nodules were maintained in suspension with the use of a 5-position magnetic stirrer (IKA ROS, CEP 13087-534, Campinas, Brazil). The parameters studied were time, particle size, acid concentration, F_2O_3/MnO_2 ratio, stirring speed and temperature.

2.4. Experimental Design

Design of experiments (DOE) can be used to investigate the simultaneous effects of input variables (factors) on an output variable (response). 729 experimental tests were carried out, studying the effects of time, particle size, sulfuric acid (H_2SO_4) concentration, Fe_2O_3/MnO_2 ratio, agitation speed, and temperature on Mn recovery. The operational parameters considered in the factorial design of six factors and three levels by factor are presented in the Table 2.

Table 1. Mineralogical composition of tailings, as determined by QEMSCAN.

Mineral	Amount% (*w/w*)
Chalcopyrite/Bornite $CuFeS_2/Cu_5FeS_4$	0.47
Tennantite/Tetrahedrite ($Cu_{12}As_4S_{13}/Cu_{12}Sb_4S_{13}$)	0.03
Other Cu Minerals	0.63
Cu–Fe Hydroxides	0.94
Pyrite (FeS_2)	0.12
Magnetite (Fe_3O_4)	58.52
Specular Hematite (Fe_2O_3)	0.89
Hematite (Fe_2O_3)	4.47
Ilmenite/Titanite/Rutile ($FeTiO_3/CaTiSiO_3/TiO_2$)	0.04
Siderite ($FeCO_3$)	0.22
Chlorite/Biotite ($Mg_3Si_4O_{10}(OH)_2(Mg)_3(OH)_6/K(Mg)_3AlSi_3O_{10}(OH)_2$)	3.13
Other Phyllosilicates	11.61
Fayalite (Fe_2SiO_4)	4.59
Dicalcium Silicate (Ca_2SiO_4	8.30
Kirschsteinite ($CaFeSiO_4$)	3.40
Forsterita (Mg_2SiO_4)	2.30
Baritine ($BaSO_4$)	0.08
Zinc Oxide (ZnO)	0.02
Lead Oxide (PbO)	0.01
Sulfate (SO_4)	0.20
Others	0.03
Total	100.00

Table 2. Experimental values for operational parameters.

Parameter/Value	Low	Medium	High
Time (min)	5	10	20
Particle Size (µm)	−150 + 106	−75 + 53	−47 + 38
Sulfuric Acid (H_2SO_4)	0.1	0.3	0.5
Fe_2O_3/MnO_2 ratio	1/2	1/1	2/1
Stirring Speed (rpm)	600	700	800
Temperature (°C)	25	35	50

The general form of the experimental model is described by:

$$Y = F(X)\big|X : \{x_1, x_2, x_3, x_4, x_5, x_6\}$$

in which x_1 corresponds to time, x_2 to the size of the particle, x_3 to the concentration of sulfuric acid, x_4 to the ratio Fe_2O_3/MnO_2, x_5 to the speed of agitation and x_6 to the temperature.

2.5. Adjustment of an Analytical Model

The following is the analytical model for leaching [31,32], where it is considered that leaching behavior could generally be modeled using a system of first order equations as shown in Equation (1):

$$\frac{\partial y}{\partial \tau} = -k_\tau y^{n_\tau} \tag{1}$$

In which y is a dynamic quantity, such as concentration or recovery (R_t), k_τ is the kinetic constant and n_τ is the order of the reaction. The subscript τ represents a time scale that depends on the phenomenon to be modeled. To solve Equation (1), an initial condition is required, introducing a delay. The general solution for this problem for $n_\tau = 1$ (see Mellado et al. [19], for example), is given by:

$$R_\tau = R_\tau^\infty \left(1 - e^{-k_\tau(\tau - \omega)}\right) \tag{2}$$

R_τ^∞ is the maximum expected recovery in operational conditions, and ω is the delay of the reaction. Dixon and Hendrix [31,33] considered that the leaching phenomenon occurs at different scales (mainly related to characteristics such as heap height) and time, and that different phenomena participate in the leaching process. However, the current study assumes only a single time scale, with the understanding that additional time scales could be developed as a result of future experiments. Modifying the equation to fit a model to the experimental design, it is possible to explain the recovery of manganese from marine nodules according to the equation:

$$R(X) = R^\infty\left(1 - e^{-g(X)}\right) \tag{3}$$

For simplicity, $R^\infty = 100\%$ has been taken to be the maximum expected recovery of ore under the experimental conditions (laboratory conditions), and $g(X)$ is a polynomial equation, which is explained by the independent variables' time, particle size, sulfuric acid and potentially other variables, such as temperature and the Fe_2O_3/MnO_2 ratio. The analytical model presented in Equation (3) can be expressed as:

$$g(X) = ln\left|\frac{R^\infty}{R^\infty - R(X)}\right| \tag{4}$$

To ensure the fulfillment of an initial condition for the development of the first-order differential equation, the exponent must be directly proportional to the difference between time and delay ω, which is, $g(X) \propto (t - \omega)$. Adjusting a multiple linear regression model for the function presented in terms of y, and considering the proportionality of $g(y)$, the recovery of Mn can be modeled by the equation:

$$g(y(X)) = k_\tau \cdot y(X) \cdot (t - \omega) \tag{5}$$

in which,

$$y(X) = \alpha + \sum_{i=1}^{n} \beta_i x_i + \sum_{i=1}^{n}\sum_{j=1}^{n} \beta_{ij} x_{ij} \tag{6}$$

The substituting Equation (6) into Equation (3) gives:

$$R_\tau = R_\tau^\infty\left(1 - e^{-k_\tau\left(\sum\limits_{i=1}^{n}\beta_i x_i + \sum\limits_{i=1}^{n}\sum\limits_{j=1}^{n}\beta_{ij} x_{ij}\right)(\tau-\omega)}\right) \tag{7}$$

Considering that H_2SO_4 concentration μ and stirring speed v are proportional to Mn recovery, and that the square of particle size r is inversely linear to Mn recovery [32,34], the following model is proposed:

$$R_\tau = R_\tau^\infty\left(1 - e^{-\frac{\lambda v \rho \mu}{r^2+\beta}\left(\sum\limits_{i=1}^{n}\beta_i x_i + \sum\limits_{i=1}^{n}\sum\limits_{j=1}^{n}\beta_{ij} x_{ij}\right)(\tau-\omega)}\right) \tag{8}$$

in which λ and β are mathematical fitting parameters.

The goodness of fit statistics used to study the fitted model are: The mean absolute deviation (MAD, Equation (9)), a statistic that measures the dispersion of forecast error; the mean square error (MSE, Equation (10)), measuring of error dispersion, which penalizes the periods where the error is larger than the average value; and the absolute average percentage error (MAPE, Equation (11)), a statistic that gives the deviation in percentage terms, calculating the averages of the absolute values between the real value and fitted (forecast) values [35].

$$MAD = \frac{\sum|Real - Forecast|}{n} \tag{9}$$

$$MSE = \frac{\sum(Real - Forecast)^2}{n} \tag{10}$$

$$\text{MAPE} = \frac{1}{n} \sum \frac{|\text{Real} - \text{Forecast}|}{|\text{Real}|} \tag{11}$$

R software environment (Version 3.6.0) [36] was used to develop the experimental design transformations presented in Equations (4) and (5), while the version 18 of Minitab software [37] was used to adjust a multiple linear regression of the independent variables (excluding time) to the mathematical model presented in Equation (6).

3. Results and Discussion

3.1. Multilinear Regression of Experimental Data

The analysis of this experimental data shows that only three factors have a significant effect upon the response variable (Figure 1). The factor with the greatest impact is the Fe_2O_3/MnO_2 ratio.
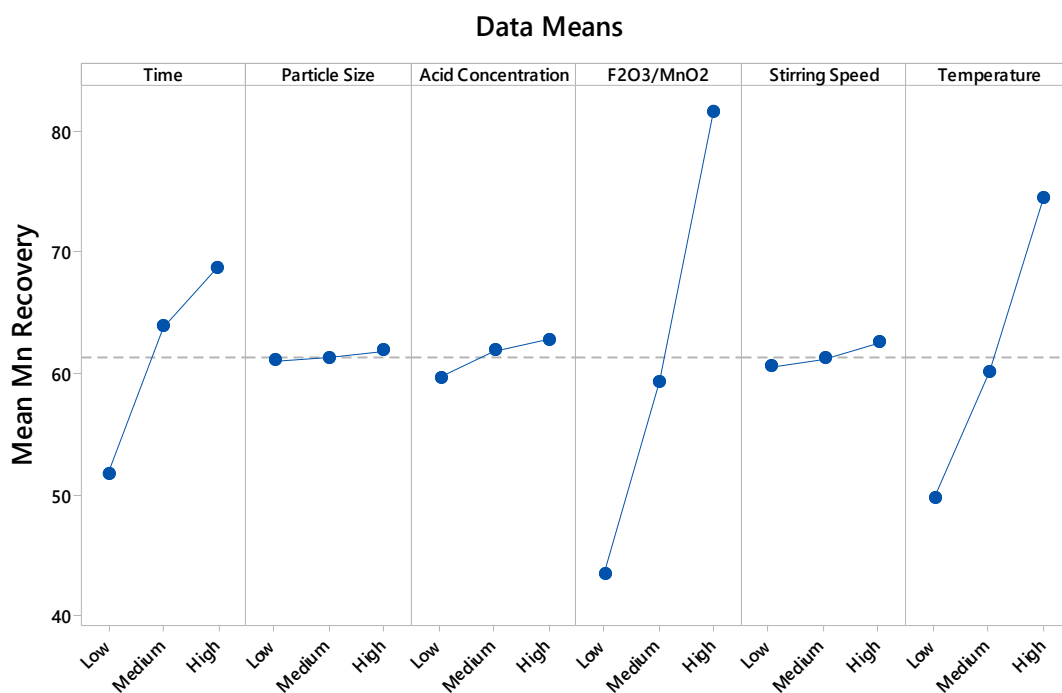
Figure 1. Graph of the main effects for manganese extraction (Figure created with Minitab 18).

Considering only the static variables (i.e., excluding the time x_1), to the following quadratic regression considers only x_4 and x_6, which are the Fe_2O_3/MnO_2 ratio and the temperature, respectively. This, response variable y is hence approximated by:

$$y = 0.2310 - 0.1680\,x_4 - 0.0094\,x_6 + 0.0370\,x_4{}^2 + 0.0001\,x_6{}^2 + 0.0050\,x_4 x_6 \tag{12}$$

A subsequent Analysis of Variance (ANOVA) analysis indicates that the regression is adequate to represent the extraction of Mn under the range of parameters sampled, including an R^2 value of 85.93% (Figure 2); this implies that 85.93% of the total variation is represented by Equation (12). The ANOVA analysis further confirms the significance of the model, as the computed F score greatly exceeds the 95% level, 539.87 > 1.9512. Equivalently, the *p*-value (Figure 3) of the model represented by the equation also indicates that the model is statistically significant.
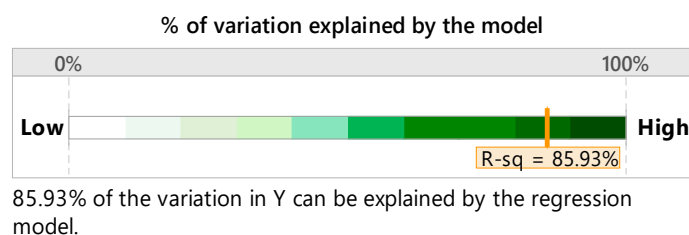
% of variation explained by the model

85.93% of the variation in Y can be explained by the regression model.

Figure 2. R^2 Statistic (Figure created with Minitab 18).

Is there a relationship between Y and the X variables?

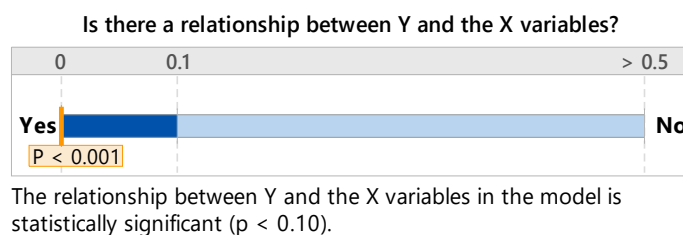The relationship between Y and the X variables in the model is statistically significant (p < 0.10).

Figure 3. Statistic p (Figure created with Minitab 18).

The value of the predictive R^2 is 85.35%, indicating that the model has a good capacity for predicting responses to new observations. The small difference between the value of R^2 and the predictive R^2 is an indicator that the model is not over fitted. Moreover, the residuals fall relatively close to the adjusted normal distribution line, and it is not possible to reject the normality assumption with $\alpha = 0.05$. Equation (12) will be further developed in the following section. Figure 4 describes the full quadratic behavior, in which all three critical variables are maintained: Time, MnO_2/Fe_3O_4 and temperature. As expected, the manganese recovery increases with the passage of time. Figure 4a,b show that Fe_2O_3/MnO_2 and temperature have a qualitatively similar effect over time, although the former is more pronounced. Indeed, Figure 4c confirms the scalable equivalence between Fe_2O_3/MnO_2 and temperature, showing recovery as an approximately linear function, increasing in both temperature and Fe_2O_3/MnO_2. Nonetheless, the full dynamic behavior is not well-represented by such a function, as it does not capture the asymptotic tendency of reaction kinetics [30,31].

3.2. Fitting of the Exponential Function

Substituting Equation (12) into Equation (5), the following equation represents the exponent of Equation (3):

$$g(X) = k_\tau \Big(0.2310 - 0.1680\, x_4 - 0.0094\, x_6 + 0.0370\, x_4{}^2 + 0.0001\, x_6{}^2 + 0.0050\, x_4 x_6 \Big)(t) \tag{13}$$

Thus, the recovery is given by:

$$R_\tau = R_\tau^\infty \left(1 - e^{-k_\tau \frac{v\rho\mu}{r^2+\beta}(0.2310-\, 0.1680\, x_4-\, 0.0094\, x_6+\, 0.0370\, x_4^2+\, 0.0001\, x_6^2+\, 0.0050\, x_4 x_6)(t-\omega)} \right) \tag{14}$$

In which r, v and μ are taken to be 64 μm, 600 rpm and 0.5 M, respectively. The fitting of parameters results in the following expression, which is supported by the goodness of fit statistics of Table 3.

$$R_t(\%) = 100 \left(1 - e^{-1.3376(0.2310-\, 0.1680\, x_4-\, 0.0094\, x_6+\, 0.0370\, x_4^2+\, 0.0001\, x_6^2+\, 0.0050\, x_4 x_6)t} \right) \tag{15}$$
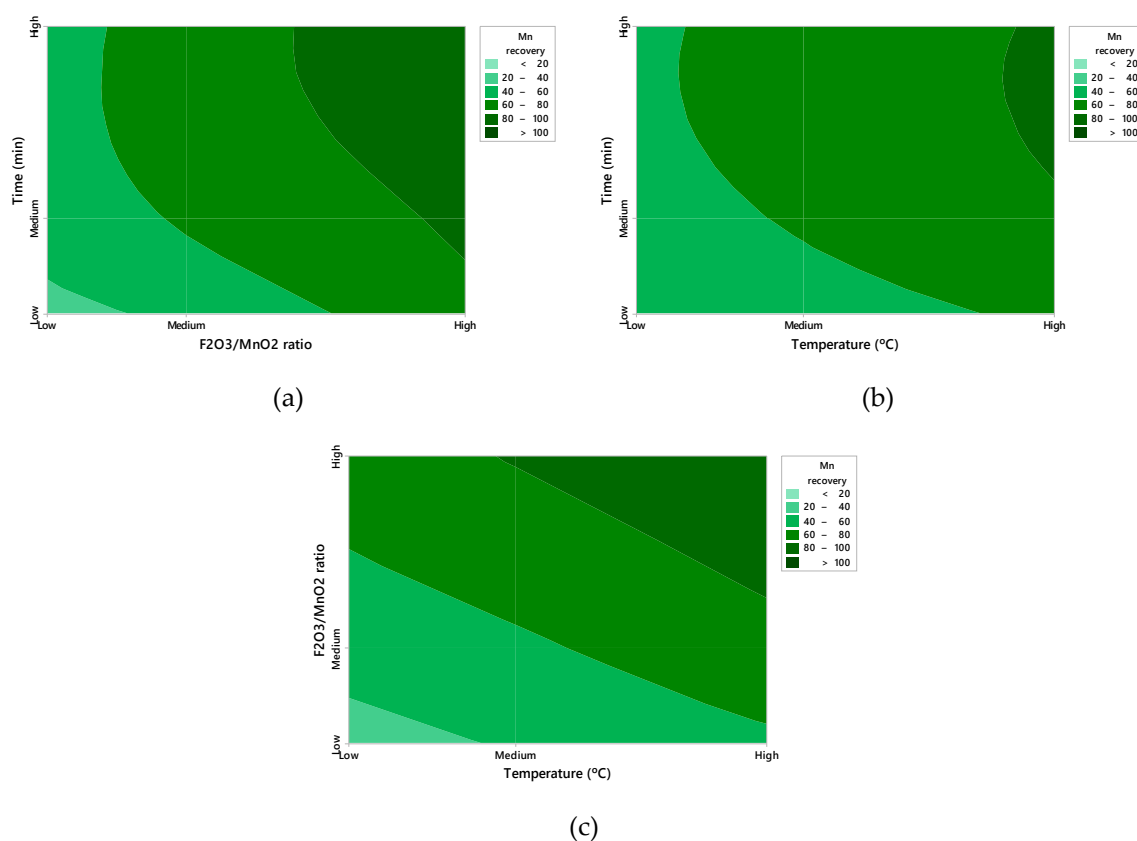
(a)

(b)

(c)

Figure 4. Contour plot of the independent variables Fe_2O_3/MnO_2 ratio, Time (**a**); Temperature, Time (**b**); and Temperature, Fe_2O_3/MnO_2 ratio (**c**) in Mn recovery (%) (Figures created with Minitab 18).

Table 3. Statistics of analytical model of the leaching of marine nodules.

Model/Statistic	MAD	MSE	MAPE
$R(t)$	6.19×10^{-5}	3.57×10^{-7}	3.88×10^{-4}

On the other hand, Figure 5 shows that the assumption of residue normality is reached, because the *p*-value of the test is greater than the level of significance ($p > 0.05$), indicating that the mathematical model is relatively accurate in representing the experimental design, although some points away from the line imply a distribution with outliers.

Following the example of Saldaña et al. [38], Equation (15) can be incorporated into a simulation framework that can quantify benefits, potentially leading to pilot tests and the implementation of nodule processing within copper producing regions [16,17]. Furthermore, there are several mines in Chile that have significant reserves of so-called black copper minerals, including Spence Mine, Mina Sur, Lomas Bayas Mine and Centinela Mine [39]. These black copper minerals are usually excluded from extraction processes, and may be stockpiled for long periods without being treated [40]. These minerals exhibit a semi-crystalline or amorphous structure that is similar to that of manganese nodules; indeed, the extraction of Cu from these black minerals by conventional hydrometallurgical processes is affected by this structure [41], and is therefore comparable to the extraction of Mn from marine nodules. The development of novel methods that may be applicable to both black copper minerals and manganese nodules is thus especially relevant for the Chilean context. Experiment-based parameterization of analytical models is a necessary step to developing alternative leaching methods for potential feeds that are not currently being treated.
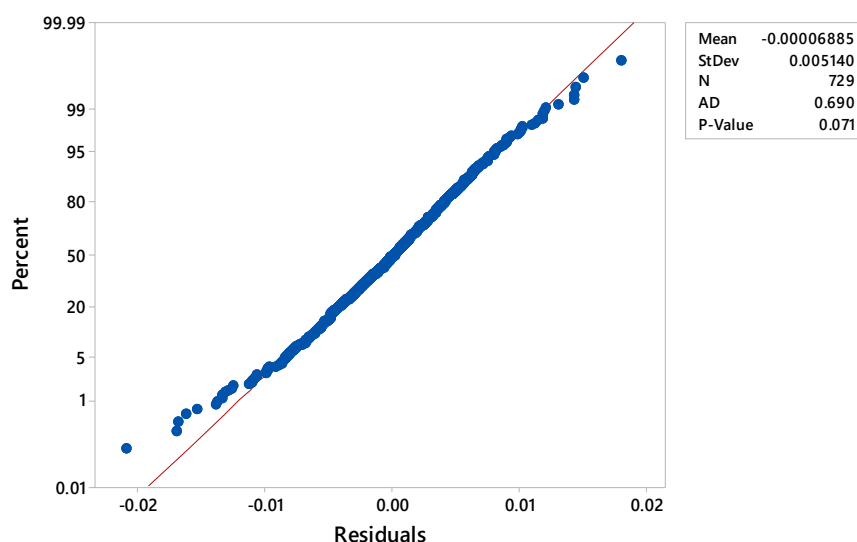
Figure 5. Probability plot of residuals values (Figure created with Minitab 18).

4. Conclusions

In the present investigation, the fitting of an analytical model for the extraction of manganese from marine nodules results in an exponential function, which considers the most critical static variables: MnO_2/Fe_2O_3 ratio and temperature. This work demonstrates the use of laboratory-level testing for the extraction of manganese from marine nodules in an acid medium at different temperatures, and with the use of iron-containing tailings, as a potential step toward industrialization of the process. This source of iron is indeed an effective reducing agent. Future experimental work will be carried out to characterize the constants in Equation (15) better through more batch tests, and to represent the effects of different time scales [30,32]. From the modelling perspective, future work will be to simulate an industrial implementation, and test potential operational responses to feed variations and related risks [38].

On the other hand, the form of developing an analytical model can be extended to other scales of time, and can be modified according to the kinetics that describe or dominate the operation. The Dixon and Hendrix's model [31,33] was used to identify the dimensionless times, but the fit to experimental design can be applied to other models proposed within the literature, considering operational scales how pile height [18–20,29]. The generation of analytical models to represent complex processes such as mineral leaching could be used for analysis, scale-up, and in optimization tasks, given that they capture the essence of the process to be modeled, they are rapid and relatively precise, and could be used to predict interpolations and extrapolations of Mn recuperation, at least with regard to time, particle size, H_2SO_4 concentration, Fe_2O_3/MnO_2 ratio, stirring speed and temperature.

Author Contributions: M.S. and N.T. contributed in the methodology, conceptualization and modeling; J.C. and P.H. investigation and resources and E.T. and A.N. contributed with supervision and validation.

References

1. Marino, E.; González, F.J.; Somoza, L.; Lunar, R.; Ortega, L.; Vázquez, J.T.; Reyes, J.; Bellido, E. Strategic and rare elements in Cretaceous-Cenozoic cobalt-rich ferromanganese crusts from seamounts in the Canary Island Seamount Province (northeastern tropical Atlantic). *Ore Geol. Rev.* **2017**, *87*, 41–61. [CrossRef]
2. Nishi, K.; Usui, A.; Nakasato, Y.; Yasuda, H. Formation age of the dual structure and environmental change recorded in hydrogenetic ferromanganese crusts from Northwest and Central Paci fi c seamounts. *Ore Geol. Rev.* **2017**, *87*, 62–70. [CrossRef]
3. Lenoble, J.P. *Polymetallic Nodules*; International Seabed Authority: Kingston, CA, USA, 2000.
4. Toro, N.; Herrera, N.; Castillo, J.; Torres, C.; Sepúlveda, R. Initial Investigation into the Leaching of Manganese from Nodules at Room Temperature with the Use of Sulfuric Acid and the Addition of Foundry Slag—Part I. *Minerals* **2018**, *8*, 565. [CrossRef]
5. Premchand, P.; Jana, R.K. Processing of Polymetallic Sea Nodules: An Overview. In Proceedings of the Ocean Mining Symposium, Goa, India, 8–10 November 1999; p. 3.
6. Hein, J.R.; Cherkashov, G.A. Preface for Ore Geology Reviews Special Issue: Marine mineral deposits: New resources for base, precious, and critical metals. *Ore Geol. Rev.* **2017**, *100*, 1–2. [CrossRef]
7. Konstantinova, N.; Cherkashov, G.; Hein, J.R.; Mirão, J.; Dias, L.; Madureira, P.; Kuznetsov, V.; Maksimov, F. Composition and characteristics of the ferromanganese crusts from the western Arctic Ocean. *Ore Geol. Rev.* **2017**, *87*, 88–99. [CrossRef]
8. Sharma, R. Environmental Issues of Deep-Sea Mining. *Procedia Earth Planet. Sci.* **2015**, *11*, 204–211. [CrossRef]
9. Senanayake, G. Acid leaching of metals from deep-sea manganese nodules—A critical review of fundamentals and applications. *Miner. Eng.* **2011**, *24*, 1379–1396. [CrossRef]
10. Usui, A.; Nishi, K.; Sato, H.; Nakasato, Y.; Thornton, B.; Kashiwabara, T. Continuous growth of hydrogenetic ferromanganese crusts since 17 Myr ago on Takuyo-Daigo Seamount, NW Pacific, at water depths of 800–5500 m. *Ore Geol. Rev.* **2017**, *87*, 71–87. [CrossRef]
11. Randhawa, N.S.; Hait, J.; Jana, R.K. A brief overview on manganese nodules processing signifying the detail in the Indian context highlighting the international scenario. *Hydrometallurgy* **2016**, *165*, 166–181. [CrossRef]
12. Kanungo, S.B. Rate process of the reduction leaching of manganese nodules in dilute HCl in presence of pyrite. Part I. Dissolution behaviour of iron and sulphur species during leaching. *Hydrometallurgy* **1999**, *52*, 313–330. [CrossRef]
13. Kanungo, S.B. Rate process of the reduction leaching of manganese nodules in dilute HCl in presence of pyrite. *Part II: Leaching behavior of manganese Hydrometallurgy* **1999**, *52*, 331–347.
14. Zakeri, A.; Bafghi, M.S.; Shahriari, S.; Das, S.C.; Sahoo, P.K.; Rao, P.K. Dissolution kinetics of manganese dioxide ore in sulfuric acid in the presence of ferrous ion. *Hydrometallurgy* **2007**, *8*, 22–27.
15. Bafghi, M.S.; Zakeri, A.; Ghasemi, Z.; Adeli, M. Reductive dissolution of manganese ore in sulfuric acid in the presence of iron metal. *Hydrometallurgy* **2008**, *90*, 207–212. [CrossRef]
16. Toro, N.; Saldaña, M.; Castillo, J.; Higuera, F.; Acosta, R. Leaching of Manganese from Marine Nodules at Room Temperature with the Use of Sulfuric Acid and the Addition of Tailings. *Minerals* **2019**, *9*, 289. [CrossRef]
17. Toro, N.; Saldaña, M.; Gálvez, E.; Cánovas, M.; Trigueros, E.; Castillo, J.; Hernández, P.C. Optimization of Parameters for the Dissolution of Mn from Manganese Nodules with the Use of Tailings in An Acid Medium. *Minerals* **2019**, *9*, 387. [CrossRef]
18. Mellado, M.; Cisternas, L.; Lucay, F.; Gálvez, E.; Sepúlveda, F. A Posteriori Analysis of Analytical Models for Heap Leaching Using Uncertainty and Global Sensitivity Analyses. *Minerals* **2018**, *8*, 44. [CrossRef]
19. Mellado, M.E.; Cisternas, L.A.; Gálvez, E.D. An analytical model approach to heap leaching. *Hydrometallurgy* **2009**, *95*, 33–38. [CrossRef]
20. Mellado, M.E.; Casanova, M.P.; Cisternas, L.A.; Gálvez, E.D. On scalable analytical models for heap leaching. *Comput. Chem. Eng.* **2011**, *35*, 220–225. [CrossRef]
21. Mellado, M.E.; Gálvez, E.D.; Cisternas, L.A. On the optimization of flow rates on copper heap leaching operations. *Int. J. Miner. Process.* **2011**, *101*, 75–80. [CrossRef]
22. Moghaddam, M.Y.; Tonkaboni, S.Z.S.; Noaparast, M.; Ardejani, F.D. A mathematical model to simulate Heap (bio)-leaching process: An exact conceptual model, Homotopy theory and comparative insights with conventional methods. *Int. J. Model. Simul Sci. Comput.* **2017**, *8*, 1750018. [CrossRef]

23. Hernández, I.F.; Ordóñez, J.I.; Robles, P.A.; Gálvez, E.D.; Cisternas, L.A. A Methodology for Design and Operation of Heap Leaching Systems. *Miner. Process. Extr. Metall. Rev.* **2017**, *38*, 180–192. [CrossRef]

24. Fekete, V.; Deconinck, E.; Bolle, F.; van Loco, J. Modelling aluminium leaching into food from different foodware materials with multi-level factorial design of experiments. *Food Addit. Contam. Part A Chem. Anal. Control. Exp. Risk Assess.* **2012**, *29*, 1322–1333. [CrossRef] [PubMed]

25. Liu, C.; Wu, A.X.; Yin, S.H.; Chen, X. Nonlinear chaotic characteristic in leaching process and prediction of leaching cycle period. *J. Cent. South Univ.* **2016**, *23*, 2935–2940. [CrossRef]

26. Bezerra, M.A.; Santelli, R.E.; Oliveira, E.P.; Villar, L.S.; Escaleira, L.A. Response surface methodology (RSM) as a tool for optimization in analytical chemistry. *Talanta* **2008**, *76*, 965–977. [CrossRef] [PubMed]

27. Çetintaş, S.; Bingöl, D. Response surface methodology approach to leaching of nickel laterite and evaluation of different analytical techniques used for the analysis of leached solutions. *Anal. Methods* **2016**, *8*, 3075–3087. [CrossRef]

28. Botane, P.; Brochot, S.; D'Hugues, P.; Spolaore, P. Material size distribution in concurrent bio-leaching and precipitation: Experimental procedure and modelling. *Hydrometallurgy* **2013**, *133*, 7–14. [CrossRef]

29. Mellado, M.E.; Gálvez, E.D.; Cisternas, L.A. Stochastic analysis of heap leaching process via analytical models. *Miner. Eng.* **2012**, *33*, 93–98. [CrossRef]

30. Komnitsas, K.; Manousaki, K.; Zaharaki, D. Assessment of reactivity of sulphidic tailings and river sludges. *Geochem. Explor. Environ. Anal.* **2009**, *9*, 313–318. [CrossRef]

31. Dixon, D.G.; Hendrix, J.L. A general model for leaching of one or more solid reactants from porous ore particles. *Metall. Trans. B* **1993**, *24*, 157–169. [CrossRef]

32. Schlesinger, M.; King, M.; Sole, K.; Davenport, W. *Extractive Metallurgy of Copper*, 5th ed.; Elsevier: Amsterdam, The Netherlands, 2011; ISBN 978-0-08-096789-9.

33. Dixon, D.G.; Hendrix, J.L. A mathematical model for heap leaching of one or more solid reactants from porous ore pellets. *Metall. Trans. B* **1993**, *24*, 1087–1102. [CrossRef]

34. Free, M. *Hidrometallurgy: Fundamentals and Applications*; John Wiley & Sons: Hoboken, NJ, USA, 2013; ISBN 978-1-118-23077-0.

35. Devore, J. *Probability & Statistics for Engineering and the Sciences*, 8th ed.; Cengage Learning: Boston, MA, USA, 2010; ISBN 0-538-73352-7.

36. R Core Team. *R: The R Project for Statistical Computing*; R Foundation for Statistical Computing: Vienna, Austria, 2019.

37. Minitab, LLC. *Getting Started with Minitab 18*; Minitab Inc.: State College, PA, USA, 2017; p. 73.

38. Saldaña, M.; Toro, N.; Castillo, J.; Hernández, P.; Navarra, A. Optimization of the Heap Leaching Process through Changes in Modes of Operation and Discrete Event Simulation. *Minerals* **2019**, *9*, 421. [CrossRef]

39. Riquelme, R.; Tapia, M.; Campos, E.; Mpodozis, C.; Carretier, S.; González, R.; Muñoz, S.; Fernández-Mort, A.; Sanchez, C.; Marquardt, C. Supergene and exotic Cu mineralization occur during periods of landscape stability in the Centinela Mining District, Atacama Desert. *Basin Res.* **2018**, *30*, 395–425. [CrossRef]

40. Benavente, O.; Hernández, M.C.; Melo, E.; Núñez, D.; Quezada, V.; Zepeda, Y. Copper Dissolution from Black Copper Ore under Oxidizing and Reducing Conditions. *Metals* **2019**, *9*, 799. [CrossRef]

41. Helle, S.; Pincheira, M.; Jerez, O.; Kelm, U. Sequential extraction to predict the leaching potential of refractory. In Proceedings of the Mineral Processing Congress, Sozopol, Bulgaria, 12–16 June 2013; pp. 109–111.

6. Dissolution of pure chalcopyrite with manganese nodules and waste water

Publicación 4: N. Toro*, K. Pérez, M. Saldaña, R. I. Jeldres, M. Jeldres and M. Cánovas. "Dissolution of pure chalcopyrite with manganese nodules and waste water" Q1 ISI WoS. Journal of Materials Research and Technology, 2019 https://doi.org/10.1016/j.jmrt.2019.11.020

7. Statistical and kinetic study for leaching of covellite in a chloride media

Statistical and kinetic study for leaching of covellite in a chloride media

Norman Toro[a]*; Kevin Pérez[b], Williams Briceño[b]; Alessandro Navarra[c]; Manuel Cánovas[a]; Emilio Trigueros[d].

[a] Department of Metallurgical and Mining Engineering, Universidad Católica del Norte, Chile

[b] Department of industrial engineering, Universidad Católica del Norte, Chile

[c] Department of Mining and Materials Engineering, McGill University, Canada

[d] Department of Mining, Geological and Cartographic Department, Universidad Politécnica de Cartagena, Spain

Corresponding author: Norman Toro, ntoro@ucn.cl

Abstract

Covellite is a relatively rare copper sulfide with slow dissolution kinetics. The present investigation used the surface optimization methodology to evaluate the effect of three independent variables (time, chloride concentration and sulfuric acid concentration) on the rate of extracting Cu from covellite. The effects of chloride concentration and temperature over time were also studied. An ANOVA indicated that the linear variables of time and chloride concentration have the greatest influence, this being highly representative (R^2 = 0.9945). The highest copper extraction rate (71.23%) at room temperature, was obtained with a high chloride concentration (100 g/L), a low concentration of sulfuric acid (0.5 M), and a leaching period of 600 h. The dissolution is described by the model of the unreacted core, the rate of leaching of the covellite is controlled by the chemical surface reaction at temperatures between 50 and 90°C, with concentrations of 0.5 M of H_2SO_4, 100 g/L of chloride, and a leaching period of up to 6 hours, where an activation energy of 72.36 kJ/mol was obtained.

Keywords: Leaching, covellite, chloride media, kinetic study
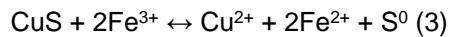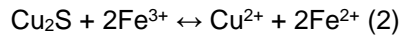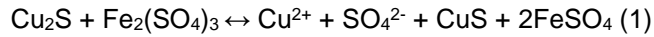
1. Introduction

While Covellite is not abundant, it is found in many copper deposits as a supergenic mineral, usually as a coating in the sulfide enrichment zone. It is associated with other minerals, mainly chalcocite, chalcopyrite, bornite and enargite, from which it is derived by alteration (Klein & Hurlbut, 1996). Covellite is of interest because of the quantity found in oxide ores, and because it is an intermediate product in converting chalcopyrite (Lundström et al., 2016) and in transforming dignite to covellite in oxygenated media (Ruiz et al., 1998; Senanayake, 2007)

Sulfurized copper ores are generally treated by flotation-smelting-refining (Schlesinger et al., 2011; Shuva et al., 2016; Turan et al., 2017). Although they have reported economic (Kelm et al., 2014) and metallurgical viability, there are environmental problems associated with the emission of sulfur dioxide and arsenic (Afif et al., 2008; Dijksira et al., 2017; Dimitrijević et al., 2009; Sánchez de la Campa et al., 2008; Serbula et al., 2017). Arsenic emissions, which have been increasing steadily in recent decades with increasing extraction of copper sulfide (Balladares et al., 2018), present a danger to human health related to higher incidence of cardiovascular and respiratory diseases and cancer (World Health Organization, 2018). This has resulted in stricter environmentally-motivated controls. Hydrometallurgical methods are generally preferred to recover copper from complex low-grade minerals because of the low cost, short construction time, operational simplicity, and good
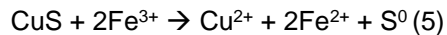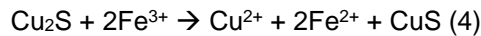
performance (Baba et al., 2017), as well as environmental benefits (González et al., 2005; Lü et al., 2018; Rabadjieva et al., 2009), in terms of yielding solid waste that is not considered hazardous.

Sulfuric acid and an oxidizing agent are required to break down sulfurized copper ores and release Cu^{2+} in solution. All copper sulfides require the presence of Fe^{3+} and O_2 as oxidizing agents for leaching to occur. Copper sulfide is oxidized by the presence of Fe^{3+}. The resulting Fe^{2+} is reoxidized to Fe^{3+} by O_2. The redox pair Fe^{2+}/Fe^{3+} act as a catalyst in these reactions. The following reactions occur with the main secondary copper mineral, chalcocite, when the temperature is high (Equation 1) and the sulfur is in the form of sulphate and not elemental sulfur, as in natural conditions (Equations 2 and 3) (Schlesinger et al., 2011):

$$Cu_2S + Fe_2(SO_4)_3 \leftrightarrow Cu^{2+} + SO_4^{2-} + CuS + 2FeSO_4 \text{ (1)}$$

$$Cu_2S + 2Fe^{3+} \leftrightarrow Cu^{2+} + 2Fe^{2+} \text{ (2)}$$

$$CuS + 2Fe^{3+} \leftrightarrow Cu^{2+} + 2Fe^{2+} + S^0 \text{ (3)}$$

Several investigations into leaching covellite have proposed hydrometallurgical approaches with different dissolution media, including ammonia (Baba et al., 2017; Reilly & Scott, 1976), nitrates (Fisher, 1994; Vračar, et al., 2003), chlorides (Cheng & Lawson, 1991; Miki et al., 2011; Nicol & Basson, 2017; Senanayake, 2007) and bioleaching with bacteria like thiobacillus ferrooxidans, acidithiobacillus ferrooxidans and acidithiobacillus thiooxidans, which can grow under anaerobic conditions where ferric ions are used as electron receptors (Donati et al., 1997; F. Monteiro et al., 1999; Falco et al., 2003; Lee et al., 2011).

The oxidative dissolution of the chalcocite occurs in two stages in sulphated or chlorinated media (Cheng & Lawson, 1991; Miki et al., 2011; Niu et al., 2015; Ruiz et al., 2007; Senanayake, 2009).

$$Cu_2S + 2Fe^{3+} \rightarrow Cu^{2+} + 2Fe^{2+} + CuS \text{ (4)}$$

$$CuS + 2Fe^{3+} \rightarrow Cu^{2+} + 2Fe^{2+} + S^0 \text{ (5)}$$

According to Niu et al. (2015), leaching from chalcocite to covellite is rapid (Equation 4) because of the low activation energy needed (4-25 kJ/mol), the reaction being controlled by the diffusion of the oxidant on the mineral surface, while the process expressed in Equation 5 is slower. Ruan et al. (2013) and Miki et al. (2011) argued this Equation 5 is slow because this reaction is chemically and/or electrochemically controlled and therefore requires activation energy of around 71.5-72 kJ/mol to transform covellite into dissolved copper. Nicol & Basson (2017) recently suggested that covellite oxidation occurs as an intermediate stage in which it is transformed into polysulfide CuS_2:

$$Cu_2S_2 \rightarrow CuS_2 + Cu^{2+} + 2e^- \text{ (6)}$$

$$CuS_2 \rightarrow Cu^{2+} + 2S^0 + 2e^- \text{ (7)}$$
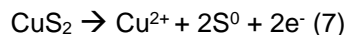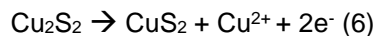
Covellite can be oxidized over a wide range of chloride concentrations or potential to the CuS_2 polysulfide, but oxidation of CuS_2 can only occur under conditions of high chloride concentrations or high potentials (Nicol & Basson, 2017).

Copper chloride-based processes are especially suitable for leaching non-ferrous minerals like chalcocite, digenite and covellite, since in these cases the leaching solutions contain low levels of dissolved iron (Ruiz et al., 1998).

In this study, two pure covellite leaching tests will be carried out in a chlorided medium in addition to oxygen. The first one will be under temperature and pressure ambient to determine the influence of the parameters to be statistically analyzed; such as sulfuric acid dosage, sodium chloride dosage

and the effect of time in copper extraction until a representative quadratic model of copper extraction is obtained based on these parameters. The second part consists of tests with the temperature to analyze its effect on the kinetics of copper dissolution, calculate the activation energy and the controlling stage of the mineral under the described conditions and according to the model of the unreacted core.

Thermodynamics

A covellite leaching is performed with the injection of O_2 at ambient pressure into a solution of H_2SO_4-NaCl. In this leaching investigation of copper sulfide, no ferric ions are added but copper-chloride complexes are added, hence, the leaching agents change. It is proposed to obtain a soluble product of $CuCl_2^-$ so the general reaction is:

$2CuS + 0{,}5O_2 + 2H^+ + 4Cl^- = 2CuCl_2^- + 2S^0 + H_2O$ (8)
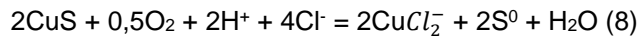
The general reaction for the dissolution of a sulfide with metal in a chlorinated environment is described by Lundstrom et al. (2016) in equation:

$MeS_x + 2CuCl^+ + 2Cl^- = Me^{2+} + 2\ CuCl_2^- + xS^0$ (9)
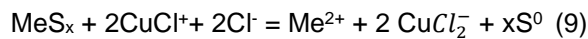
And in the case of the leaching of covellite in chlorinated environment, the following reaction is obtained:

$CuS + 2CuCl^+ + 2Cl^- = Cu^{2+} + 2CuCl_2^- + S^0$ (10)
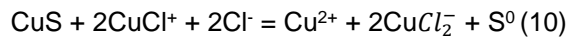
According to the information given in table 1, the difference between equation 8 and 10 is the addition of O_2 and H^+, with equation 8 above 10 being very favorable due to the diffusion of oxygen in covellite leaching.

Cu^{2+}, $CuCl^+$ and $CuCl_2^-$ are the stable species of Cu^{2+}/Cu^+ in a solution at 25 ° C, and with a chloride concentration range of between 0.02 - 2 M. According to Senanayake (2007), $CuCl^+$ is the predominant species of Cu^{2+} at a low chloride concentration (<0.5 M) (Cheng & Lawson, 1991), while $CuCl_2^-$ is the predominant Cu^+ species at 25 ° C. In contrast, $CuCl_2$ is the most stable Cu^{2+} species at high temperature (102 °C) and high concentrations of chloride.

Within the reactions that occur in the leaching of covellite with the use of NaCl, Cu^{2+} and the addition of O_2, leaching agents, such as Cu^{2+}, $CuCl^+$, $CuCl_2$ and $CuCl_3^-$, are continuously generated during leaching (Herreros & Viñals, 2007; Senanayake, 2007) where finally a soluble product of $CuCl_2^-$ (chloro complex), and a residue of elemental sulfur (S^0) will be obtained.
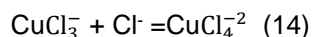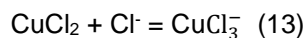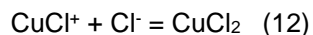
$Cu^{+2} + Cl^- = CuCl^+$ (11)

$CuCl^+ + Cl^- = CuCl_2$ (12)

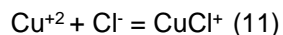$CuCl_2 + Cl^- = CuCl_3^-$ (13)
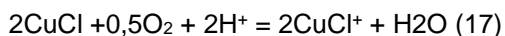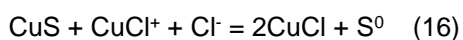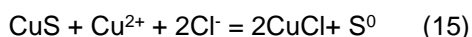
$CuCl_3^- + Cl^- = CuCl_4^{-2}$ (14)

Table 1 shows all the interesting reactions within the leaching of covellite in a chlorinated medium, analyzing the free energy of Gibbs at temperatures of 25 ° C and 90 ° C.Equilibrium constants are based on Outokumpu HSC 5,1 Software.

Table 1. Equilibrium constants for reactions at temperatures of 25°C and 90°C.

No Rx	Equilibrium constant (K)		Gibbs free energy (kJ)
	25°C	90°C	25°C
3	4,433x10^4	6.962x10^5	-26,521
8	6,253x10^14	6.942x10^11	-84,448
10	5,033x10^-7	2.276x10^-5	35,946
11	2,982	5.343	-2,708
12	2,843x10^-5	1.185x10^-3	25,947
13	6,053x10^1	1.318	-10,17
14	5x10^-3	1.207x10^-3	13,133
15	4,249x10^-3	3.206x10^-1	13,536
16	1,425x10^-3	6.002x10^-2	16.244
17	2,924x10^23	9.513x10^16	-133,93
18	3,245x10^-2	4,501x10^-2	8,497

In the reactions of the covellite solution, there is the possibility of obtaining a solid product of CuCl, although this can be reoxidized in $CuCl^+$ which is used as a leaching agent.

$CuS + Cu^{2+} + 2Cl^- = 2CuCl + S^0$ (15)

$CuS + CuCl^+ + Cl^- = 2CuCl + S^0$ (16)

$2CuCl + 0,5O_2 + 2H^+ = 2CuCl^+ + H_2O$ (17)

It is emphasized that with the addition of oxygen and H^+, this reaction is spontaneous.

The CuCl can also be reduced to $CuCl_2^-$ (18) $CuCl + Cl^- = CuCl_2^-$
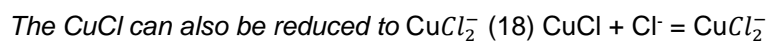
However, this reaction is not spontaneous even at a temperature of 90 ° C.

2. Experimental

2.1 Materials

The covellite sample used in this research was obtained from Michilla mine Using a porcelain mortar, the sample (apparently pure) was reduced to a size range of -150 to +106 µm, and then chemically analyzed by atomic emission spectrometry via induction-coupled plasma (ICP-AES) at the applied geochemistry laboratory of the Geological Sciences Department of the Universidad Católica del Norte. Table 2 shows the chemical composition of the samples.

Table 2. Chemical analysis of the covellite ore

Element	Cu	S	Ca	O	H
Mass (%)	56.14	31.08	3.66	8.76	0.36

The studied sample was also analyzed mineralogically. Fig. 1 shows the chemical species identified by QEMSCAN. Covellite was the most abundant mineral present (84.29%), followed by a much lower percentage of gypsum (15.71%).
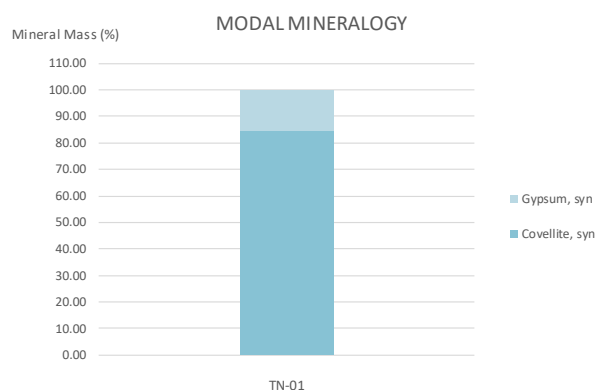

Fig. 1. Detailed modal mineralogy

2.2 Reagent and leaching test

The sulfuric acid used in the leaching tests was grade P.A, Merck brand, with a purity of 95-97%, a density of 1.84 kg/L, and a molecular weight of 98.08 g/mol.

The leaching tests were carried out in a 50-mL glass reactor with a 0.01 S/L ratio of leaching solution. A total of 200 mg of covellite ore was maintained in agitation and suspension in a 5-position magnetic stirrer (IKA ROS, CEP 13087-534, Campinas, Brazil) at a speed of 600 rpm with an oxygen addition of 6 mL/min connecting a hose to the reactor. The tests were conducted at a room temperature of 25°C, with variations in sulfuric acid and chloride concentrations and leaching time. In the temperature-controlled experimental trials, a coolant was added to the top, thereby avoiding evaporation losses. The coolant was added in combination with water, at ambient temperature (25°C), and interacts with the outgoing hot gas, causing it to condense back into liquid form. Also, the tests were performed in duplicate, measurements (or analyses) were carried on 5 mL undiluted samples using atomic absorption spectrometry with a coefficient of variation ≤ 5% and a relative error between 5 to 10%. Measurements of pH and oxidation-reduction potential (ORP) of leach solutions were made using a pH-ORP meter (HANNA HI-4222). The solution ORP was measured in a combination ORP electrode cell composed of a platinum working electrode and a saturated Ag/AgCl reference electrode.

2.3 Experimental Design

The effects of independent variables on Cu extraction rates from leaching covellite were studied using the response surface optimization method (Aguirre et al., 2016; Bezerra et al., 2008; Dean et al., 2017; Toro et al., 2018). The central composite face design (CCF) and a quadratic model were applied to the experimental design for leaching CuS.

Twenty-seven experimental tests were carried out to study the effects of time, and chloride and H_2SO_4 concentrations as independent variables. Minitab 18 software was used in the modeling and experimental design to study the linear and quadratic effects of the independent variables. The experimental data were fitted by multiple linear regression analysis to a quadratic model, considering only those factors that helped to explain the variability of the model. The empirical model contained coefficients of linear, quadratic, and two-factor interaction effects.

The general form of the experimental model is represented by (Equation 19):

$$Y = b_0 + b_1 x_1 + b_2 x_2 + b_3 x_3 + b_{12} x_1 x_2 + b_{13} x_1 x_3 + b_{23} x_2 x_3 + b_{11} x_1^2 + b_{22} x_2^2 + b_{33} x_3^2 \qquad (19)$$

Where, x_1 is time, x_2 is Chloride, x_3 is H_2SO_4 concentration, and b is the variable coefficients

Table 3 shows the ranges of the parameters used in the experimental model. The following equation (Equation 20) transformed real values (Z_i) into coded values (X_i) according to the experimental design:

$$X_i = \frac{Z_i - \dfrac{Z_{high} + Z_{low}}{2}}{\dfrac{Z_{high} - Z_{low}}{2}} \qquad (20)$$

Where Z_{high} and Z_{low} are respectively the highest and lowest levels of a variable (Montgomery, 2012).

Table 3. Experimental configuration and Cu extraction data

Exp. No.	Time (h)	Cl (g/L)	H_2SO_4 (M)	Cu extraction rate (%)
1	48	20	0.5	2.50
2	48	50	0.5	3.50
3	48	100	0.5	6.00
4	48	20	1	3.00
5	48	50	1	3.63
6	48	100	1	9.13
7	48	20	2	3.25
8	48	50	2	5.50
9	48	100	2	11.38
10	72	20	0.5	5.13
11	72	50	0.5	8.75
12	72	100	0.5	11.25
13	72	20	1	5.88
14	72	50	1	9.25
15	72	100	1	13.88
16	72	20	2	6.38
17	72	50	2	11.63
18	72	100	2	18.75
19	144	20	0.5	24.63
20	144	50	0.5	24.88
21	144	100	0.5	28.75
22	144	20	1	26.25
23	144	50	1	29.75
24	144	100	1	35.00
25	144	20	2	28.75
26	144	50	2	31.25
27	144	100	2	38.75

The statistical R^2, R^2_{adj}, p-values and Mallows's Cp indicate whether the model obtained is adequate to describe Cu extraction under a given domain. The R^2 coefficient is a measure of the goodness of fit, that is, it measures the proportion of total variability of the dependent variable with respect to its mean, which is explained by the regression model. The p-values represent statistical significance, which indicates whether there is a statistically significant association between the response variable and the term. The predicted R^2 was used to determine how well the model predicts the response for new observations. Finally, Mallows's Cp is a precise measure in the model, estimating the true parameter regression (Montgomery et al., 2012).

3. Results

3.1. Methodology

An ANOVA analysis (Table 4) showed no significant effect of the interaction {time, Cl} ($p > 0.05$) on the copper extraction rate. The effects of the curvature of chloride are not significant in explaining the variability of the model. However, the effects of the curvature of time and H_2SO_4 must also be considered ($p < 0.1$).
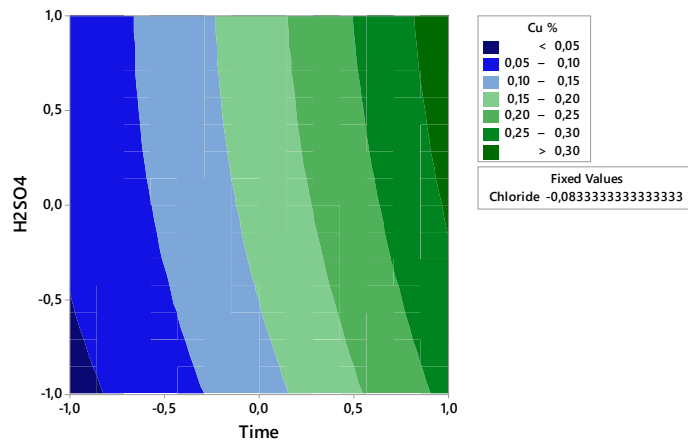
Table 4. ANOVA Cu extraction

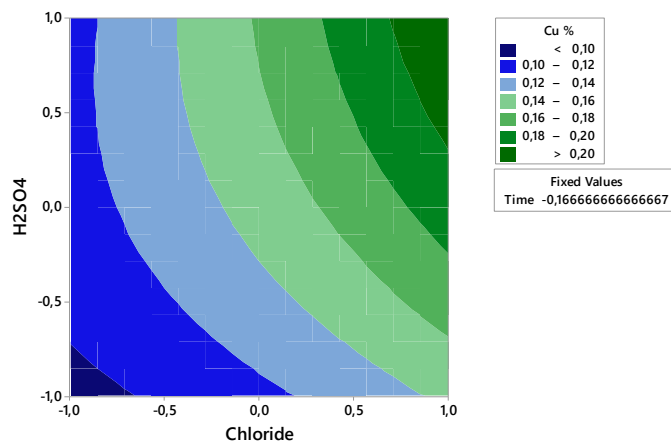| Source	F-Value	p-Value
Regression	371.42	0.000
Time	2624.36	0.000
Cl	257.04	0.000
H_2SO_4	105.5	0.000
Time*Time	9.7	0.006
Cl*Cl	0.56	0.466
H_2SO_4*H_2SO_4	3.39	0.083
Time*Cl	0.81	0.379
Time*H_2SO_4	11.22	0.004
Cl*H_2SO_4	22.6	0.000

The contour plot in Fig. 2 shows that the Cu extraction rate increases with more time, and higher concentrations of chloride and H_2SO_4.
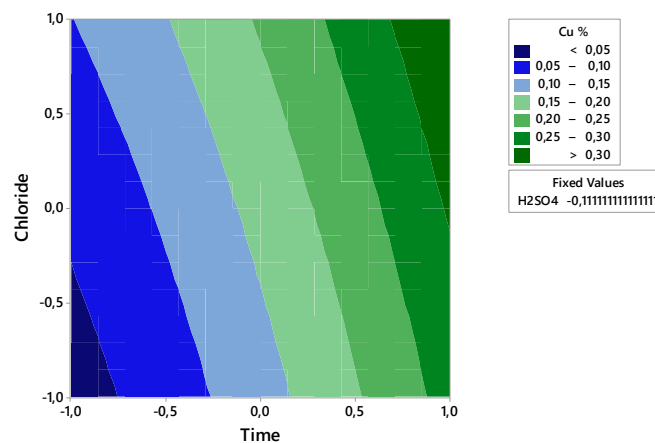
(a)

(b)

(c)

Fig. 2. Experimental contour plot of Cu extraction in response to the independent variables of time and chloride (a), time and H_2SO_4 concentration (b), and chloride concentration and H_2SO_4 concentration (c).

Fig. 3 and 4 show that the interactions of time, chloride and H_2SO_4 concentration, and of time-H_2SO_4 and Cl-H_2SO_4 affected the Cu extraction rate.
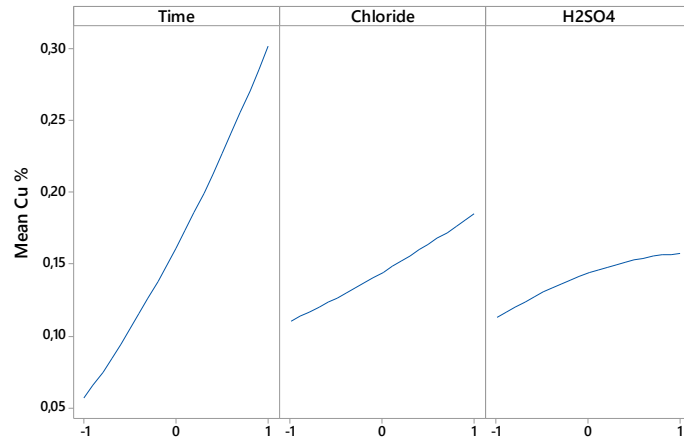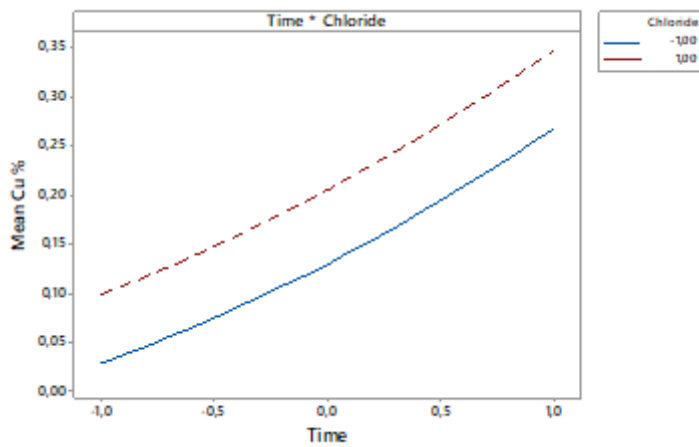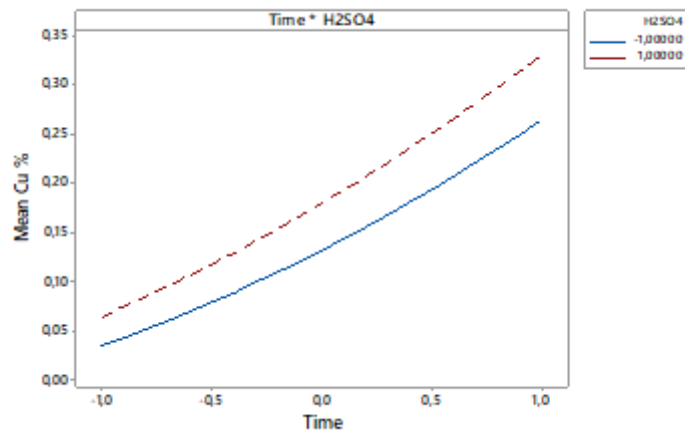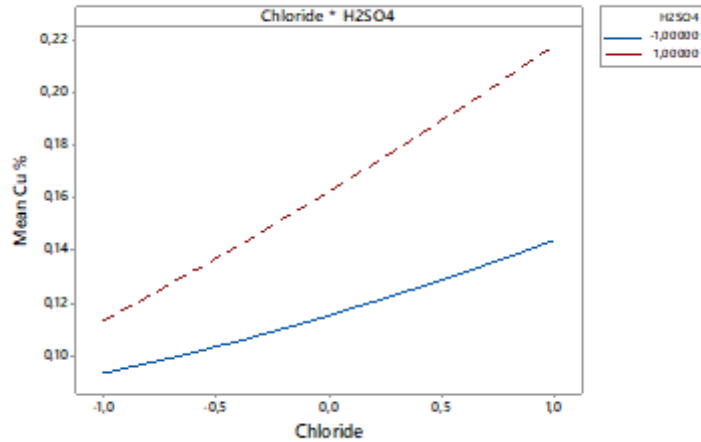
Fig. 3. Linear effect plot for Cu extraction

(a)

(b)

(c)

Fig. 4. Plot for the effect on Cu extraction of the Interactions of time-chloride (a), time-H_2SO_4 concentration (b), and chloride-H_2SO_4 (c).

Equation (21) presents the Cu extraction rate over the range of experimental conditions after eliminating non-significant coefficients.

$$\% \, Extraction = 0{,}16969 + 0{,}12332 \, x_1 + 0{,}03904 \, x_2 + 0{,}02502 \, x_3 + 0{,}01782 \, x_1^2 - 0{,}00870 \, x_3^2 + 0{,}00921 \, x_1 x_3 + 0{,}01347 \, x_2 x_3$$

(21)

where $x_1, x_2 \, y \, x_3$ are codified variables that respectively represent time and chloride and H_2SO_4 concentrations.

An ANOVA test indicated that the quadratic model adequately represents Cu extraction from CuS under the established ranges of the parameters. The model did not require adjustment and was validated by the R^2 (0.9945) and R^2_{adj} values (0.9925). The ANOVA showed that the indicated factors influence Cu extraction from CuS, as indicated by regression F_{reg} (371.42) > $F_{T, 95\% \, confidence \, level}$ $F_{7,19}$ (2.543).

The p-value of the model is 0.000 < 0.05, as represented by Equation (21), which indicates that the model is statistically significant.

The Mallows's Cp = 7.37 (constant + 7 predictors) indicates that the model is accurate and does not present bias in estimating the true regression coefficients. It also allows for prediction with an acceptable margin of error of R^2_{pred} = 0.9888.

Finally, the adjustment of the ANOVA analysis indicated that the factors considered explained the variations in the response. The difference between R^2 and R^2_{pred} of the model was minimal, thus reducing the possibility that the model was overly adjusted, that is, a lower probability that the model only fits the sample data. The ANOVA analysis indicated that time, chloride and H_2SO_4 concentrations, and the interactions of time-H_2SO_4 and chloride-H_2SO_4 are the most important factors in explaining the behavior of the system for the sampled data set.
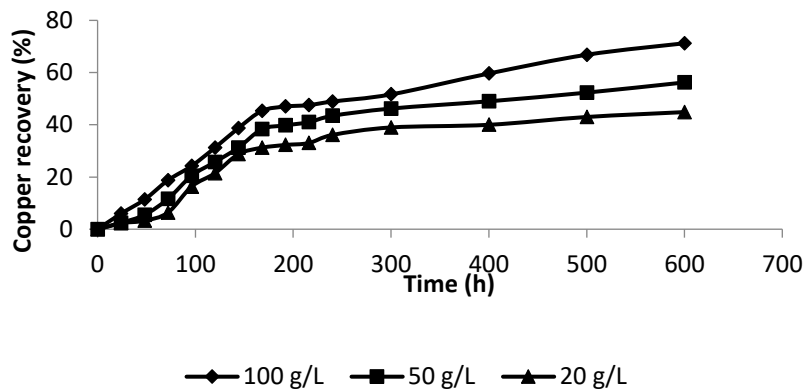
3.2 Effect of chloride concentration

Fig. 5. Extraction of Cu (%) vs time (h), depending on the addition of chloride

Fig. 5 shows that the highest rate of copper extraction (71.23%) was obtained with high concentrations of chloride ions (100 g/L), thus demonstrating the effect of a higher chloride ion concentration on copper extraction (Miki et al., 2011;Senanayake, 2007). However, according to Cheng and Lawson (1991), there is a ceiling of 0.25 M, above which higher concentrations of chloride have insignificant effects on covellite dissolution, while in the range of 20 to 50 (g/L), chloride has no positive effects based on the leaching time, obtaining maximum copper extractions of 44.87 and 56.23%, respectively. This concurs with the results of other investigations (Miki et al., 2011), which indicate that CuS oxidation to CuS_2 is possible with any chloride concentration, but the oxidation of CuS_2 is only possible with very high potential or high chloride concentrations (Nicol & Basson, 2017).
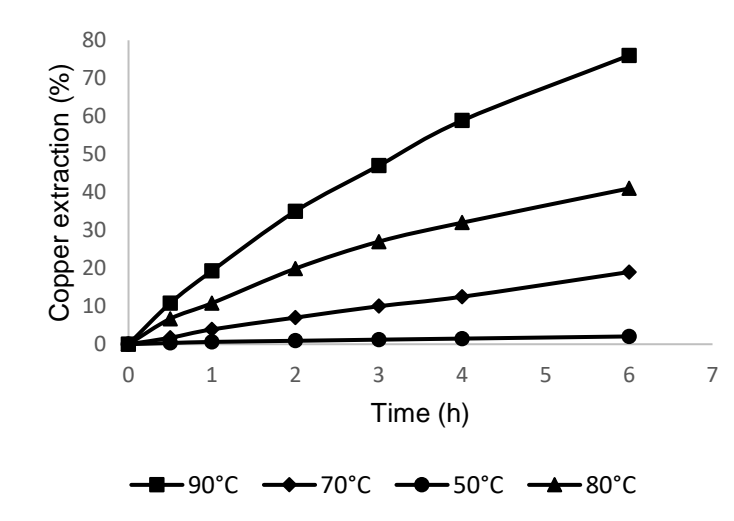
3.3 Effect of temperature

Fig. 6. Cu extraction (%) vs time (h), based on the T ° C

Fig. 6 shows the effect of temperature on a covellite solution in a medium with a high concentration of chloride and a low concentration of sulfuric acid. The copper extraction rate varied by up to 74% with temperatures of 90 °C and 50 °C, with a leaching period of 6 hours. The analysis of the effect of

temperature on the copper extraction rate confirmed the significant effect of this parameter on leaching, and in this case, the increase in leaching kinetics with 0.5 M of H_2SO_4, 100 g/L of chloride and a leaching time of up to 9 hours. According to Ruan et al. (2013) and Miki et al. (2011), covellite dissolution is controlled by chemical surface reaction. The unreacted core model is used to describe the kinetics of covellite leaching with the application of Equation 22:

$Kt=1-(1-\alpha)^{1/3}$ (22)

where:

α is the fraction of dissolved copper, t is leaching time, and k is the reaction rate constant

Using the slopes of the extraction curves as a function of temperature, the linear zones were shortened by approximately 2 hours), yielding the Arrhenius plot in Fig. 7, and resulting in an activation energy of 72.36 kJ/mol, which was similar to the levels in other investigations under similar conditions, such as in Cheng and Lawson (1991), who obtained an activation energy of 77 kJ/mol with the addition of 0.5 M of H_2SO_4 and 0.5 M of NaCl, and in Miki et al. (2011), who obtained an activation energy of 72 kJ/mol, with low temperature (25-45 °C), an extended leaching period, and the addition of iron and copper catalysts.
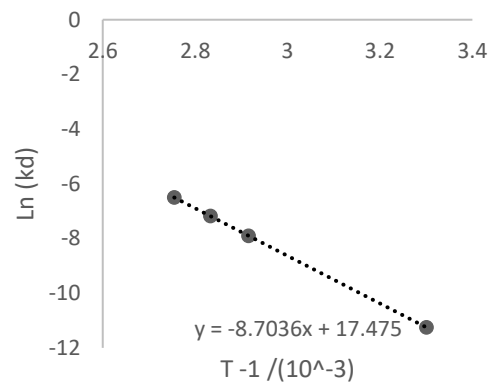

Fig. 7: Arrhenius plot for covellite dissolution using linear slopes of the curves in Fig. 6.
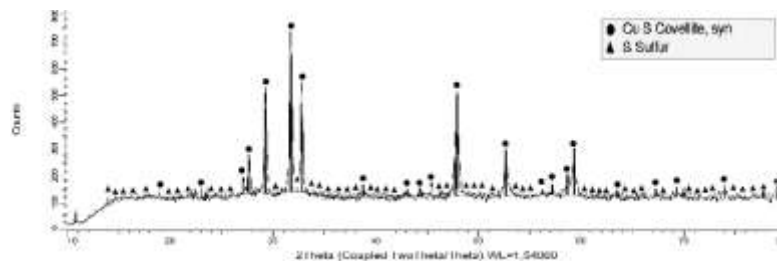
Residues analysis:

Fig. 8: X-ray diffractogram for the covellite mineral after being leached at 90 ° C in a time of two hours.
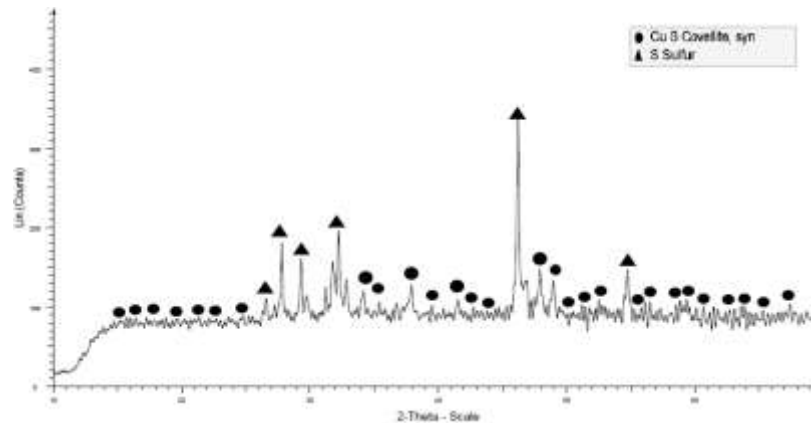
Fig. 9: X-ray diffractogram for the covellite mineral after being leached at 90 ° C in a time of six hours

An analysis is made about the XRD of the residues comparing them with the initial state which contains an approximate 15.71% of gypsum. In fig. 8, the difractogram is presented where the transformation of the covellite is observed after a leaching of two hours at a temperature of 90 ° C under conditions of 1 M H_2SO_4 and 100 g/L NaCl a 35% of copper is extracted in solution, with 85.34% covellite and 14.66% elemental sulfur remain in the residue. In fig. 9, the XRD shows the covellite transformation after six hours of leaching at a temperature of 90 ° C under conditions of 1 M H_2SO_4 and 100 g/L NaCl, achieving the extraction of 76% of copper, remaining in the residual of 47% "synthetic covellite", which is presumed to be CuS and CuS2, as mentioned by Nicol & Basson (2017). Although the XRD only shows a synthetic covellite, accompanied by 53% of elemental sulfur, what stands out is that the gypsyum remains that were present in the initial mineral were not observed in figures 8 and 9. The CuS_2 mineral is slower than the covellite and therefore requires more demanding conditions and/or longer times to complete the extraction of Cu.

4. Conclusions

The present investigation shows the laboratory results of dissolving Cu from covellite in chlorinated media. The highest Cu extraction rate was obtained with high concentrations of chloride in the system. The findings of this study were:

1. The linear variables of time and chloride concentration have the greatest influence in the model.
2. Under normal conditions of pressure and temperature, H_2SO_4 concentration-time and chloride concentration-time have synergistic effects on copper extraction from covellite.
3. The Anova analysis indicates that the presented quadratic model adequately represents copper extraction, which is validated by the R^2 value (0.9945).
4. The highest copper extraction rate working at room temperature of 71.23% was obtained with a low concentration of sulfuric acid (0.5 M), a high concentration of chloride (100 g/L) and an extended leaching time (600 h).
5. Regarding the temperature control (50-90°C) in leaching conditions of 0.5 M of H_2SO_4, 100 g/L chloride and leaching time of 6 hours, an activation energy of 72.36 kJ/mol is observed, indicating that the rate of dissolution of the mineral is indeed limited by the chemical reaction.
6. In the XRD carried out in the leaching residues at 2 and 6 hours at a temperature of 90 ° C, the formation of elemental sulfur is observed, which is expected as a stable and non-polluting residue.

References

Afif, C., Chélala, C., Borbon, A., Abboud, M., Adjizian-Gérard, J., Farah, W., … Rizk, T. (2008). So2in Beirut: Air quality implication and effects of local emissions and long-range transport. *Air Quality, Atmosphere and Health*, *1*(3), 167–178. https://doi.org/10.1007/s11869-008-0022-y

Aguirre, C. L., Toro, N., Carvajal, N., Watling, H., & Aguirre, C. (2016). Leaching of chalcopyrite (CuFeS2) with an imidazolium-based ionic liquid in the presence of chloride. *Minerals Engineering*, *99*, 60–66. https://doi.org/10.1016/j.mineng.2016.09.016

Baba, A. A., Balogun, A. F., Olaoluwa, D. T., Bale, R. B., Adekola, F. A., & Alabi, A. G. F. (2017). Leaching kinetics of a Nigerian complex covellite ore by the ammonia-ammonium sulfate solution. *Korean Journal of Chemical Engineering*, *34*(4), 1133–1140. https://doi.org/10.1007/s11814-017-0005-5

Balladares, E., Jerez, O., Parada, F., Baltierra, L., Hernández, C., Araneda, E., & Parra, V. (2018). Neutralization and co-precipitation of heavy metals by lime addition to effluent from acid plant in a copper smelter. *Minerals Engineering*, *122*(March), 122–129. https://doi.org/10.1016/j.mineng.2018.03.028

Bezerra, M. A., Santelli, R. E., Oliveira, E. P., Villar, L. S., & Escaleira, L. A. (2008). Response surface methodology (RSM) as a tool for optimization in analytical chemistry. *Talanta*, *76*(5), 965–977. https://doi.org/10.1016/j.talanta.2008.05.019

Cheng, C. Y., & Lawson, F. (1991). The kinetics of leaching covellite in acidic oxygenated sulphate-chloride solutions. *Hydrometallurgy*, *27*(3), 249–268. https://doi.org/10.1016/0304-386X(91)90053-O

Dean, A., Voss, D., & Draguljic, D. (2017). Response Surface Methodology. In *Design and Analysis of Experiments* (pp. 565–614). https://doi.org/10.1007/978-3-319-52250-0

Dijksira, R., Senyard, B., Shah, U., & Lee, H. (2017). Economical abatement of high-strength SO2off-gas from a smelter. *Journal of the Southern African Institute of Mining and Metallurgy*, *117*(11), 1003–1007. https://doi.org/10.17159/2411-9717/2017/v117n11a2

Dimitrijević, M., Kostov, A., Tasić, V., & Milosević, N. (2009). Influence of pyrometallurgical copper production on the environment. *Journal of Hazardous Materials*, *164*(2–3), 892–899. https://doi.org/10.1016/j.jhazmat.2008.08.099

Donati, E., Pogliani, C., & Boiardi, J. L. (1997). Anaerobic leaching of covellite by Thiobacillus ferrooxidans. *Applied Microbiology and Biotechnology*, *47*(6), 636–639. https://doi.org/10.1007/s002530050987

F. Monteiro, V., Garcia, O., & Tuovinen, O. (1999). *Oxidative dissolution of covellite by Thiobacillus ferrooxidans. Process Metallurgy* (Vol. 9). https://doi.org/10.1016/S1572-4409(99)80028-5

Falco, L., Pogliani, C., Curutchet, G., & Donati, E. (2003). A comparison of bioleaching of covellite using pure cultures of Acidithiobacillus ferrooxidans and Acidithiobacillus thiooxidans or a mixed culture of Leptospirillum ferrooxidans and Acidithiobacillus thiooxidans. *Hydrometallurgy*, *71*(1–2), 31–36. https://doi.org/10.1016/S0304-386X(03)00170-1

Fisher, W. W. (1994). Comparison of chalcocite dissolution in the sulfate, perchlorate, nitrate,

chloride, ammonia, and cyanide systems. *Minerals Engineering*, *7*(1), 99–103. https://doi.org/10.1016/0892-6875(94)90150-3

González, C., Parra, R., Klenovcanova, A., Imris, I., & Sánchez, M. (2005). Reduction of Chilean copper slags: A case of waste management project. *Scandinavian Journal of Metallurgy*, *34*(2), 143–149. https://doi.org/10.1111/j.1600-0692.2005.00740.x

Herreros, O., & Viñals, J. (2007). Leaching of sulfide copper ore in a NaCl-H2SO4-O2 media with acid pre-treatment. *Hydrometallurgy*, *89*(3–4), 260–268. https://doi.org/10.1016/j.hydromet.2007.07.011

Kelm, U., Avendaño, M., Balladares, E., Helle, S., Karlsson, T., & Pincheira, M. (2014). The use of water-extractable Cu, Mo, Zn, As, Pb concentrations and automated mineral analysis of flue dust particles as tools for impact studies in topsoils exposed to past emissions of a Cu-smelter. *Chemie Der Erde*, *74*(3), 365–373. https://doi.org/10.1016/j.chemer.2013.12.001

Klein, C., & Hurlbut, C. S. (1996). *Manual de mineralogía*. Reverté. Retrieved from https://books.google.cl/books/about/Manual_de_mineralogía.html?id=4z8EMkxqfe4C&redir_esc=y

Lee, J., Acar, S., Doerr, D. L., & Brierley, J. A. (2011). Comparative bioleaching and mineralogy of composited sulfide ores containing enargite, covellite and chalcocite by mesophilic and thermophilic microorganisms. *Hydrometallurgy*, *105*(3–4), 213–221. https://doi.org/10.1016/j.hydromet.2010.10.001

Lü, C., Wang, Y., Qian, P., Liu, Y., Fu, G., Ding, J., … Chen, Y. (2018). Separation of chalcopyrite and pyrite from a copper tailing by ammonium humate. *Chinese Journal of Chemical Engineering*, *26*(9), 1814–1821. https://doi.org/10.1016/j.cjche.2018.02.014

Lundström, M., Liipo, J., Taskinen, P., & Aromaa, J. (2016). Copper precipitation during leaching of various copper sulfide concentrates with cupric chloride in acidic solutions. *Hydrometallurgy*, *166*, 136–142. https://doi.org/10.1016/j.hydromet.2016.10.017

Miki, H., Nicol, M., & Velásquez-Yévenes, L. (2011). The kinetics of dissolution of synthetic covellite, chalcocite and digenite in dilute chloride solutions at ambient temperatures. *Hydrometallurgy*, *105*(3–4), 321–327. https://doi.org/10.1016/j.hydromet.2010.11.004

Montgomery, D. C. (2012). Cap. 3, 6, 7 and 10. In *Design and Analysis of Experiments*. Wiley; 8 edition (April 10, 2012).

Nicol, M., & Basson, P. (2017). The anodic behaviour of covellite in chloride solutions. *Hydrometallurgy*, *172*(June), 60–68. https://doi.org/10.1016/j.hydromet.2017.06.018

Niu, X., Ruan, R., Tan, Q., Jia, Y., & Sun, H. (2015). Study on the second stage of chalcocite leaching in column with redox potential control and its implications. *Hydrometallurgy*, *155*, 141–152. https://doi.org/10.1016/j.hydromet.2015.04.022

Rabadjieva, D., Tepavitcharova, S., Todorov, T., Dassenakis, M., Paraskevopoulou, V., & Petrov, M. (2009). Chemical speciation in mining affected waters: The case study of Asarel-Medet mine. *Environmental Monitoring and Assessment*, *159*(1–4), 353–366. https://doi.org/10.1007/s10661-008-0634-6

Reilly, I. G., & Scott, D. S. (1976). The Leaching of Cupric Sulfide in Ammonia. *Industrial and Engineering Chemistry Process Design and Development*, *15*(1), 60–67. https://doi.org/10.1021/i260057a012

Ruan, R., Zou, G., Zhong, S., Wu, Z., Chan, B., & Wang, D. (2013). Why Zijinshan copper bioheapleaching plant works efficiently at low microbial activity-Study on leaching kinetics of copper sulfides and its implications. *Minerals Engineering*, *48*, 36–43. https://doi.org/10.1016/j.mineng.2013.01.002

Ruiz, M. C., Abarzúa, E., & Padilla, R. (2007). Oxygen pressure leaching of white metal. *Hydrometallurgy*, *86*(3–4), 131–139. https://doi.org/10.1016/j.hydromet.2006.10.009

Ruiz, M. C., Honores, S., & Padilla, R. (1998). Leaching kinetics of digenite concentrate in oxygenated chloride media at ambient pressure. *Metallurgical and Materials Transactions B: Process Metallurgy and Materials Processing Science*, *29*(5), 961–969. https://doi.org/10.1007/s11663-998-0064-4

Sánchez de la Campa, A. M., de la Rosa, J. D., Sánchez-Rodas, D., Oliveira, V., Alastuey, A., Querol, X., & Gómez Ariza, J. L. (2008). Arsenic speciation study of PM2.5 in an urban area near a copper smelter. *Atmospheric Environment*, *42*(26), 6487–6495. https://doi.org/10.1016/j.atmosenv.2008.04.016

Schlesinger, M. E., King, M. J., Sole, K. C., & Davenport, W. G. (2011). *Extractive Metallurgy of Copper* (fifth edit). Elsevier.

Senanayake, G. (2007). Chloride assisted leaching of chalcocite by oxygenated sulphuric acid via Cu(II)-OH-Cl. *Minerals Engineering*, *20*(11), 1075–1088. https://doi.org/10.1016/j.mineng.2007.04.002

Senanayake, G. (2009). A review of chloride assisted copper sulfide leaching by oxygenated sulfuric acid and mechanistic considerations. *Hydrometallurgy*, *98*(1–2), 21–32. https://doi.org/10.1016/j.hydromet.2009.02.010

Serbula, S. M., Milosavljevic, J. S., Radojevic, A. A., Kalinovic, J. V, & Kalinovic, T. S. (2017). Science of the Total Environment Extreme air pollution with contaminants originating from the mining – metallurgical processes. *Science of the Total Environment*, *586*, 1066–1075. https://doi.org/10.1016/j.scitotenv.2017.02.091

Shuva, M. A. H., Rhamdhani, M. A., Brooks, G. A., Masood, S., & Reuter, M. A. (2016). Thermodynamics data of valuable elements relevant to e-waste processing through primary and secondary copper production: A review. *Journal of Cleaner Production*, *131*, 795–809. https://doi.org/10.1016/j.jclepro.2016.04.061

Toro, N., Herrera, N., Castillo, J., Torres, C., & Sepúlveda, R. (2018). Initial Investigation into the Leaching of Manganese from Nodules at Room Temperature with the Use of Sulfuric Acid and the Addition of Foundry Slag—Part I. *Minerals*, *8*(12), 565. https://doi.org/10.3390/min8120565

Turan, M. D., Sari, Z. A., & Miller, J. D. (2017). Leaching of blended copper slag in microwave oven. *Transactions of Nonferrous Metals Society of China (English Edition)*, *27*(6), 1404–1410. https://doi.org/10.1016/S1003-6326(17)60161-4

Vračar, R. Ž., Vučković, N., & Kamberović, Ž. (2003). Leaching of copper(I) sulphide by sulphuric acid solution with addition of sodium nitrate. *Hydrometallurgy*, *70*(1–3), 143–151. https://doi.org/10.1016/S0304-386X(03)00075-6

World Health Organization. (2018). *World Health Statistics*. Retrieved from http://e-journal.uajy.ac.id/14649/1/JURNAL.pdf

8. Conclusiones

El presente estudio muestra los resultados mediante el uso de modelos estadísticos, así como curvas de extracción versus tiempo para investigar la lixiviación de dos tipos de minerales, sulfuros de cobre (primarios y secundarios) y minerales con altos contenidos de MnO_2 (nódulos de manganeso y cobres negros). Para todas las pruebas se trabajó en un medio ácido con el uso de H_2SO_4 y temperatura ambiente (25 °C). Los principales hallazgos son los siguientes:

Minerales de Manganeso

- Trabajar a razones de agente reductor/MnO_2 sobre 1/1, permite obtener extracciones de Mn sobre un 70% en tiempos inferiores a 10 min.

- Una razón de agente reductor/MnO_2 de 3/1 presenta las mayores extracciones de Mn en cortos periodos de tiempo, aunque presentando muy poca diferencia respecto a razones de 2/1.

- Altas concentraciones de agente reductor (hierro) en el sistema, permiten trabajar en rangos de potencial y pH que favorecen la generación de Fe^{2+} y Fe^{3+}; así, se evita la formación de precipitados de Fe. Además, vuelve irrelevante la concentración de ácido sulfúrico en la disolución de Mn.

Minerales sulfurados de Cobre

- El agua de descarte presenta mejores resultados para la disolución de Cu desde minerales sulfurados, respecto al agua de mar, en donde compuestos presentes en el agua de descarte como MgO y $CaSO_4$ no afectaron significativamente en la extracción de cobre. Además, se resalta que se generan residuos estables y no contaminantes, como el azufre elemental.

- Bajo condiciones normales de presión y temperatura, sólo la concentración de cloruro en el sistema ejerce un efecto significativo en la extracción de cobre desde calcosina.

- Altas concentraciones de MnO_2 (4/1 y 5/1) en el sistema, permiten valores de potencial entre 580 y 650mV, favoreciendo la disolución de $CuFeS_2$.

Se puede apreciar en base a los resultados obtenidos en la presente investigación, que es posible extraer los elementos de interés a partir de minerales refractarios a procesos convencionales, adicionando los aditivos adecuados (aguas de descarte, agua de mar, MnO_2, Fe^{2+}), proporcionando los rangos de potencial y pH adecuados para su disolución. A pesar de que ninguno de los procesos propuestos en este estudio han sido aplicados a escala industrial (excepto uso de agua de mar), y no se ha estudiado en el presente manuscrito u otras publicaciones a la fecha su viabilidad económica, no se ve un impedimento en hacer pruebas a nivel escala piloto, para su posible futura implementación en la gran minería. Esto debido a que los aditivos adicionados son principalmente residuos industriales masivos, que no tienen un costo económico de por medio. Sólo en el caso del MnO_2 se presenta una dificultad para obtener nódulos de manganeso, sin embargo, se tiene una gran cantidad de minerales de cobre negro en la gran minería del cobre, los cuales son considerados como residuos actualmente por la industria, y podrían ser un reemplazo viable.

En futuros trabajos es necesario hacer un análisis más detallado de los residuos sólidos, y también un análisis sobre todos los iones presentes en la solución líquida posterior a la lixiviación. Esto debido a que la visión industrial, desde mi punto de vista, se enfocará en cómo poder utilizar aguas alternativas y no solamente el agua de mar. Para poder satisfacer los problemas hídricos que se presentan a nivel mundial a causa del cambio climático, y el nuevo impulso de tecnologías limpias y economía circular con el fin de disminuir la contaminación. Por este motivo, mis investigaciones futuras tratarán sobre procesos de lixiviación con aguas residuales de otros procesos industriales, más el tratamiento de sus residuos.

Referencias

[1] SERNAGEOMIN (2017).Anuario de la minería de Chile. Retrieved from:

http://www.sernageomin.cl/wp-content/uploads/2018/06/Anuario_2017.pdf

[2] USGS (2017). U.S. Geological Survey. Retrieved from:

https://minerals.usgs.gov/minerals/pubs/commodity/copper/mcs-2017-coppe.pdf

[3] CM (2017). Cifras actualizadas de la minería. Retrieved from:

http://consejominero.cl/inicio/chile-pais- minero/mineria-en-cifras/

[4] COCHILCO. (2017). Sulfuros primarios: desafíos y oportunidades I Comisión Chilena del Cobre. Retrieved from:

https://www.cochilco.cl/Listado%20Temtico/sulfuros%20primarios_desaf%C3%ADos%20y%20oportunidades.pdf

[5] Toro, N.; Briceño, W.; Pérez, K.; Cánovas, M.; Trigueros, E.; Sepúlveda, R.; Hernández, P. Leaching of Pure Chalcocite in a Chloride Media Using Sea Water and Waste Water. Metals 2019, 9, 780.

[6] Saldaña, M.; Toro, N.; Castillo, J.; Hernández, P.; Navarra, A. Optimization of the heap leaching process through changes in modes of operation and discrete event simulation. Minerals 2019, 9, 421.

[7] Devore J., Probability & Statistics for Engineering and the Sciences, 8th ed. 2010.

[8] Mathews P. G., Design of Experiments with MINITAB. Milwaukee: William A. Tony, 2005.

[9] Toro N., Saldaña M., Gálvez E., Cánovas M., Trigueros E., Castillo J., and Hernández P. C., "Optimization of Parameters for the Dissolution of Mn from Manganese Nodules with the Use of Tailings in An Acid Medium," Minerals, vol. 9, no. 7, p. 387, Jun. 2019.

[10] Saldaña M., Toro N., Castillo J., Hernández P., Trigueros E., and Navarra A., "Development of an Analytical Model for the Extraction of Manganese from Marine Nodules," Metals (Basel)., vol. 9, no. 8, p. 903, Aug. 2019.

[11] Mellado M. E., Casanova M. P., Cisternas L. A., and Gálvez E. D., "On scalable analytical models for heap leaching," Comput. Chem. Eng., vol. 35, no. 2, pp. 220–225, 2011.

[12] Mellado M. E., Gálvez E. D., and Cisternas L. A., "On the optimization of flow rates on copper heap leaching operations," Int. J. Miner. Process., vol. 101, no. 1–4, pp. 75–80, 2011.

[13] Mellado M. E., Gálvez E. D., and Cisternas L. A, "Stochastic analysis of heap leaching process via analytical models," Miner. Eng., vol. 33, pp. 93–98, 2012.

[14] Dixon D. G. and Hendrix J. L., "A mathematical model for heap leaching of one or more solid reactants from porous ore pellets," Metall. Trans. B, vol. 24, no. 6, pp. 1087–1102, 1993.

[15] Dixon D. G. and Hendrix J. L., "A general model for leaching of one or more solid reactants from porous ore particles," Metall. Trans. B, vol. 24, no. 1, pp. 157–169, 1993.

[16] Habashi, F. 1997. Handbook of Extractive Metallurgy. Laval, Wiley-VCH. 2426p

[17] Lide, D. 2003. Handbook of chemistry and physics. 84ª ed. Florida, CRC Press. 2616p

[18] Post, J.E. 1999. Manganese Oxide Minerals: Crystal Structures and Economic and Environmental Significance. Proceedings of the National Academy of Sciences 96(7):3447-3454

[19] Nordberg G. et al., 2007. HANDBOOK ON the Toxicology of Metals. 3ª ed. Oxford, Elsevier. 1024p.

[20] Randhawa, N.S.; Hait, J.; Jana, R.K. A brief overview on manganese nodules processing signifying the detail in the Indian context highlighting the international scenario. Hydrometallurgy 2016, 165, 166–181

[21] HEIN, J.R. 2016. Manganese nodules. En: HARFF J., MESCHEDE M., PETERSEN S. Y THIEDE J. (Eds.). Encyclopedia of Marine Geosciences. Estados Unidos. Springer. pp. 408-412.

[22] Cronan, D.S. 1977. Chapter 2 Deep-Sea Nodules: Distribution and Geochemistry. Journal of Geophysical Research 80(27):11-44.

[23] Gálvez, J. 1980. Panorama actual de la Hidrometalurgia. Los nódulos de manganeso. Anales de la Universidad de Murcia. 34(1):279-292

[24] Cuadra, P., & Rojas, G. (2001). Oxide Mineralization at the Radomiro Tomic Porphyry Copper Deposit, Northern Chile. Economic Geology, 96(2), 387–400.

[25] Mora, R., Artal, J., Brockway, H., Martinez, E., & Muhr, R. (2003). El Tesoro exotic copper deposit, Antofagasta region, northern Chile. Economic Geology: Special Publication, 11, 187–197.

[26] Kojima, S., Astudillo, J., Rojo, J., Tristá, D., & Hayashi, K. I. (2003). Ore mineralogy, fluid inclusion, and stable isotopic characteristics of stratiform copper deposits in the coastal Cordillera of northern Chile. Mineralium Deposita, 38(2), 208–216.

[27] Menzies, A., Campos, E., Hernández, V., Sola, S., & Riquelme, R. (2015). Understanding Exotic-Cu Mineralisation Part II : Characterization of " Black Copper " ore (" Cobre Negro "). (September), 3–6.

[28] Pincheira, M. ., Dagnino, A., Kelm, U., & Helle, S. (2003). "Copper Pitch Y Copper Wad": Contraste Entre Las Fases Presentes En Las Cabezas Y En Los Ripios En Pruebas De Mina sur, Chuquicamata.

[29] mindat. (2019). Black Copper. Retrieved November 12, 2019, from https://www.mindat.org/min-4225.html

[30] Sokić, M. D., Milošević, V. D., Stanković, V. D., Matković, V. L., & Marković, B. R. (2015). Acid leaching of oxide-sulfide copper ore prior the flotation - A way for an increased metal recovery. Hemijska Industrija, 69(5), 453–458.

[31] Navarra, A.; Oyarzun, F.; Parra, R.; Marambio, H.; Mucciardi, F. System dynamics and discrete event simulation of copper smelters. Miner. Metall. Process. 2017, 34, 96–106

[32] International Copper Study Group. The World Copper Factbook 2017; International Copper Study Group: Lisbon, Portugal, 2017.

[33] Velásquez-Yévenes, L., Torres, D., & Toro, N. (2018). Leaching of chalcopyrite ore agglomerated with high chloride concentration and high curing periods. Hydrometallurgy, 181, 215–220.

[34] Baba A, I. Ayinla K, A. Adekola F, K. Ghosh M, S. Ayanda O, B. Bale R, et al. A Review on Novel Techniques for Chalcopyrite Ore Processing. Int J Min Eng Miner Process 2012;1:1–16.

[35] Niu, X., Ruan, R., Tan, Q., Jia, Y., & Sun, H. (2015). Study on the second stage of chalcocite leaching in column with redox potential control and its implications. Hydrometallurgy, 155, 141–152.

[36] Miki, H., Nicol, M., & Velásquez-Yévenes, L. (2011). The kinetics of dissolution of synthetic covellite, chalcocite and digenite in dilute chloride solutions at ambient temperatures. Hydrometallurgy, 105(3–4), 321–327.

[37] mindat. (2019). Chalcocite. Retrieved November 12, 2019, from: https://www.mindat.org/min-962.html

[38] Klein, C., & Hurlbut, C. S. (1996). Manual de mineralogía. Reverté. Retrieved from https://books.google.cl/books/about/Manual_de_mineralogía.html?id=4z8EMkxqfe4C&redir_esc=y

[39] Lundström, M., Liipo, J., Taskinen, P., & Aromaa, J. (2016). Copper precipitation during leaching of various copper sulfide concentrates with cupric chloride in acidic solutions. Hydrometallurgy, 166, 136–142.

[40] Ruiz, M. C., Honores, S., & Padilla, R. (1998). Leaching kinetics of digenite concentrate in oxygenated chloride media at ambient pressure. Metallurgical and Materials Transactions B: Process Metallurgy and Materials Processing Science, 29(5), 961–969. https://doi.org/10.1007/s11663-998-0064-4

[41] Senanayake, G. (2009). A review of chloride assisted copper sulfide leaching by oxygenated sulfuric acid and mechanistic considerations. Hydrometallurgy, 98(1–2), 21–32.

[42] mindat. (2019). Covellite. Retrieved November 12, 2019, from https://www.mindat.org/min-1144.html.

[43] Aguirre C.L., Toro N., Carvajal N., Watling H., Aguirre C. Leaching of chalcopyrite

(CuFeS2) with an imidazolium-based ionic liquid in the presence of chloride. Miner Eng 2016;99:60–6.

[44] Toro, N.; Pérez, K.; Saldaña, M.; Jeldres, R.I.; Jeldres, M.; Cánovas, M. Dissolution of pure chalcopyrite with manganese nodules and waste water. J. Mater. Res. Technol (in press). 2019. doi:10.1016/j.jmrt.2019.11.020.

[45] mindat. (2019). Chalcopirite. Retrieved December 12, 2019, from https://www.mindat.org/min-4965.html

[46] Córdoba, E.M. Muñoz, J.A. Blázquez, M.L. González, F. ballester, A. 2008. Leaching of chalcopyrite with ferric ion. Part I: General aspects. Hydrometallurgy 93: 81-87

[47] Cherkaev, A. 2010. Mathematical and Computer Modellingof Heap Leaching at the Agglomerate Scale with Application to Chloride Leaching of Chalcopyrite. Tesis para optar al grado de Master of Science in Engineering. Department of Chemical Engineering. University of Cape Town.

[48] Domic E., (2001). Hidrometalurgia: Fundamentos Procesos y Aplicaciones. Hidrometalurgia: Fundamentos Procesos y Aplicaciones. Santiago. https://doi.org/10.1016/j.geobios.2005.01.003

[49] Dresher W.H., 2004. Producing copper Nature's way: bioleaching. Copper application in mining and extraction. Innovations.

Anexos

Anexos

Otras publicaciones realizadas durante el periodo de tesis:

- **Publicación 1: N. Toro***, M. Saldaña, J. Castillo, F. Higuera and R. Acosta. "Leaching of Manganese from Marine Nodules at Room Temperature with the Use of Sulfuric Acid and the Addition of Tailings" Q2 ISI WoS. Minerals, 2019; https://doi.org/10.3390/min9050289

- **Publicación 2:** M. Saldaña, **N. Toro***, J. Castillo, P. Hernández and A. Navarra. "Optimization of the Heap Leaching Process through Changes in Modes of Operation and Simulation of Discrete Events" Q2 ISI WoS. Minerals, 2019; https://doi.org/10.3390/min9070421

- **Publicación 3**: K. Pérez, **N. Toro***, E. Campos, J. González, R. I. Jeldres, A. Nazer and M.H. Rodríguez. "Extraction of Mn from black copper using iron oxides from tailings and Fe2+ as reducing agents in acid medium" Q1 ISI WoS. Metals, 2019; https://doi.org/10.3390/met9101112

- **Publicación 4:** K. Pérez, A. Villegas, M. Saldaña, R. I. Jeldres, J. González and **N. Toro***. "Initial Investigation into the Leaching of Manganese from Nodules at Room Temperature with the Use of Sulfuric Acid and the Addition of Foundry Slag—Part II" Q3 ISI WoS. Separation Science and Technology, 2020; https://doi.org/10.1080/01496395.2020.1713816

Leaching of Manganese from Marine Nodules at Room Temperature with the Use of Sulfuric Acid and the Addition of Tailings

Norman Toro [1],*, Manuel Saldaña [2], Jonathan Castillo [3] , Freddy Higuera [2] and Roxana Acosta [4]

[1] Departamento de Ingeniería en Metalurgia y Minas, Universidad Católica del Norte, Antofagasta 1270709, Chile

[2] Departamento de Ingeniería Industrial, Universidad Católica del Norte, Antofagasta 1270709, Chile; msp018@alumnos.ucn.cl (M.S.); fhiguera@ucn.cl (F.H.)

[3] Departamento de Ingeniería en Metalurgia, Universidad de Atacama, Copiapó 1531772, Chile; jonathan.castillo@uda.cl

[4] Departamento de Educación, Universidad de Antofagasta, Antofagasta 1270300, Chile; roxana.acosta@uantof.cl

* Correspondence: ntoro@ucn.cl; Tel.: +56-552651021

Abstract: Based on the results obtained from a previous study investigating the dissolution of Mn from marine nodules with the use of sulfuric acid and foundry slag, a second series of experiments was carried out using tailings produced from slag flotation. The proposed approach takes advantage of the Fe present in magnetite contained in these tailings and is believed to be cost-efficient. The surface optimization methodology was used to evaluate the independent variables of time, particle size, and sulfuric acid concentration in the Mn solution. Other tests evaluated the effect of agitation speed and the MnO_2/Fe_2O_3 ratio in an acid medium. The highest Mn extraction rate of 77% was obtained with an MnO_2/Fe_2O_3 ratio of 1/2 concentration of 1 mol/L of H_2SO_4, particle size of −47 + 38 μm, and 40 min of leaching. It is concluded that higher rates of Mn extraction were obtained when tailings instead of slag were used, while future research needs to focus on determination of the optimum Fe_2O_3/MnO_2 ratio to improve dissolution of Mn from marine nodules.

1. Introduction

Ferromanganese (Fe–Mn) deposits are present in the oceans across the world, marine ridges, and plateaus where the currents have delivered sediments for millions of years [1]. These deposits form through the accumulation of iron and manganese oxides in seawater, within either volcanic or sedimentary rocks that act as substrates, as observed in the central and northeastern ocean beds of the Pacific [2]. They may have economic potential [3], due to the high concentrations of Co, Ni, Te, Ti, Pt, and rare earth elements [4]. These Fe–Mn oceanic deposits include ferromanganese crusts, as well as cobalt-rich crusts, polymetallic nodules, and hydrothermal infusions [5]. Polymetallic nodules have a particular importance for the steel industry as an they may eventually become an alternate source of manganese [6].

In order to extract manganese and other metals from marine nodules, the use of a reducing agent is necessary [7]. Acid leaching of marine nodules, with the use of iron as a reducing agent, has shown good results [8–10]. In a previous study carried out by Toro et al. [11], several parameters were evaluated for dissolving Mn from marine nodules using slag at room temperature in an acid medium. This study established that high MnO_2/Fe_2O_3 ratios significantly shorten the manganese dissolution

time from 30 to 5 min. They also conclude that MnO_2 particle size does not significantly affect the Mn extraction rate in an acid medium in the presence of Fe contained in ferrous slag.

The positive effect of Fe as a reducing agent for dissolving Mn from marine nodules was noted when lower Mn/Fe ratios were used [8–11]. Bafghi et al. [12] and Toro et al. [11] determined that sulfuric acid concentration is less important than Fe concentration in dissolving Mn.

The Mn extraction rate increases with a higher agitation speed [13–15]. Jiang et al. [13] evaluated the kinetic aspects of manganese and silver extraction during leaching of pyrolusite in sulfuric acid solutions in the presence of H_2O_2, and concluded that agitation speed was one of the most important variables affecting the Mn extraction rate. Su et al. [14] indicated that the Mn extraction rate increases significantly when the agitation speed increases from 100 to 700 rpm because high speed improves mixing and allows better contact between reagents and reactants. Jiang et al. [13] also reported that the extraction rate decreases slightly at 1000 rpm because excessive agitation can cause material to adhere to the walls of the reactor and prevent it from being leached. Velásquez et al. [16] indicated that it is only necessary to keep particles in suspension and prevent agglomeration.

The addition of Fe as a reducing agent in temperature-controlled acid media has already been studied [8,10,12]. In particular, Zakeri et al. [10] used ferrous ions with a Fe^{2+}/MnO_2 ratio of 2.4 and sulfuric acid as a leaching agent with a H_2SO_4/MnO_2 ratio of 2.0 over a temperature range of 20 to 60 °C, and found out that Mn extraction was notably higher at 60 °C and reached 96% after 60 min. Bafghi et al. [12] used Fe sponge with a molar ratio of 2, and H_2SO_4 with a molar ratio of 4 (both ratios with respect to MnO_2), under the same temperatures as Zakeri et al. [10]; at 60 °C, 100% of the Mn present within the nodules was dissolved in 3 min. Both cases demonstrate the positive impact of higher temperature on the extraction rate; however, the positive impact of the presence of iron indicated that effective processing may take place even at ambient temperatures. Furthermore, both studies demonstrate that the acid concentration is less significant than the Fe/MnO_2 ratio.

The present work investigates the effect of using of tailings, obtained after flotation of slag at the Altonorte Foundry Plant, on the dissolution of Mn from marine nodules. A report by SERNAGEOMIN [17] indicates that the production of copper concentrate in Chile has been increasing steadily, and is expected to almost double by 2026 from its 2014 level, from 3.9 to 5.4 million tons. For every ton of Cu concentrate obtained by flotation, 151 tons of tailings are generated [18], which are disposed of in tailing dams and have significant impacts on the environment [19]. Consequently, it is necessary to find new uses for tailings with the application of more environmentally friendly hydrometallurgical techniques [20]. This results in an attractive proposal given the quantities of waste generated in the country by flotation, providing an added value for this material while introducing a new initiative in the context of the need to overcome stagnation in the mining sector [21].

2. Materials and Methods

2.1. Manganese Nodule Sample

The marine nodules used in this work were the same as those used in Toro et al. [11]. They were composed of 15.96% Mn and 0.45% Fe. Table 1 shows the chemical composition. The sample material was analyzed with a Bruker®M4-Tornado μ-FRX tabletop device (Fremont, CA, USA). The μ-XRF data shows that the nodules were composed of fragments of preexisting nodules that formed their nuclei, with concentric layers that precipitated around the nuclei in later stages.

Table 1. Chemical analysis (in the form of oxides) of manganese nodules.

Component	MgO	Al_2O_3	SiO_2	P_2O_5	SO_3	K_2O	CaO	TiO_2	MnO_2	Fe_2O_3
Weight (%)	3.54	3.69	2.97	7.20	1.17	0.33	22.48	1.07	29.85	26.02

2.2. Tailings

The sample of tailings used in this study was obtained after flotation of slag during the production of copper concentrate at the Altonorte Smelting Plant. The methods used to determine the chemical and mineralogical composition of the tailings were the same as those used to determine marine nodule content. Chemical species were determined by QEMSCAN. Several iron-containing phases were present, while the Fe content was estimated at 41.9%. Table 2 shows the mineralogical composition of the tailings. As the Fe was mainly in the form of magnetite, the most appropriate method of extraction was the same as that used in Toro et al. [11].

Table 2. Mineralogical composition of tailings, as determined by QEMSCAN.

Mineral	Amount % (w/w)
Chalcopyrite/Bornite $(CuFeS_2/Cu_5FeS_4)$	0.47
Tennantite/Tetrahedrite $(Cu_{12}As_4S_{13}/Cu_{12}Sb_4S_{13})$	0.03
Other Cu Minerals	0.63
Cu–Fe Hydroxides	0.94
Pyrite (FeS_2)	0.12
Magnetite (Fe_3O_4)	58.52
Specular Hematite (Fe_2O_3)	0.89
Hematite (Fe_2O_3)	4.47
Ilmenite/Titanite/Rutile $(FeTiO_3/CaTiSiO_5/TiO_2)$	0.04
Siderite $(FeCO_3)$	0.22
Chlorite/Biotite $(Mg)_3(Si)_4O_{10}(OH)_2(Mg)_3(OH)_6/K(Mg)_3AlSi_3O_{10}(OH)_2$	3.13
Other Phyllosilicates	11.61
Fayalite (Fe_2SiO_4)	4.59
Dicalcium Silicate (Ca_2SiO_4)	8.30
Kirschsteinite $(CaFeSi\,O_4)$	3.40
Forsterita (Mg_2SiO_4)	2.30
Baritine $(BaSO_4)$	0.08
Zinc Oxide (ZnO)	0.02
Lead Oxide (PbO)	0.01
Sulfate (SO_4)	0.20
Others	0.03
Total	100.00

2.3. Reagents Used—Leaching Parameters

The sulfuric acid used for the leaching tests was grade P.A., with 95%–97% purity, a density of 1.84 kg/L, and a molecular weight of 98.8 g/mol. The leaching tests were carried out in a 50 mL glass reactor with a 0.01 solid/liquid ratio. A total of 200 mg of Mn nodules were maintained in suspension with the use of a 5-position magnetic stirrer (IKA ROS, CEP 13087-534, Campinas, Brazil) at a speed of 600 rpm. The tests were conducted at a room temperature of 25 °C, while the parameters studied were additives, particle size, and leaching time. Also, the tests were performed in duplicate, measurements (or analyses) were carried on 5 mL of undiluted samples using atomic absorption spectrometry with a coefficient of variation ≤5% and a relative error between 5% to 10%.

2.4. Experimental Design

The effect of the independent variables on the extraction rate of Mn from manganese nodules was studied using the response surface method [22,23], which helped in understanding and optimizing the response by refining the determinations of relevant factors using the model. An experiment was designed involving three factors that could influence the response variable, and with three levels for each factor for a total of 27 experimental tests (Table 3), the purpose of which was to study the effects of H_2SO_4 concentration, particle size, and time on the dependent variable. Minitab 18 software was used for modeling and experimental design, providing the same analytical approach as used in Toro et al. [11].

Table 3. Experimental configuration and Mn extraction data.

Exp. No.	Time (min)	Sieve Fraction (Tyler Mesh)	Particle Size (μm)	Sulfuric Acid Conc. (mol/L)	Mn Extraction (%)
1	10	−320 + 400	−47 + 38	0.1	8.12
2	20	−100 + 140	−150 + 106	0.5	29.10
3	20	−320 + 400	−47 + 38	1	55.51
4	30	−320 + 400	−47 + 38	1	71.00
5	10	−200 + 270	−75 + 53	0.5	19.12
6	20	−100 + 140	−150 + 106	0.1	7.63
7	30	−100 + 140	−150 + 106	1	49.8
8	30	−200 + 270	−75 + 53	0.1	17.79
9	10	−100 + 140	−150 + 106	0.5	13.98
10	10	−100 + 140	−150 + 106	1	41.22
11	20	−320 + 400	−47 + 38	0.5	52.51
12	30	−100 + 140	−150 + 106	0.1	10.89
13	20	−320 + 400	−47 + 38	0.1	19.12
14	10	−100 + 140	−150 + 106	0.1	5.24
15	10	−320 + 400	−47 + 38	1	46.23
16	10	−200 + 270	−75 + 53	0.1	9.54
17	20	−200 + 270	−75 + 53	0.1	11.11
18	20	−200 + 270	−75 + 53	0.5	29.41
19	30	−320 + 400	−47 + 38	0.1	19.43
20	30	−320 + 400	−47 + 38	0.5	59.16
21	10	−200 + 270	−75 + 53	1	46.77
22	20	−200 + 270	−75 + 53	1	54.00
23	20	−100 + 140	−150 + 106	1	47.24
24	30	−200 + 270	−75 + 53	0.5	33.67
25	10	−320 + 400	−47 + 38	0.5	38.23
26	30	−200 + 270	−75 + 53	1	63.50
27	30	−100 + 140	−150 + 106	0.5	30.00

The response variable can be expressed as showed in Equation (1):

$$Y = (\text{overall constant}) + (\text{linear effects}) + (\text{interaction effects}) + (\text{curvature effects}) \tag{1}$$

Table 4 shows the ranges for values of the parameters used for the experimental design.

Table 4. Experimental conditions.

Parameters/Values	Low	Medium	High
Sieve fraction (Tyler mesh)	−100 + 140	−200 + 270	−320 + 400
Particle size (μm)	−150 + 106	−75 + 53	−47 + 38
Time (in min)	10	20	30
H_2SO_4 (mol/L)	0.1	0.5	1

The levels of the factors are coded as (−1, 0, 1), where each number represents a particular value of the factor, with (−1) as the lowest value, (0) as the intermediate, and (1) as the highest. Equation (2) is used to transform a real value (Z_i) into a coded value (X_i) according to the experimental design:

$$X_i = \frac{Z_i - \frac{Z_{high} + Z_{low}}{2}}{\frac{Z_{high} - Z_{low}}{2}} \tag{2}$$

where Z_{high} and Z_{low} are, respectively, the highest and lowest values of a variable [22].

The statistics used to determine whether the model can adequately describe the extraction of Mn from marine nodules are similar with those used in the study of Toro et al. [11].

2.5. Effect of Stirring Speed

The effect of particle size was evaluated by Toro et al. [11]. It was concluded that this variable did not significantly influence the manganese solutions. Consequently, the present work assessed the effect of agitation speed on Mn dissolution kinetics.

This investigation determined the effect of increasing agitation speed (200, 400, 600, 800, and 1000 rpm) on leaching manganese nodules, using a particle size of $-75 + 53$ μm, MnO_2/Fe_2O_3 ratio of 1, leaching solution volume of 20 mL, 1 mol/L sulfuric acid, and room temperature (25 °C).

2.6. Effect of the MnO_2/Fe_2O_3 Ratio

The present study evaluated the effect of the MnO_2/Fe_2O_3 ratio on leaching time with the use of tailings, using a particle size of $-75 + 53$ μm, agitation speed of 600 rpm, leaching solution volume of 20 mL, 1 mol/L sulfuric acid, and room temperature (25 °C).

3. Results and Discussion

3.1. Effect of Variables

Based on the information obtained from the ANOVA analysis (Table 5), the linear effects of particle size, H_2SO_4, and time contribute greatly to explaining the experimental model, as shown in the contour plots (Figures 1 and 2), while there was no significant effect of any of the curvatures and interactions of the variables considered ($p >> 0.05$) on the manganese extraction rate.

Table 5. ANOVA of the Mn extraction rate.

Source	F-Value	p-Value
Regression	32.13	0.000
Time	27.12	0.000
Particle size	30.39	0.000
Sulfuric acid	226.50	0.000
Time × Time	0.43	0.522
Particle size × Particle size	0.67	0.423
Sulfuric acid × Sulfuric acid	0.39	0.542
Time × Particle size	1.81	0.196
Time × Sulfuric acid	1.57	0.228
Particle size × Sulfuric acid	0.34	0.568
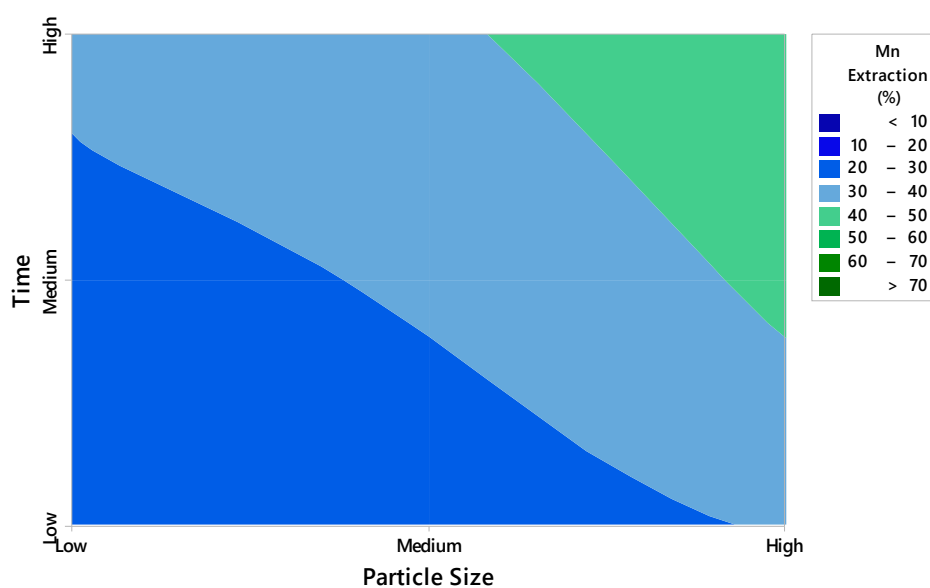
Figure 1. Experimental contour plot of Mn extraction (25 °C; $-150 + 106$, $-75 + 53$, $-47 + 38$ μm particle size; 10, 20, 30 min leaching time).
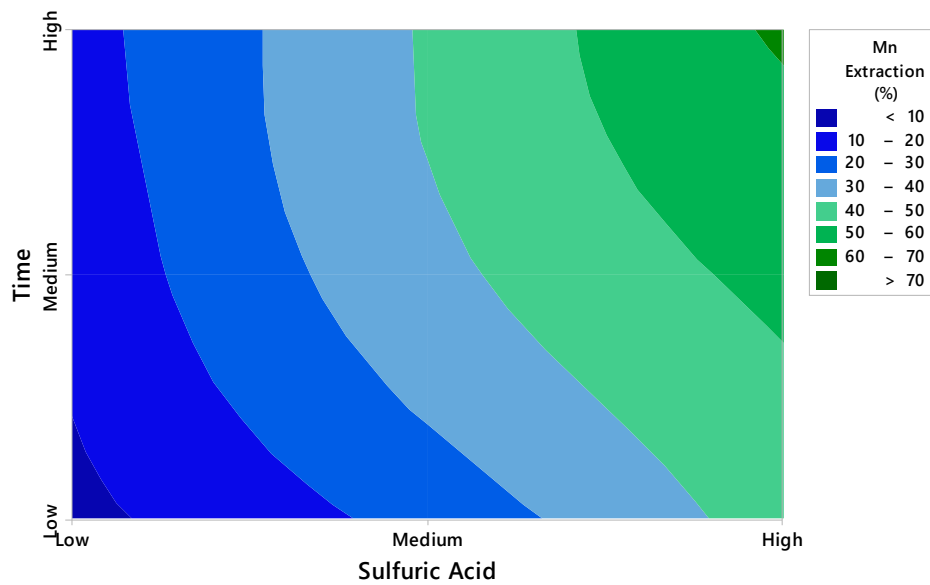
Figure 2. Experimental contour plot of Mn extraction (25 °C; 10, 20, 30 min leaching time; 0.1, 0.5, 1 mol/L H_2SO_4).

Figures 3–5 show that the linear effects of time, particle size, and H_2SO_4 concentration had the most significant impact on Mn extraction rates.
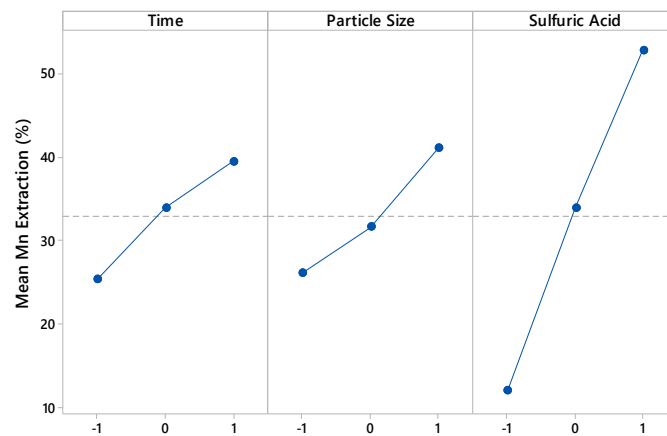

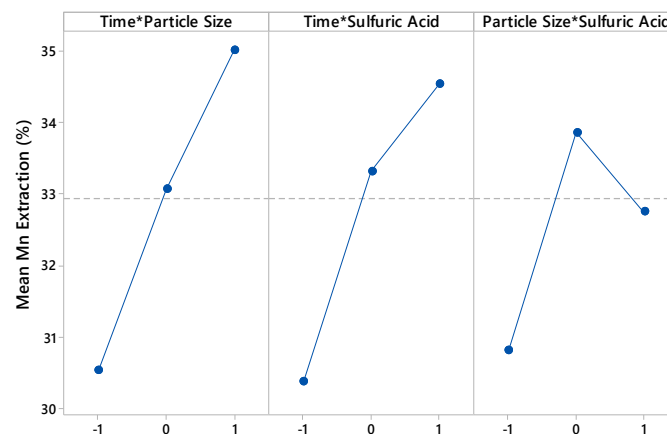**Figure 3.** Linear effect plot for Mn extraction.

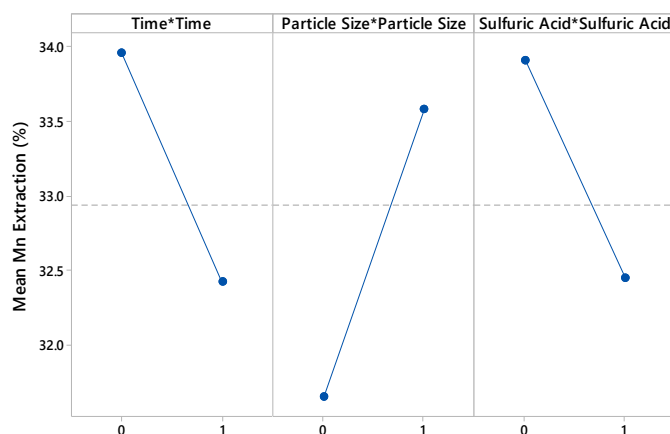**Figure 4.** Interaction effect plot for Mn extraction.

Figure 5. Curvature effect plot for Mn extraction.

After eliminating non-significant coefficients, the model developed to predict ore extraction over the range of experimental conditions is presented in Equation (3).

$$\text{Mn Extraction} = 0.3294 + 0.0704x_1 + 0.0746x_2 + 0.2036x_3 \tag{3}$$

where x_1, x_2, and x_3 are coded variables representing time, particle size, and H_2SO_4 concentration, respectively.

Figure 6 shows the order of adding parameters to the model, graphically showing the contribution to explaining the variability of each new parameter.
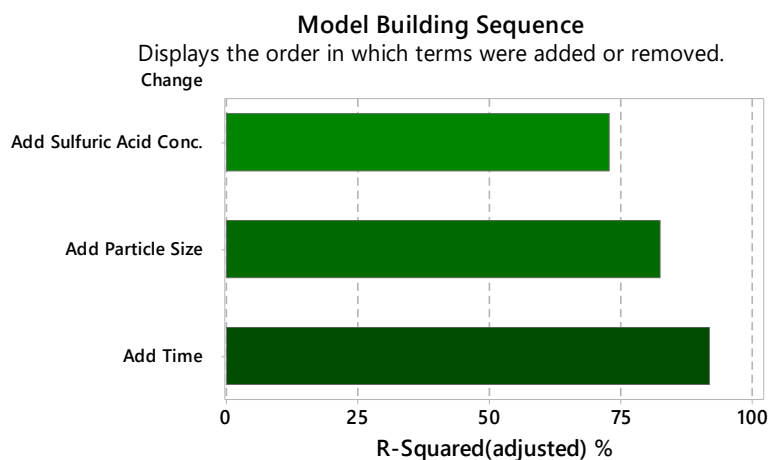
Figure 6. Construction sequence of the model.

The ANOVA indicates that the model adequately represents Mn extraction under the range of established parameters. The model does not require adjustment and is validated by the value of R^2 (0.9275) (Figure 7). The ANOVA shows that the effect of the indicated factors on manganese extraction is $F_{\text{regression}}$ (98.07) > F_{Table}, at the 95% confidence level $F_{4.22}$ (2.8167).
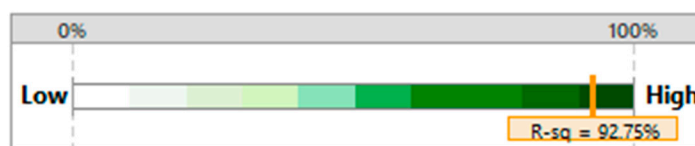
Figure 7. Statistic R^2 (% of variation explained by the model).

Additionally, the p-value (Figure 8) of the model represented by the Equation (3) indicates that the model is statistically significant.
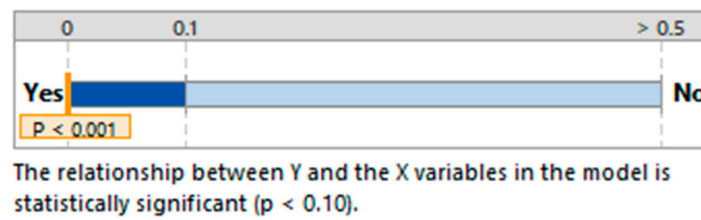

Figure 8. Statistic p.

In favor of the above analysis, the number of parameters plus the constant of the regression does not differ greatly from Mallows' Cp statistic, which indicates that the model is relatively accurate and does not present a bias in estimating the true coefficients of the regression, in addition to making predictions with an acceptable margin of error (R_{pred} = 90.02%).

The data points from the normality test applied to the residuals resulting from the regression in Figure 9 are relatively close to the adjusted normal distribution line, and the p-value of the test is greater than the level of significance of 0.05, so it is not possible to reject the assumption of the regression model, that the residuals are distributed normally.
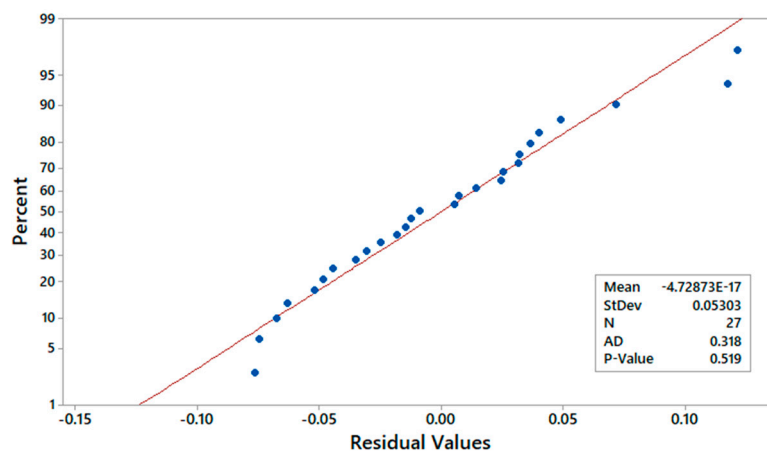
Figure 9. Probability plot of residual values.

Figure 10 shows that residuals do not correlate, indicating that they are independent of each other as there are no obvious trends or patterns.
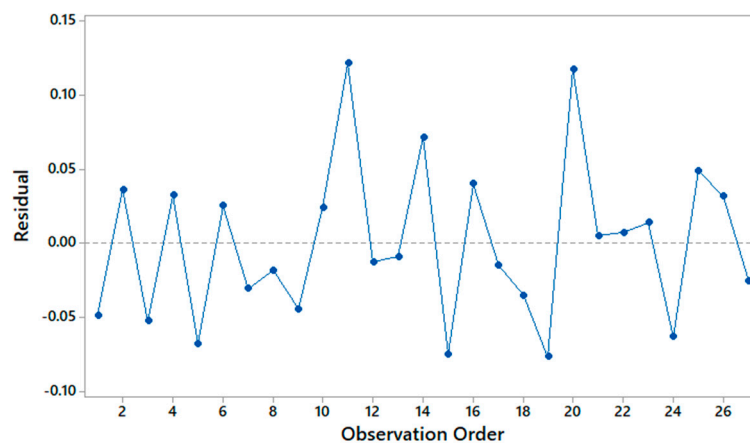

Figure 10. Residuals according to observations.

The response surface graphs in Figure 11A show that manganese extraction increases with time and particle size, while Figure 11B shows, graphically, that the effect of the variable H_2SO_4 concentration is greater than that of time, resulting in a more significant increase in extraction only when the acid concentration increases. The effect described above occurs analogously with variations in particle size and sulfuric acid concentration (Figure 11C).
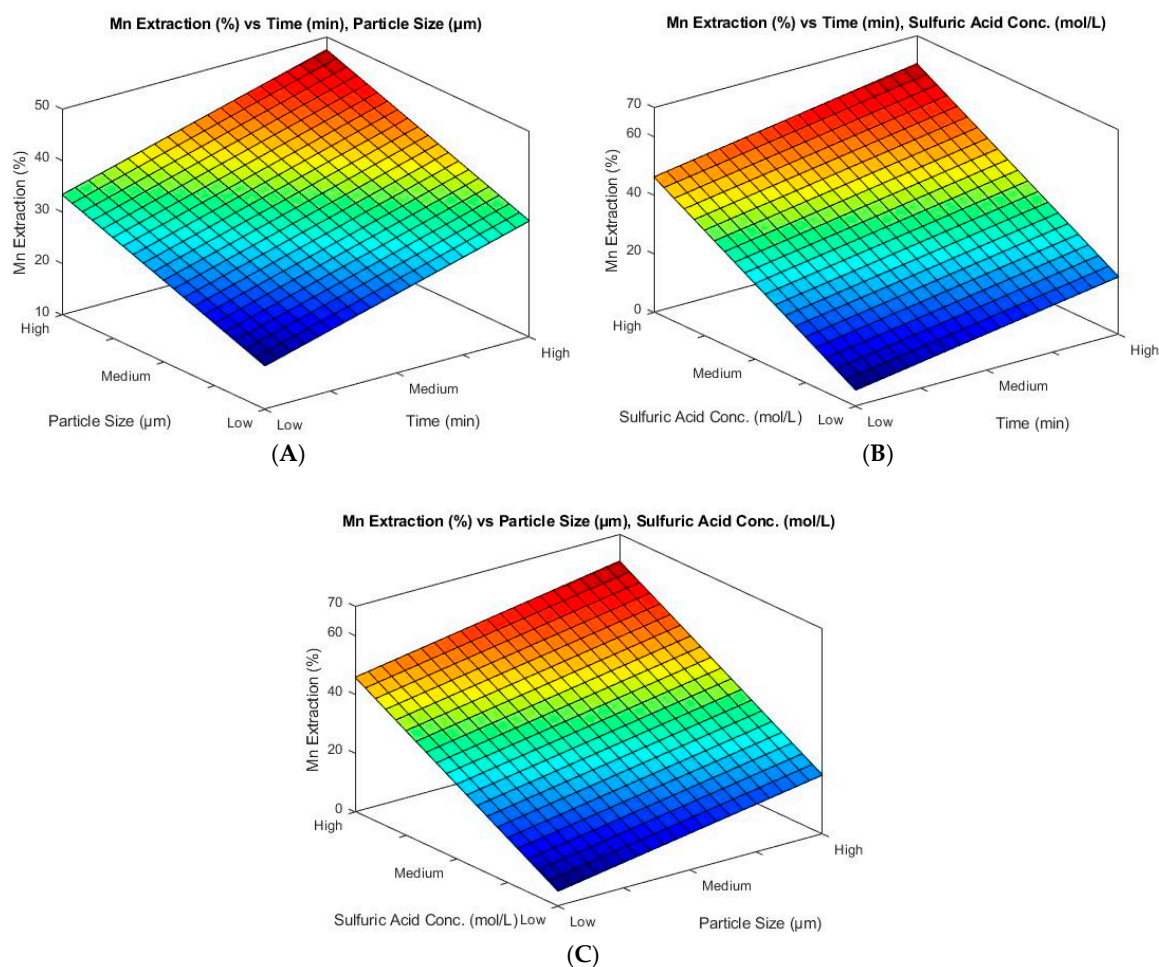

Figure 11. Response surface of the independent variables of time and particle size (**A**); time and H_2SO_4 concentration (**B**); and particle size and H_2SO_4 concentration (**C**) on the dependent variable of Mn extraction.

3.2. Effect of Agitation Speed

In Figure 12, it can be seen that higher Mn extraction rates are obtained at higher agitation speeds. In this study, the highest rate of 69% was obtained with a speed of 600 rpm and a time of 30 min. The extraction rate was lower at 800 and 1000 rpm because, at these speeds, some of the mineral breaks away and adheres to the reactor wall. Jiang et al. [13] had a similar observation at the speed of 1000 rpm. The extraction rate, at 400 rpm (58%), was not significantly different from what was obtained at 600 rpm, while at a low speed of 200 rpm, the Mn extraction rate was only 35% at 30 min. It was observed that not all the particles were in suspension at a stirring speed of 200 rpm, which explains why the extraction rate was so much lower. This is consistent with what Velásquez et al. [16] found in a study of leaching chalcopyrite mineral in chlorinated media. These authors concluded that agitation speed was not the most important factor in determining extraction rates as long as all the particles of the system are kept in suspension.
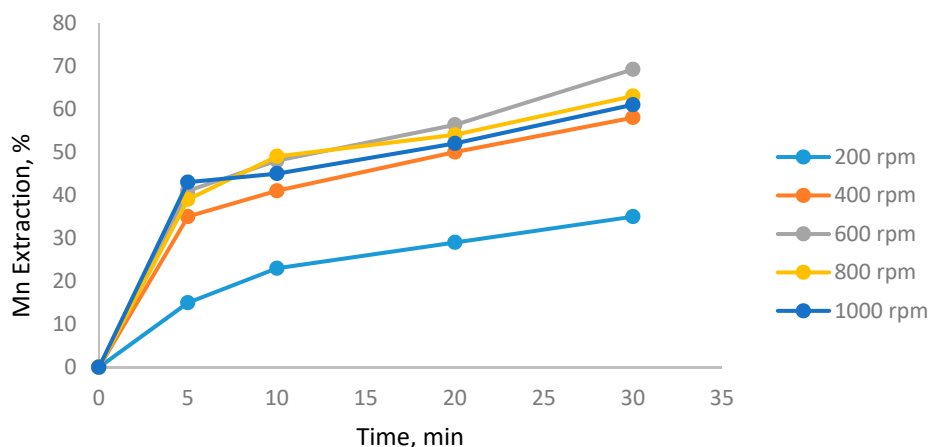
Figure 12. Effect of stirring speed on manganese extraction (25 °C, MnO$_2$/Fe$_2$O$_3$ ratio of 1, −75 + 53 μm, 1 mol/L H$_2$SO$_4$).

3.3. Effect of the MnO$_2$/Fe$_2$O$_3$ Ratio

The results presented in Figure 13 show the benefit of operating at high concentrations of reducing agent (Fe) in terms of shortening the dissolution time. The highest Mn extraction of 77% was obtained after 40 min with an MnO$_2$/Fe$_2$O$_3$ ratio of 1/2. Notably, at this MnO$_2$/Fe$_2$O$_3$ ratio, the leaching time required to reach a 70% extraction rate has been shortened significantly, while 67% extraction was reached in 5 min. However, the extraction graph shows asymptotic behavior, with no significant increase in the extraction rate vs. time. It can be observed that the extraction rate for 30 min with an MnO$_2$/Fe$_2$O$_3$ ratio of 1/1 is close to that obtained with a ratio of 1/2. However, the differences in dissolution rates are more significant for short periods of time (between 5 and 20 min). Finally, the Mn extraction rate was lower (maximum of 47% in 40 min) with an MnO$_2$/Fe$_2$O$_3$ ratio of 2/1 than with the ratios mentioned above. The tests conducted in this investigation were in pH ranges between −2 to 0.1, and potentials from −0.4 to 1.4 V, because the presence of Fe$_2$O$_3$ maintains the regeneration of ferrous ions, which results in high levels of ferrous ion concentration and activity, favoring the dissolution of Mn and avoiding the formation of precipitates through oxidation–reduction reactions.
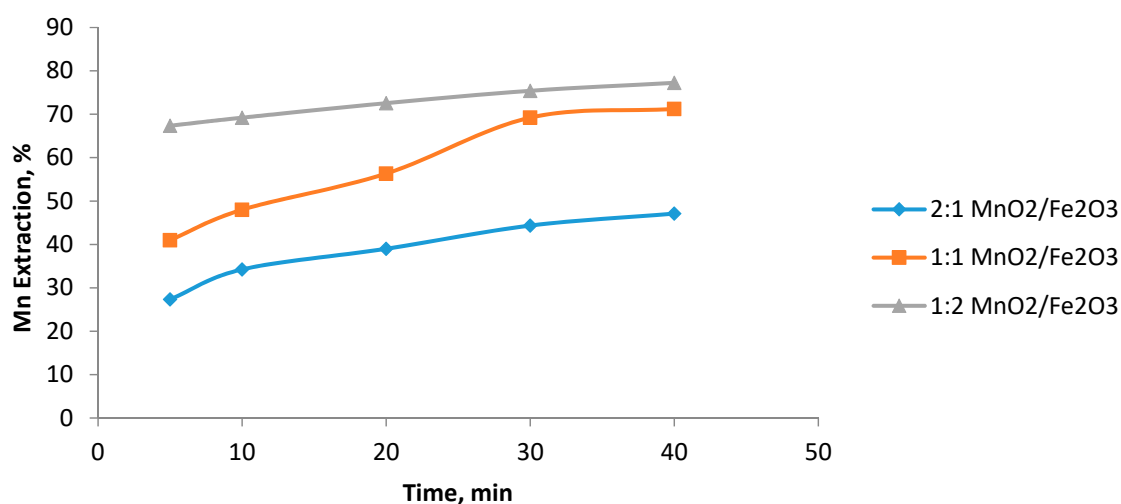

Figure 13. Effect of the MnO$_2$/Fe$_2$O$_3$ ratio on manganese extraction (25 °C, −75 + 53 μm, 1 mol/L H$_2$SO$_4$).

Table 6 compares the results using Fe present in slag and tailings as a reducing agent for Mn dissolution under the same operational conditions. In both cases, dissolution over a short period of time (5 min) immediately reached values close to 70%, with almost identical levels in the two investigations.

However, better results were obtained at 40 min using tailings instead of slag, although the difference is small (7%). This is possibly due to the presence of 13.07% Cu in the slag, which consumes protons. However, this issue requires additional study, since the reactivity of Cu in acid media is associated with slag mineralogy, and the presence of high silica often results in gel formation when leaching is carried out in low pH values [24]. In addition, the tailings are more reactive since they are derived from flotation, and have been attacked by chemicals, resulting in exposure of their surface [25]. These results are promising for future hydrometallurgical studies to investigate the use of slag and tailings as reducing agents for manganese ores. In future studies, it is proposed that this research be continued under the same operating parameters and by applying elemental iron (Fe^0) to determine if it is possible to achieve better results within short periods of time (5 min). In addition, when slag and tailings are used for Mn reduction, the effect of temperature should be evaluated to determine if it is possible to obtain 100% extraction in short periods of time. Finally, an optimal MnO_2/Fe_2O_3 ratio must be found.

Table 6. Comparison of the experimental results.

Experimental Conditions	Toro et al. [11] (2018)	Present Investigation
Temperature (°C)	25	25
Particle size of Mn nodules and slag/tailings (μm)	−75 + 53	−75 + 53
H_2SO_4 concentration (mol/L)	1	1
MnO_2/Fe_2O_3 ratio	1/2	1/2
Mn dissolution rate at 5 min (%)	68	67
Mn dissolution rate at 40 min (%)	70	77

For the recovery of Mn from the solution, the use of zerovalent iron (ZVI) is proposed. In a study by Bartzas et al. [26], the performance of a Fe^0 permeable reactive barrier (PRB) was evaluated for the treatment of acid leachates, where it was observed that metals, such as aluminum, manganese, nickel, cobalt, and zinc, were mainly removed from solution, as metal hydroxides, by precipitation. This can be an attractive proposal because zerovalent iron is a cheap byproduct obtained from the metal finishing industries.

Table 6 shows a comparison of the experimental results of Mn extraction from marine nodules with the use of slag and slag flotation tailings.

4. Conclusions

This investigation presents the results of dissolving Mn from marine nodules in an acid medium at room temperature (25 °C) with the use of tailings obtained from flotations of smelter slag. The Fe present in the tailings proved to be a good reducing agent, increasing MnO_2 dissolution kinetics. The findings of this study are as follows:

(1) The ANOVA test indicates that sulfuric acid is the factor that has the greatest impact on manganese extraction under the studied conditions.
(2) The manganese dissolution rate was generally higher when tailings were used instead of slag, possibly because tailings are more reactive to leaching.
(3) Increase of the agitation speed did not significantly increase Mn extraction.
(4) The highest Mn extraction rate of 77% was obtained at an MnO_2/Fe_2O_3 ratio 0.5, 1 mol/L H_2SO_4, particle size of −47 + 38 μm, and leaching time of 40 min.

In future work, the leaching of marine nodules should be studied using different Fe reducing agents but under the same operational conditions. It is also necessary to determine the optimal MnO_2/Fe_2O_3 ratio that improves dissolution of Mn. In addition, SEM studies need to be carried out on the tailings and manganese nodules after leaching, in order to observe their morphology and determine the possible formation of any iron precipitates.

References

1. Marino, E.; González, F.J.; Somoza, L.; Lunar, R.; Ortega, L.; Vázquez, J.T.; Reyes, J.; Bellido, E. Strategic and rare elements in Cretaceous-Cenozoic cobalt-rich ferromanganese crusts from seamounts in the Canary Island Seamount Province (northeastern tropical Atlantic). *Ore Geol. Rev.* **2017**, *87*, 41–61. [CrossRef]

2. Nishi, K.; Usui, A.; Nakasato, Y.; Yasuda, H. Formation age of the dual structure and environmental change recorded in hydrogenetic ferromanganese crusts from Northwest and Central Paci fi c seamounts. *Ore Geol. Rev.* **2017**, *87*, 62–70. [CrossRef]

3. Konstantinova, N.; Cherkashov, G.; Hein, J.R.; Mirão, J.; Dias, L.; Madureira, P.; Kuznetsov, V.; Maksimov, F. Composition and characteristics of the ferromanganese crusts from the western Arctic Ocean. *Ore Geol. Rev.* **2017**, *87*, 88–99. [CrossRef]

4. Usui, A.; Nishi, K.; Sato, H.; Nakasato, Y.; Thornton, B.; Kashiwabara, T. Continuous growth of hydrogenetic ferromanganese crusts since 17 Myr ago on Takuyo-Daigo Seamount, NW Pacific, at water depths of 800–5500 m. *Ore Geol. Rev.* **2017**, *87*, 71–87. [CrossRef]

5. Josso, P.; Pelleter, E.; Pourret, O.; Fouquet, Y.; Etoubleau, J.; Cheron, S.; Bollinger, C. A new discrimination scheme for oceanic ferromanganese deposits using high fi eld strength and rare earth elements. *Ore Geol. Rev.* **2017**, *87*, 3–15. [CrossRef]

6. Senanayake, G. Acid leaching of metals from deep-sea manganese nodules—A critical review of fundamentals and applications. *Miner. Eng.* **2011**, *24*, 1379–1396. [CrossRef]

7. Randhawa, N.S.; Hait, J.; Jana, R.K. A brief overview on manganese nodules processing signifying the detail in the Indian context highlighting the international scenario. *Hydrometallurgy* **2016**, *165*, 166–181. [CrossRef]

8. Kanungo, S.B. Rate process of the reduction leaching of manganese nodules in dilute HCl in presence of pyrite. Part I. Dissolution behaviour of iron and sulphur species during leaching. *Hydrometallurgy* **1999**, *52*, 313–330. [CrossRef]

9. Kanungo, S.B. Rate process of the reduction leaching of manganese nodules in dilute HCl in presence of pyrite. Part II: leaching behavior of manganese. *Hydrometallurgy* **1999**, *52*, 331–347. [CrossRef]

10. Zakeri, A.; Bafghi, M.S.; Shahriari, S.; Das, S.C.; Sahoo, P.K.; Rao, P.K. Dissolution kinetics of manganese dioxide ore in sulfuric acid in the presence of ferrous ion. *Hydrometallurgy* **2007**, *8*, 22–27.

11. Toro, N.; Herrera, N.; Castillo, J.; Torres, C.; Sepúlveda, R. Initial Investigation into the Leaching of Manganese from Nodules at Room Temperature with the Use of Sulfuric Acid and the Addition of Foundry Slag—Part I. *Minerals* **2018**, *8*, 565. [CrossRef]

12. Bafghi, M.S.; Zakeri, A.; Ghasemi, Z.; Adeli, M. Reductive dissolution of manganese ore in sulfuric acid in the presence of iron metal. *Hydrometallurgy* **2008**, *90*, 207–212. [CrossRef]

13. Jiang, T.; Yang, Y.; Huang, Z.; Zhang, B.; Qiu, G. Leaching kinetics of pyrolusite from manganese-silver ores in the presence of hydrogen peroxide. *Hydrometallurgy* **2004**, *72*, 129–138. [CrossRef]

14. Su, H.; Liu, H.; Wang, F.; Lü, X.; Wen, Y. Kinetics of reductive leaching of low-grade pyrolusite with molasses alcohol wastewater in H2SO4. *Chin. J. Chem. Eng.* **2010**, *18*, 730–735. [CrossRef]

15. Zhang, Y.; You, Z.; Li, G.; Jiang, T. Manganese extraction by sulfur-based reduction roasting-acid leaching from low-grade manganese oxide ores. *Hydrometallurgy* **2013**, *133*, 126–132. [CrossRef]

16. Velásquez Yévenes, L.; Miki, H.; Nicol, M. The dissolution of chalcopyrite in chloride solutions: Part 2: Effect of various parameters on the rate. *Hydrometallurgy* **2010**, *103*, 80–85. [CrossRef]

17. SERNAGEOMIN. *Anuario de la mineria de Chile 2017*; SERNAGEOMIN: Santiago, Chile, 2017.

18. COCHILCO. *Sulfuros primarios: desafíos y oportunidades I Comisión Chilena del Cobre*; COCHILCO: Santiago, Chile, 2017.

19. Oyarzun, R.; Oyarzún, J.; Lillo, J.; Maturana, H.; Higueras, P. Mineral deposits and Cu-Zn-As dispersion-contamination in stream sediments from the semiarid Coquimbo Region, Chile. *Environ. Geol.* **2007**, *53*, 283–294. [CrossRef]

20. Baba, A.A.; Ayinla, K.I.; Adekola, F.A.; Ghosh, M.K.; Ayanda, O.S.; Bale, R.B.; Sheik, A.R.; Pradhan, S.R. A Review on Novel Techniques for Chalcopyrite Ore Processing. *Int. J. Min. Eng. Miner. Process.* **2012**, *1*, 1–16. [CrossRef]

21. Centro de Estudios del Cobre y la Minería (CESCO). Available online: http://www.cesco.cl/en/home-en/ (accessed on 11 May 2019).

22. Montgomery, D.C. *Design and Analysis of Experiments*; Wiley: Hoboken, NJ, USA, 2012.

23. Bezerra, M.A.; Santelli, R.E.; Oliveira, E.P.; Villar, L.S.; Escaleira, L.A. Response surface methodology (RSM) as a tool for optimization in analytical chemistry. *Talanta* **2008**, *76*, 965–977. [CrossRef] [PubMed]

24. Komnitsas, K.; Zaharaki, D.; Perdikatsis, V. Effect of synthesis parameters on the compressive strength of low-calcium ferronickel slag inorganic polymers. *J. Hazard. Mater.* **2009**, *161*, 760–768. [CrossRef] [PubMed]

25. Komnitsas, K.; Manousaki, K.; Zaharaki, D. Assessment of reactivity of sulphidic tailings and river sludges. *Geochemistry Explor. Environ. Anal.* **2009**, *9*, 313–318. [CrossRef]

26. Bartzas, G.; Komnitsas, K.; Paspaliaris, I. Laboratory evaluation of Fe0 barriers to treat acidic leachates. *Miner. Eng.* **2006**, *19*, 505–514. [CrossRef]

Optimization of the Heap Leaching Process through Changes in Modes of Operation and Discrete Event Simulation

Manuel Saldaña [1], Norman Toro [2,3,*], Jonathan Castillo [4], Pía Hernández [5] and Alessandro Navarra [6]

[1] Departamento de Ingeniería Industrial, Universidad Católica del Norte, Av. Angamos 610, Antofagasta 1270709, Chile

[2] Departamento de Ingeniería en Metalurgia y Minas, Universidad Católica del Norte, Av. Angamos 610, Antofagasta 1270709, Chile

[3] Departamento de Ingeniería Minera y Civil. Universidad Politécnica de Cartagena, Paseo Alfonso Xlll N°52, Cartagena 30203, Spain

[4] Departamento de Ingeniería en Metalurgia, Universidad de Atacama, Copiapó 1531772, Chile

[5] Departamento de Ingeniería Química y Procesos de Minerales, Universidad de Antofagasta, Avda. Angamos 601, Antofagasta 1240000, Chile

[6] Department of Mining and Materials Engineering, McGill University, 3610 University Street, Montreal, QC H3A 0C5, Canada

* Correspondence: ntoro@ucn.cl; Tel.: +56-552-651-021

Abstract: The importance of mine planning is often underestimated. Nonetheless, it is essential in achieving high performance by identifying the potential value of mineral resources and providing an optimal, practical, and realistic strategy for extraction, which considers the greatest quantity of options, materials, and scenarios. Conventional mine planning is based on a mostly deterministic approach, ignoring part of the uncertainty presented in the input data, such as the mineralogical composition of the feed. This work develops a methodology to optimize the mineral recovery of the heap leaching phase by addressing the mineralogical variation of the feed, by alternating the mode of operation depending on the type of ore in the feed. The operational changes considered in the analysis include the leaching of oxide ores by adding only sulfuric acid (H_2SO_4) as reagent and adding chloride in the case of sulfide ores (secondary sulfides). The incorporation of uncertainty allows the creation of models that maximize the productivity, while confronting the geological uncertainty, as the extraction program progresses. The model seeks to increase the expected recovery from leaching, considering a set of equiprobable geological scenarios. The modeling and simulation of this productive phase is developed through a discrete event simulation (DES) framework. The results of the simulation indicate the potential to address the dynamics of feed variation through the implementation of alternating modes of operation.

Keywords: process optimization process; heap leaching; modes of operation; discrete event simulation

1. Introducion:

1.1. Overview

Conventional mine planning is traditionally applied in the industry through methodologies that consider an important part of the data to be deterministic. However, critical information used for mining calculations may exhibit statistical variations [1]. When a parameter is uncertain, the expected result is uncertain, since the calculations have considered a potentially unrepresentative value of the parameter,

instead of another that could have the same or different probability of occurrence. Due to this, modern approaches consider the uncertainty and the risk associated with input parameters, which provide a wider vision of the possible losses and gains of the project [2]. The uncertainty of not knowing the real value of the metal content of interest to a certain process is indeed a real risk, so finding a way to organize resources or define alternative operational strategies is a very difficult calculation problem, mainly due to variables that are subject to geological uncertainty; there is generally a range of possible scenarios of mineral grade distribution, process capacities, and commodity market conditions, among others [3,4].

Modern approaches to mine production require simulation frameworks that can increase mineral recovery and are robust in mitigating feed variations [5]. This work presents a methodology for the evaluation of heap leaching, incorporating information of the mineralogical composition of the inputs; the approach is based on discrete event simulation (DES). In general, DES models are used to study systems and processes, in which state changes are computed only at discrete points in time (i.e., discrete events); the changes that occur between these events are not computed explicitly, but can be inferred *a posteriori*. The simulation of the heap leaching allows the planner to estimate the impact on the productivity of the implementation of different modes of operation [6] in response to variations in the mineralogical composition of ores.

1.2. Heap Leaching

After the comminution phase, the copper ores pass to the leaching stage, where the metals present in the mineralized rock are extracted through the application of water and leaching agents. This process is comparatively effective for low- to medium-grade copper oxide minerals (0.3–0.7%). Secondary copper sulfides and low-grade gold ores are also processed in this way [7–9], since it provides a low cost of capital compared to other methods, and since it does not require an intensive use of energy [10]. The agglomeration of the fines around the larger particles with water and concentrated sulfuric acid is known as "curing". This process improves the resistance of the material while having a good permeability of the mineral in the heap leaching, in order to reach adequate heap heights, improve copper recovery rates, and control processing times [11,12]. The acid solution is distributed by sprinklers or drippers, in which the copper (Cu^{2+}) dissolves in the leaching solution as it percolates the heap. The realization of tests at the laboratory level and in pilot plants determine the effectiveness of a heap. The amount of ore to be treated can vary considerably from hundreds to more than one million tons [12], depending on the mine.

Another emerging method is biohydrometallurgy, which plays an important role in the recovery of copper from copper sulfides with economic, environmental, and social benefits [13]. To date, many investigations on acid bioleaching of secondary sulfides [14,15] and primary sulfides [16–18] have been reported presenting good results.

Even in its role as a surplus generator, large-scale mining faces great challenges. These include an increase in costs due to various factors, such as the deterioration of grades and other factors associated with the aging of deposits and increased operating costs to be compatible with sustainable development demands. In typical operations, heap leaching processes operate in approximate times of three months for sulfide ores in chloride media, and also with lower ore grades [19].

2. Materials and Methods

There are several processes through which minerals can be leached, depending mainly on the physical and chemical considerations, such as the solubility of the metal, the kinetics of the solution, the consumption of the reagent, etc. [20]. Heap leaching is currently the most common leaching method in the Chilean mining industry.

2.1. Discrete Event Simulation

With a DES framework, an event is a random occurrence that occurs at a discrete point in time, and whose outcome depends on chance. An event is considered simple if it consists of a specific result or compound if it consists of two or more independent events [21].

Within a system of discrete events, one or more phenomena of interest change their value in discrete points in time [22]. Discrete event simulation considers the evolution of the system, but the states are modified only at discrete moments of time, and they are caused by the occurrence of some event. For this, the state of the system does not explicitly consider variations between two consecutive events. The event *n* occurs at time t_n, and event *n* + 1 will occur at time t_{n+1}, as the simulation clock jumps directly to the instant t_{n+1}. Upon advancing to t_{n+1}, the system statistics and state variables are updated, and this process repeated until a termination condition is met [23].

2.2. Mathematical Modeling of Heap Leaching

Around 20% of the world's copper production is obtained by heap leaching. This process has been modeled by many authors; however, the validation, verification and implementation of these models are difficult since there is uncertainty about the operating conditions and parameters of the leaching model [24–26].

The performance of heap leaching depends on many input variables (operational and design), which means its optimization is complex [27]. The materials are leached with various chemical solutions that extract valuable minerals. These chemical solutions are a weak sulfuric acid solution for copper oxide ores, and chloride media [28] for copper secondary sulfides. The valuable minerals are irrigated with a chemical solution that dissolves the valuable metal of the ore, as the resulting pregnant leaching solution (PLS) passes through the ore, and is recuperated at the base of the heap. The valuable material is then extracted from the PLS, and the chemical solution is recycled back into the heap. The most common methods for recovery of valuable minerals are solvent extraction and electro-winning processes [12].

The following is an analytical model for heap leaching developed by Mellado et al. [29–31], using a system of first order equations:

$$\frac{\partial y}{\partial \tau} = -k_\tau y^{n_\tau} \tag{1}$$

where "y" is a dynamic quantity, such as the concentration or recovery R_t, k_τ are kinetic constants associated with the characteristics of the heap and grade of the mineral respectively, and n_τ is the order of the reaction. The subscript τ represents a time scale that depends on the phenomenon to be modeled. To solve Equation (1), an initial condition is required. Mellado et al. introduced a delay (i.e., a time ω where R_t begins to change ($R_t(\omega) = 0$)); the general solution for $n_\tau = 1$ is given by (see Mellado et al. [29] for the general solution):

$$R_\tau = R_\tau^\infty \left(1 - e^{-k_\tau(\tau - \omega)}\right) \tag{2}$$

Dixon and Hendrix [32,33] considered that the leaching phenomenon occurs at different scales of size and time, and that different phenomena participate in the leaching process. On the other hand, Mellado et al. [31] incorporated the different scales in an analytical model of the leaching process, introducing the parameters K_θ and K_τ, related to size and time, respectively, as can be seen in Equation (3):

$$R(t) = \frac{\alpha}{Z^\gamma + \beta}\left[1 - \lambda e^{K_\theta(t - \omega^*)} - (1 - \lambda)e^{K_\tau(t - \omega^*)}\right] \tag{3}$$

Mellado et al. develop the parameters K_θ, K_τ, and ω^* in Equations (4)–(6) respectively:

$$K_\theta = k_\theta \frac{\mu_s}{\varepsilon_b Z} \tag{4}$$

$$K_\tau = k_\tau \frac{D_{Ae}}{\varepsilon_o r^2} \tag{5}$$

$$\omega^* = \frac{\varepsilon_b Z}{\mu_s} \omega \tag{6}$$

where α, β, and γ are mathematical constants of fit, Z is the height of the heap, λ is a factor of kinetic weight, k_θ and k_τ are kinetic constants, μ_s is the surface velocity of the leaching flow in the heap, ε_b is the volumetric fraction of the bulk solution in the heap, ω is the delay of the reaction, D_{Ae} is the effective diffusivity of the solute within the pores of the particles, ε_o is the porosity of the particles, and r is the radius of the particles.

The goodness-of-fit statistics used to study the model adjusted to observations (operational data supplied from an industrial heap leaching operation at a copper mine in Antofagasta, Chile) are: The mean absolute deviation (MAD, Equation (7)), a statistic that measures the dispersion of forecast error; the mean square error (MSE, Equation (8)), measure of error dispersion that penalizes the periods or values where the error module is higher than the average value; and the absolute average percentage error (MAPE, Equation (9)), a statistic that gives the deviation in percentage terms, calculating the averages of the absolute values between the real value [21].

$$MAD = \frac{\sum |Real - Forecast|}{n} \tag{7}$$

$$MSE = \frac{\sum (Real - Forecast)^2}{n} \tag{8}$$

$$MAPE = \frac{1}{n} \sum \frac{|Real - Forecast|}{|Real|} \tag{9}$$

2.3. Adjustment of the Analytical Model for the Recovery of Copper from Copper Oxides

Adjusting the analytical model by means of a linear optimization model that minimizes the error measurements of the adjustment to operational data, considering the theoretical restrictions of the analytical model, results in the following equation:

$$R(t) = 0.9993\left(1 - 0.4e^{-0.0844(t-2.3684)} - 0.6e^{-0.0055(t-2.3684)}\right) \tag{10}$$

Figure 1 shows the adjusted models from operational data and analytical model respectively for the leaching process operating only with sulfuric acid as a leaching agent, while the goodness-of-fit statistics are shown in Table 1.
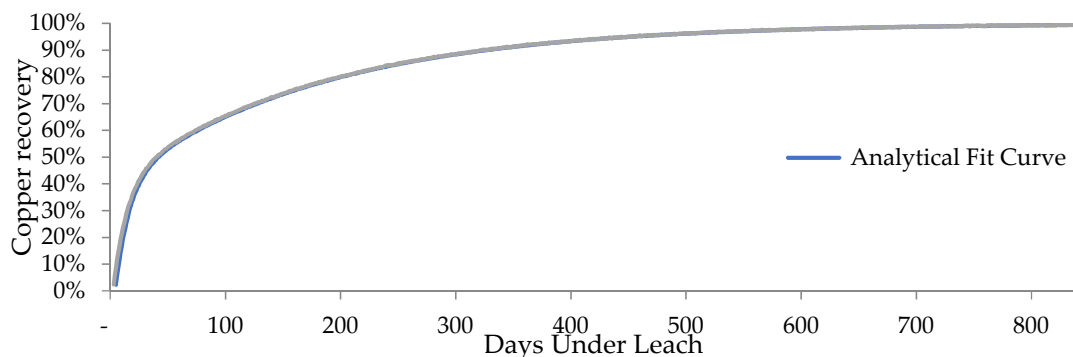

Figure 1. Operational fit curve versus analytical fit curve for copper recovery from oxide ores.

Table 1. Statistics of analytical models of leaching of copper oxides adding sulfuric acid.

Curve/Statistic	MAD	MSE	MAPE
R(t) (Oxides)	1.008×10^{-2}	1.222×10^{-4}	1.28×10^{-2}

The interpretation of the error statistics indicates the degree to which the generated model explains the system to be modeled, from which it is possible to conclude that the difference between the real and predicted values is negligible, which means that the analytical model explains the operational values.

2.4. Adjustment of Analytical Model for Copper Recovery from Secondary Copper Sulfides

The analytical model for copper recovery as a function of time for sulfide minerals (secondary sulfides) is modeled by Equation (11).

$$R(t) = 0.8841\left(1 - 0.2e^{-0.0072(t-1.91)} - 0.8e^{-0.0771(t-1.91)}\right) \tag{11}$$

The adjusted curve of Figure 2 and the error measures of the adjusted model presented in Equation (3) have the goodness-of-fit statistics and low error statistics shown in Table 2, indicating that the analytical model fits the sample data of the operation.
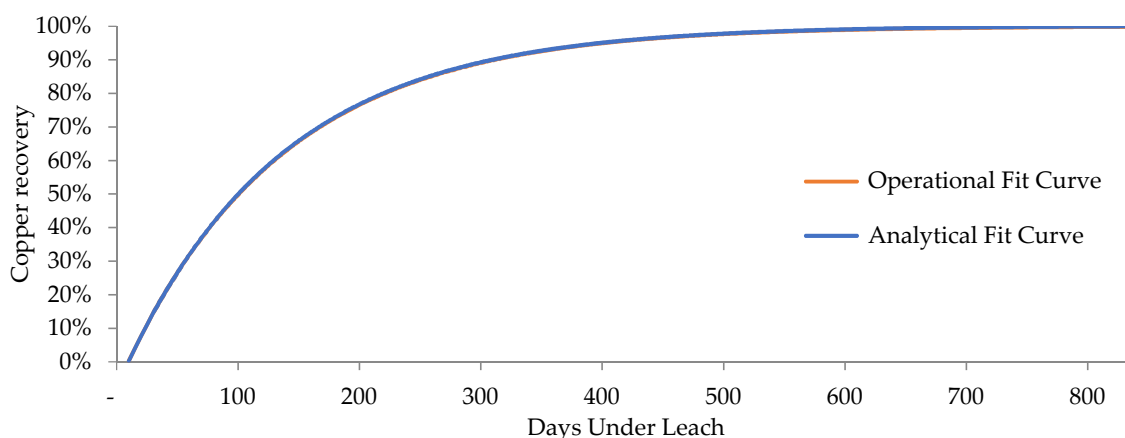

Figure 2. Operational fit curve versus analytical fit curve for copper recovery from sulfide ores.

Table 2. Statistics of analytical models of leaching of secondary copper sulfides adding sulfuric acid.

Curve/Statistic	MAD	MSE	MAPE
R(t) (Oxides)	6.63×10^{-4}	5.068×10^{-7}	8.93×10^{-4}

2.5. Adjustment of Analytical Models for Copper Recovery from Secondary Copper Sulfide Ores Adding Chlorides

Adjusting the curves for the leaching of copper sulfide minerals for two levels of chloride concentration (20 and 50 g/L) as shown in Figure 3, produces the following equations:

$$R(t)[\text{Chloride 20 g/L}] = 0.9159\left(1 - 0.3e^{-0.0168t-2.3684} - 0.7e^{-0.0057t-2.3684}\right) \tag{12}$$

$$R(t)[\text{Chloride 50 g/L}] = 0.9291\left(1 - 0.3e^{-0.0633t-2.3684} - 0.7e^{-0.0071t-2.3684}\right) \tag{13}$$
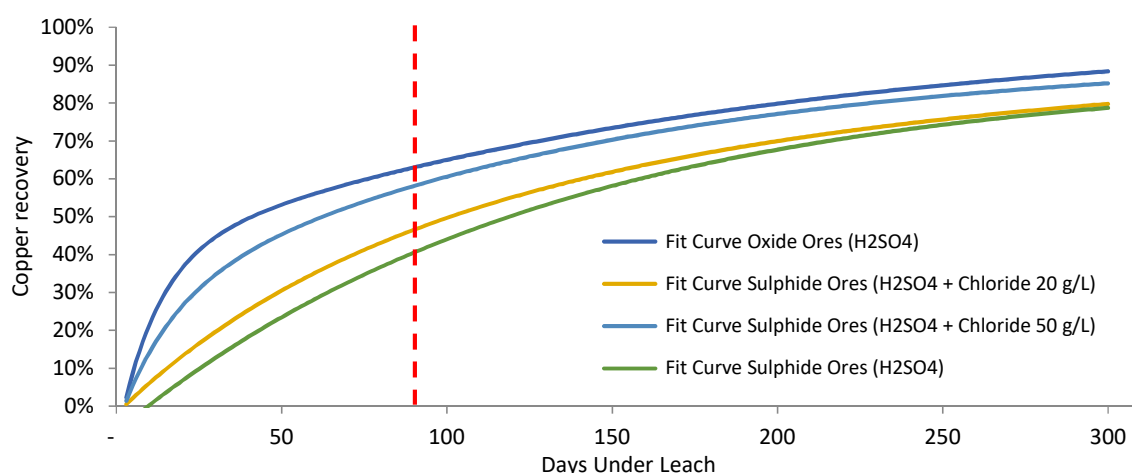
Figure 3. Copper recovery from oxide and sulfide ores using H_2SO_4 and chlorides as an additive.

The goodness-of-fit statistics for the leaching of copper sulfide minerals for two levels of chloride concentration (20 and 50 g/L) are shown in Table 3. Low error statistics indicate that the generated analytical model fits the sample data

Table 3. Statistics of analytical models of leaching adding chlorides.

Curve/Statistic	MAD	MSE	MAPE
R(t) (Chloride 20 g/L)	1.68×10^{-4}	4.59×10^{-7}	5.40×10^{-4}
R(t) (Chloride 50 g/L)	9.17×10^{-5}	5.23×10^{-7}	5.89×10^{-4}

The expected recovery of copper for the different configurations in 90 days of leaching is presented in Table 4.

Table 4. Recovery for each configuration in a 90-day leaching time.

Configuration	Recovery (%)
Leaching of secondary copper sulfides with sulfuric acid	40.5
Leaching of secondary copper sulfides adding chlorides (20 g/L)	46.5
Leaching of secondary copper sulfides adding chlorides (50 g/L)	58.1
Leaching of copper oxides with sulfuric acid	64.6

2.6. Modeling and Simulation of Heap Leaching Using a DES Framework

Once the process workflow of heap leaching has been characterized, it is possible to model the heap leach stage sequentially with the Arena simulation software. The update of copper recovery over time is simulated by parametrizing the analytical models retrieved from the literature, and incorporating them into the Arena simulation [23].

The schematic of the simulation model is presented in Figure 4, next to the subprocess responsible for the update in discrete time. The update of the recovery state is carried out whenever a production campaign is in development, while the use of the operational parameters is updated in the module "Assignment of attributes to the piles", and the recovery of ore is obtained from the analytical models derived from Equations (1) and (2), (these equations depend on the leaching time and operating conditions of the site).
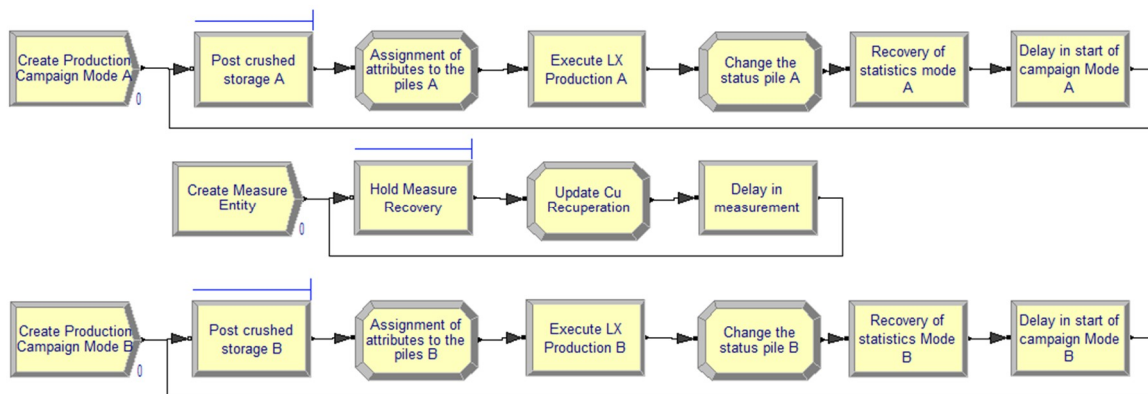
Figure 4. High-level diagram of heap leaching in Arena Simulation Software.

The heap leaching process is modeled by production campaigns, whose start is determined by the availability of inventories of the crushing phase, the development of the campaign corresponding to the production of each heap, the limited production capacity due to available physical space, and the downstream storage capacity. For each heap, the expected recovery of ore is measured according to the adjusted analytical models and the production in tons considering the variations in ore grades of the feed.

The storage of crushed material works under the logic of inventory theory [3], where the comminution product is kept waiting until the end of the leaching campaign. The module "Post crushed storage" stores the ore that will enter the leaching process when its respective mode of operation is activated. Each mode of operation is determined by the type of ore to be leached, and the decision to apply a given mode depends on the maximum and minimum stock levels established for each type of mineral. The current context considers two modes of operation:

- Mode A: Leaching of copper oxides.
- Mode B: Leaching of copper sulfide minerals (secondary sulfides).

The assignment of attributes to the heaps, such as the grade of each type of copper ore, is obtained from ore data from the *Empresa Nacional de Minería* (ENAMI), which is a Chilean state-owned enterprise. These attributes are taken as input variables for the analytical models used to estimate the expected recovery of ore under operational conditions. After a simulated leaching campaign, recovery results are saved. A comparative analysis of simulated leaching operations, with and without an additional mode, allows us to quantify the benefit of implementing the additional mode.

3. Discussion of Results

3.1. Simulated Scenarios

With the objective of evaluating the variation in the leaching productivity through the incorporation of analytical models that integrate mineralogical characteristics under conditions of uncertainty, the following scenarios are defined:

- Scenario 1 (standard operation): Leaching of copper oxides and secondary copper sulfides adding sulfuric acid only. The leaching of secondary sulfides with sulfuric acid slows down the process of extracting ore from the rock, increasing the time required until the marginal extraction of ore is negligible [12,34].
- Scenario 2 (proposed operation): Leaching of oxides with sulfuric acid and leaching of secondary sulfides with chloride. The leaching of secondary sulfides by adding chloride accelerates the recovery of copper from sulfide minerals, decreasing the leaching time [34–37].

Scenario 1:

From the graphical analysis of copper recovery for each production campaign (see Figure 5), a decrease in the expected recovery of copper ore can be observed in sulfide mineral leaching campaigns using sulfuric acid as reagent (without incorporating additives), due to the slower dissolution kinetics of the secondary copper sulfides.
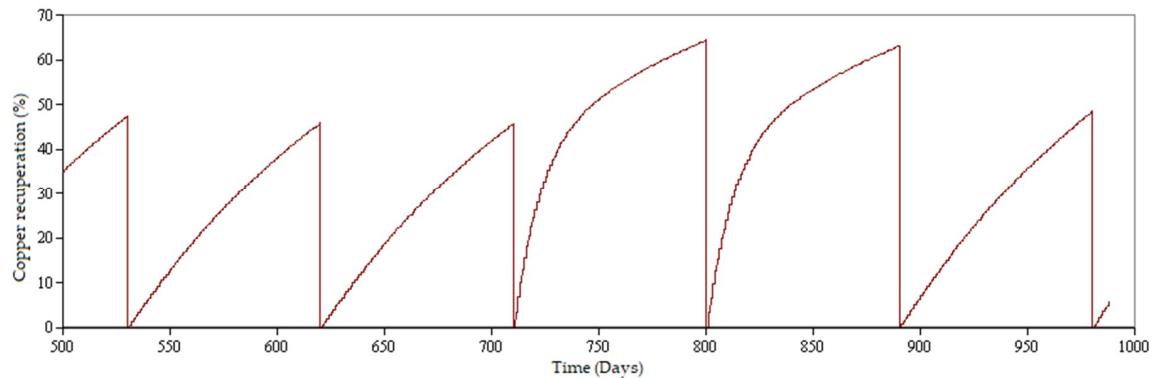

Figure 5. Copper recovery of base case maintaining a single mode of operation

Then the average copper recovery is approximately 65% in the case of oxide ores, and 40% in the case of sulfide ores. Of the total production time, 61% of the time was for processing oxide ores, and 39% for sulfide ores, hence an average recovery of approximately 55%.

Scenario 2:

A similar analysis for scenario 2 reveals that 61% of the time was spent on oxide ores, for which only sulfuric acid was used as reagent, while 39% was on sulfide minerals, using sulfuric acid and chlorides as additives. The average recovery of ore is maintained at 65% for operational mode A and increases to 58% for mode B (improvements in extraction derived from the addition of chlorides), working at a chloride concentration of 50 g/L. The resulting average recovery is approximately 62%.

The benefit of having alternate modes of operation is illustrated in Figures 6 and 7, showing that the expected copper recovery from sulfide ores is greater when varying the mode of operation, being independent of the characteristics of the feed and considering that the leaching time remains constant. (Leaching time is kept constant due to the increase in opportunity costs of maintaining a longer time of a leaching heap whose recovery rate decreases over time).
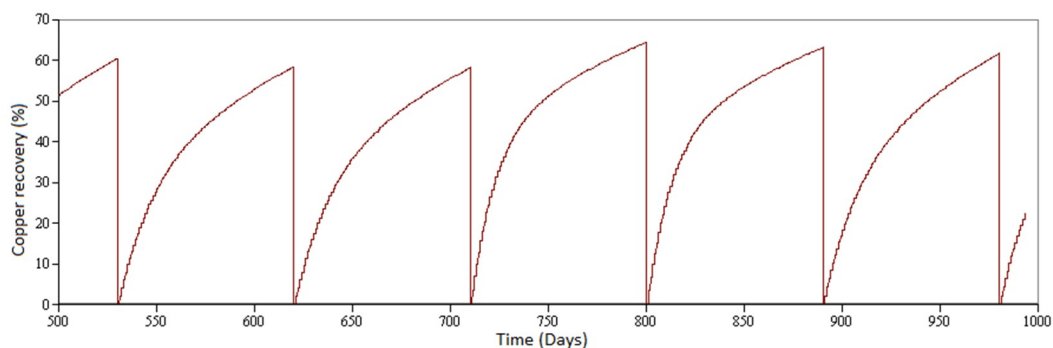

Figure 6. Copper recovery for the proposed scenario (two operation modes).
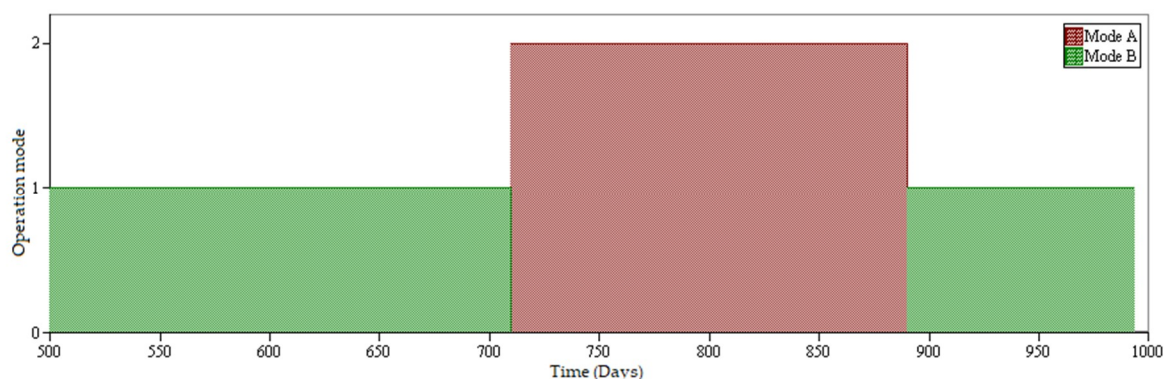
Figure 7. Mode of operation for the proposed scenario.

Considering two modes of operation, the objective is to optimize production by alternating the modes of operation as a function of the feed, avoiding instances of lower recovery of copper with mode A (leaching of oxide ores with sulfuric acid) whenever mode B (leaching of sulfides by adding chloride) will be more appropriate; this is the case when there are sufficient sulfides that a detrimental passivation layer will form in the presence of sulfuric acid. This passivation causes a decrease in recoveries when leaching secondary sulfides with sulfuric acid, that can be mitigated with longer exposure time to the leaching agent, but this means an increase in production costs, considering the increases in the consumption of acid and the opportunity costs of the use of the leaching equipment; the chloride counteracts this phenomenon.

3.2. Comparison of Samples

In order to compare the productivity of the leaching phase under the scenarios considered, a hypothesis test is carried out [38], for which the null hypothesis is defined as:

$$H_0 : \mu_2 = \mu_1$$

where μ_2 represents the average production in thousands of tons of the leaching phase considering changes in the modes of operation, and μ_1 represents the average value of production considering a single mode of production. The alternate hypothesis is given by:

$$H_a : \mu_2 > \mu_1$$

Developing the hypothesis test in the statistical analysis software Minitab 18 [39], and considering a sample size of 100 simulations, it can be concluded that the size of the production average of the proposed situation is greater than the current situation, as shown in Figure 8. It is further concluded that the hypothesis test is significant, since the *p*-value is less than the level of significance, as shown in Figure 9.

Individual Samples		
Statistics	Actually	Proposal
Sample size	100	100
Mean	3852.1	4399.0
90% CI	(3800, 3904)	(4340.1, 4457.9)
Standard deviation	313.11	354.61

Figure 8. Statistics test of 2 samples (CI: Confidence interval of 90%).

Mean Test
Is Actually less than Proposal?

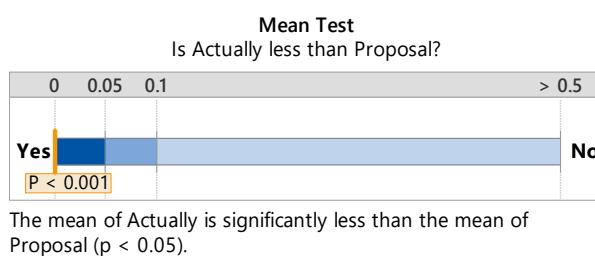The mean of Actually is significantly less than the mean of Proposal (p < 0.05).

Figure 9. *p*-value of the hypothesis test.

The confidence interval quantifies the uncertainty associated with the estimation of the difference in the means from the data of the samples, so it is possible to have more than 90% certainty that the true difference is between −625.08 and −468.71, and a 95% assurance that it is less than −468.71, as shown in Figures 10 and 11.

Difference Between Samples

Statistics	*Difference
Difference	−546.89
90% CI	(−625.08, −468.71)

*Difference = Actually − Proposal

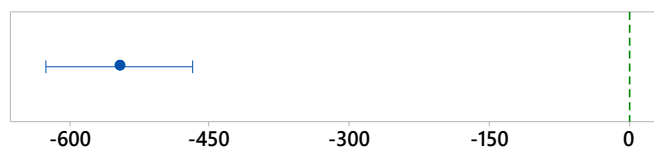**Figure 10.** Differences of the samples.

Figure 11. A 90% confidence interval for the difference.

Finally, comparing the data distributions for both samples (Figure 12), the difference of the mean values of the samples can be observed graphically. Although the distributions have some overlap, the means are several error bars away.
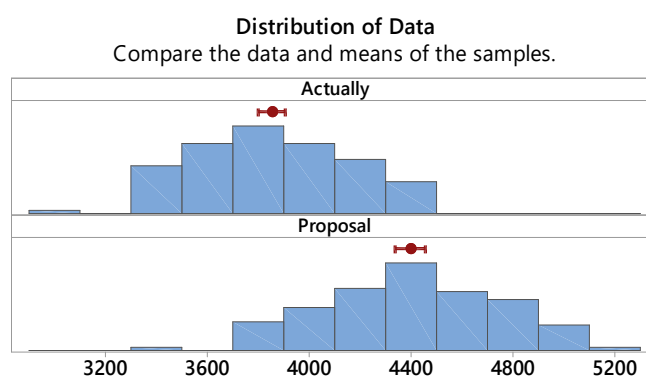
Distribution of Data
Compare the data and means of the samples.

Figure 12. Distribution of production for both samples.

In summary, when copper recovery is carried out by means of a single mode of operation (simulation based on analytical models extracted from the literature, which does not consider variations in reagent concentrations), there may not be a systemic response to the changing mineralogical characteristics of the feed, resulting in lost production.

4. Conclusions

4.1. Conclusions

Mineral deposits tend to be heterogeneous, which forces the processing parameters to evolve over time. In this document, a simulation of the production sequence of the heap leaching was considered, simplifying the feeding to only two types of ore. However, the framework could be extended to a greater number of mineral types that could come from a range of geological domains in a mine, as long as the ore to be processed is of interest and it is technically and economically possible to process it through the hydrometallurgical route.

The use of alternating modes of operation has the potential to improve the strategic mine plan, making the value chain more flexible by making a better use of assets and improving mineral recovery, addressing the varying mineralogical characteristics of the feed. The hypothesis test indicates the average production increase to incorporate the dynamics of operating modes in heap leaching, in this case increasing the expected recovery of copper, from 55% to 62%.

The quantification of the improvements by addressing uncertainty in the processing of minerals through alternating modes of operation, the incorporation of analytical models for the unit processes and the sequential simulation through a discrete event simulation framework constitute an opportunity to effectively model and plan leaching operations, from a system-wide perspective. The approach can assist in local and ultimately global mine optimizations for cash flows and asset utilization.

4.2. Future Work

To further advance the operation research of leaching processes, the following avenues are being considered:

1. Include other modes of operation and analytical models that incorporate more operational variables to the process, together with parameters that have a significant impact on recovery.
2. Study the impact on an industrial scale of operating the leaching process with alternating modes of operation, including the analysis operating and capital costs.

References

1. Navarra, A.; Alvarez, M.; Rojas, K.; Menzies, A.; Pax, R.; Waters, K. Concentrator operational modes in response to geological variation. *Miner. Eng.* **2019**, *134*, 356–364. [CrossRef]
2. Hustrulid, W.; Kuchta, M.; Martin, R. *Open Pit Mine Planning and Design*; CRC Press: Boca Raton, FL, USA, 2013; ISBN 9781466575127.
3. Dimitrakopoulos, R. Strategic mine planning under uncertainty. *J. Min. Sci.* **2011**, *47*, 138–150. [CrossRef]
4. Rahmanpour, M.; Osanloo, M. Determination of value at risk for long-term production planning in open pit mines in the presence of price uncertainty. *J. S. Afr. Inst. Min. Metall.* **2016**, *116*, 8–11. [CrossRef]
5. Upadhyay, S.P.; Askari-Nasab, H. Simulation and optimization approach for uncertainty-based short-term planning in open pit mines. *Int. J. Min. Sci. Technol.* **2018**, *28*, 153–166. [CrossRef]
6. Drebenstedt, C.; Singhal, R. *Mine Planning and Equipment Selection*; Brookfield: Rotterdam, The Netherlands, 2014; ISBN 978-3-319-02677-0.
7. Harris, G.B.; White, C.W.; Demopoulos, G.P.; Ballantyne, B. Recovery of copper fromamassive polymetallic sulphide by high concentration chloride leaching. *Can. Metall. Q.* **2008**, *47*, 347–356. [CrossRef]
8. Robertson, S.W.; Van Staden, P.J.; Seyedbagheri, A. Advances in high-temperature heap leaching of refractory copper sulphide ores. *J. S. Afr. Inst. Min. Metall.* **2012**, *112*, 1045–1050.

9. Petersen, J. Heap leaching as a key technology for recovery of values from low-grade ores—A brief overview. *Hydrometallurgy* **2016**, *165*, 206–212. [CrossRef]

10. COCHILCO. *Caracterización de los Costos de la Gran Minería del Cobre*; COCHILCO: Santiago, Chile, 2015.

11. Lu, J.; Dreisinger, D.; West-Sells, P. Acid curing and agglomeration for heap leaching. *Hydrometallurgy* **2017**, *167*, 30–35. [CrossRef]

12. Schlesinger, M.; King, M.; Sole, K.; Davenport, W. *Extractive Metallurgy of Copper*, 5th ed.; Elsevier: Amsterdam, The Netherlands, 2011; ISBN 9780080967899.

13. Liu, H.; Xia, J.; Nie, Z.; Ma, C.; Zheng, L.; Hong, C.; Zhao, Y.; Wen, W. Bioleaching of chalcopyrite by Acidianus manzaensis under different constant pH. *Miner. Eng.* **2016**, *98*, 80–89. [CrossRef]

14. Ruan, R.; Zou, G.; Zhong, S.; Wu, Z.; Chan, B.; Wang, D. Why Zijinshan copper bioheapleaching plant works efficiently at low microbial activity-Study on leaching kinetics of copper sulfides and its implications. *Miner. Eng.* **2013**, *48*, 36–43. [CrossRef]

15. Lee, J.; Acar, S.; Doerr, D.L.; Brierley, J.A. Comparative bioleaching and mineralogy of composited sulfide ores containing enargite, covellite and chalcocite by mesophilic and thermophilic microorganisms. *Hydrometallurgy* **2011**, *105*, 213–221. [CrossRef]

16. Zhang, R.; Sun, C.; Kou, J.; Zhao, H.; Wei, D.; Xing, Y. Enhancing the leaching of chalcopyrite using acidithiobacillus ferrooxidans under the induction of surfactant Triton X-100. *Minerals* **2018**, *9*, 11. [CrossRef]

17. Ma, L.; Wang, X.; Liu, X.; Wang, S.; Wang, H. Intensified bioleaching of chalcopyrite by communities with enriched ferrous or sulfur oxidizers. *Bioresour. Technol.* **2018**, *268*, 415–423. [CrossRef] [PubMed]

18. Ma, L.; Wu, J.; Liu, X.; Tan, L.; Wang, X. The detoxification potential of ferric ions for bioleaching of the chalcopyrite associated with fluoride-bearing gangue mineral. *Appl. Microbiol. Biotechnol.* **2019**, *103*, 2403–2412. [CrossRef] [PubMed]

19. CESCO. *La Minería Como Plataforma Para el Desarrollo: Hacia Una Relación Integral y Sustentable de la Industria Minera en Chile*; CESCO: Santiago, Chile, 2013.

20. Beiza, L. *Lixiviación de Mineral y Concentrado de Calcopirita en Medios Clorurados*; Universidad Católica del Norte: Antofagasta, Chile, 2012.

21. Devore, J. *Probability & Statistics for Engineering and the Sciences*, 8th ed.; Cengage Learning: Boston, MA, USA, 2010; ISBN 0-538-73352-7.

22. Neeraj, R.R.; Nithin, R.P.; Niranjhan, P.; Sumesh, A.; Thenarasu, M. Modelling and simulation of discrete manufacturing industry. *Mater. Today Proc.* **2018**, *5*, 24971–24983. [CrossRef]

23. Kelton, W.D. *Simulation with Arena*; McGraw-Hill Education: New York, NY, USA, 2015; ISBN 978-0-07-340131-7.

24. Van Staden, P.J.; Kolesnikov, A.V.; Petersen, J. Comparative assessment of heap leach production data—1. A procedure for deriving the batch leach curve. *Miner. Eng.* **2017**, *101*, 47–57. [CrossRef]

25. Ordóñez, J.; Condori, A.; Moreno, L.; Cisternas, L. Heap leaching of caliche ore. modeling of a multicomponent system with particle size distribution. *Minerals* **2017**, *7*, 180.

26. Morrison, R.D.; Shi, F.; Whyte, R. Modelling of incremental rock breakage by impact—For use in DEM models. *Miner. Eng.* **2007**, *20*, 303–309. [CrossRef]

27. Leiva, C.; Flores, V.; Salgado, F.; Poblete, D.; Acuña, C. Applying softcomputing for copper recovery in leaching process. *Sci. Prog.* **2017**, *2017*, 6. [CrossRef]

28. Miki, H.; Nicol, M.; Velásquez-Yévenes, L. The kinetics of dissolution of synthetic covellite, chalcocite and digenite in dilute chloride solutions at ambient temperatures. *Hydrometallurgy* **2011**, *105*, 321–327. [CrossRef]

29. Mellado, M.E.; Cisternas, L.A.; Gálvez, E.D. An analytical model approach to heap leaching. *Hydrometallurgy* **2009**, *95*, 33–38. [CrossRef]

30. Mellado, M.E.; Gálvez, E.D.; Cisternas, L.A. Stochastic analysis of heap leaching process via analytical models. *Miner. Eng.* **2012**, *33*, 93–98. [CrossRef]

31. Mellado, M.; Cisternas, L.; Lucay, F.; Gálvez, E.; Sepúlveda, F. A posteriori analysis of analytical models for heap leaching using uncertainty and global sensitivity analyses. *Minerals* **2018**, *8*, 44. [CrossRef]

32. Dixon, D.G.; Hendrix, J.L. A mathematical model for heap leaching of one or more solid reactants from porous ore pellets. *Metall. Trans. B* **1993**, *24*, 1087–1102. [CrossRef]

33. Dixon, D.G.; Hendrix, J.L. A general model for leaching of one or more solid reactants from porous ore particles. *Metall. Trans. B* **1993**, *24*, 157–169. [CrossRef]

34. Helle, S.; Jerez, O.; Kelm, U.; Pincheira, M.; Varela, B. The influence of rock characteristics on acid leach extraction and re-extraction of Cu-oxide and sulfide minerals. *Miner. Eng.* **2010**, *23*, 45–50. [CrossRef]

35. Jones, D.A.; Paul, A.J.P. Acid leaching behavior of sulfide and oxide minerals determined by electrochemical polarization measurements. *Miner. Eng.* **1995**, *8*, 511–521. [CrossRef]

36. Cheng, C.Y.; Lawson, F. The kinetics of leaching chalcocite in acidic oxygenated sulphate-chloride solutions. *Hydrometallurgy* **1991**, *27*, 249–268. [CrossRef]

37. Ruiz, M.C.; Honores, S.; Padilla, R. Leaching kinetics of digenite concentrate in oxygenated chloride media at ambient pressure. *Metall. Mater. Trans. B Process Metall. Mater. Process. Sci.* **1998**, *29*, 961–969. [CrossRef]

38. Douglas, C. *Montgomery: Design and Analysis of Experiments*, 8th ed.; John Wiley & Sons: New York, NY, USA, 2012; ISBN 978-1-118-14692-7.

39. Mathews, P.G. *Design of Experiments with MINITAB*; William, A., Ed.; ASQ Quality Press: Milwaukee, WI, USA, 2005; ISBN 0873896378.

Extraction of Mn from Black Copper Using Iron Oxides from Tailings and Fe^{2+} as Reducing Agents in Acid Medium

Kevin Pérez [1], **Norman Toro** [1,2,*], **Eduardo Campos** [3], **Javier González** [1], **Ricardo I. Jeldres** [4], **Amin Nazer** [5] **and Mario H. Rodriguez** [6]

1 Departamento de Ingeniería en Metalurgia y Minas, Universidad Católica del Norte, Antofagasta 1270709, Chile; kps003@alumnos.ucn.cl (K.P.); javier.gonzalez@ucn.cl (J.G.)

2 Department of Mining, Geological and Cartographic Department, Universidad Politécnica de Cartagena, Murcia 30203, Spain

3 Departamento de Ciencias Geológicas, Universidad Católica del Norte, Antofagasta 1270709, Chile; edcampos@ucn.cl

4 Departamento de Ingeniería Química y Procesos de Minerales, Universidad de Antofagasta, Antofagasta 1270300, Chile; ricardo.jeldres@uantof.cl

5 Departamento de Construcción, Universidad de Atacama, Copiapó 1531772, Chile; amin.nazer@uda.cl

6 Laboratorio de Metalurgia Extractiva y Síntesis de Materiales (MESiMat-ICB-UNCUYO-CONICET-FCEN, Padre Contreras 1300, Parque Gral. San Martín), CP 5500 Mendoza, Argentina; mrodriguez@uncu.edu.ar

* Correspondence: ntoro@ucn.cl; Tel.: +56-55-2651-021

Abstract: Exotic type deposits include several species of minerals, such as atacamite, chrysocolla, copper pitch, and copper wad. Among these, copper pitch and copper wad have considerable concentrations of manganese. However, their non-crystalline and amorphous structure makes it challenging to recover the elements of interest (like Cu or Mn) by conventional hydrometallurgical methods. For this reason, black copper ores are generally not incorporated into the extraction circuits or left unprocessed, whether in stock, leach pads, or waste. Therefore, to dilute MnO_2, the use of reducing agents is essential. In the present research, agitated leaching was performed to dissolve Mn of black copper in an acidic medium, comparing the use of ferrous ions and tailings as reducing agents. Two samples of black copper were studied, of high and low grade of Mn, respectively, the latter with a high content of clays. The effect on the reducing agent/black copper ratio and the concentration of sulfuric acid in the system were evaluated. Better results in removing Mn were achieved using the highest-grade black copper sample when working with ferrous ions at a ratio of Fe^{2+}/black copper of 2/1 and 1 mol/L of sulfuric acid. Besides, the low-grade sample induced a significant consumption of H_2SO_4 due to the high presence of gangue and clays.

Keywords: waste treatment; reducing agent; manganese

1. Introduction

Copper mining is Chile's most important economic activity, accounting for 10% of the gross national product (GNP) [1]. According to the latest figures from the Chilean Copper Commission, 5.83 million metric tons of copper were produced in 2018, making Chile the leading copper producer, accounting for 27.7% of global copper production. Experts from the Chilean Association of Geologists have stated that Chile has the largest copper deposits in the world [2], with a total copper reserve of 170 million metric tons [3].

Porphyry minerals in deposits like pyrite oxidize when submitted to geological agents. When pyrite reacts with water, it generates sulfuric acid, promoting the mobility of metals like copper that can be transported under certain potential and pH conditions, precipitating downstream and forming what are termed exotic deposits [4–8].
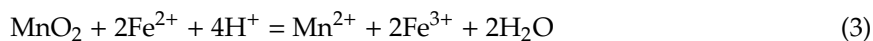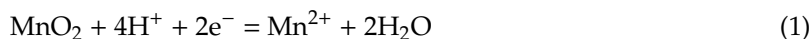
These deposits are composed of different copper containing phases such as chrysocolla, atacamite, copper pitch, and copper wad [6,9]. The latter two are defined as mineraloids because they crystalize amorphously [2]. They are also termed silicates rich in Si-Fe-Cu-Mn [10].

Some examples of exotic deposits in Chile are Mina Sur in Chuquicamata [11], Damiana in El Salvador [7], Huanquintipa in Collahuasi [12], and La Cascada, Lomas Bayas Spence, El Tesoro [2], and Angélica in Tocopilla [13]. The copper and manganese of this type of deposit are often associated with oxidized minerals, mainly chrysocolla, which, in turn, are associated with gangue that can negatively affect leaching [11]. Silicates and aluminosilicates, like mica and clay minerals, have the capacity to consume some of the acid generated by oxidization [14]. Clay minerals, like montmorillonite, kaolinite, and smectite, easily absorb acid [15]. Other minerals, like chlorites and biotite, also consume large amounts of acid over the long term [15]. Helle et al. [11] studied the effect of gangue and clay minerals on the leaching of copper oxides such as atacamite, chrysocolla, and malachite. The copper oxides were treated with a strong solution of sulfuric acid (265 g/L) in small columns at ambient temperature (18 to 21 °C), with the addition of synthetic rocks composed of 57% quartz, 1% phase mineral, and 42% reactive gangue. The authors concluded that copper retention and acid consumption were the result of the presence of smectite, mordenite gangue, kaolinite, illite, and quartz.
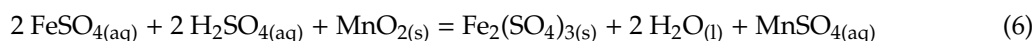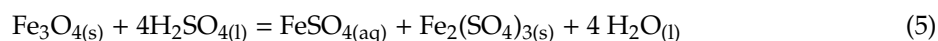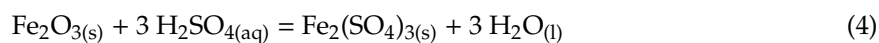
Researchers have indicated that it is not possible to recover copper associated with these silicates using conventional hydrometallurgical methods for oxidized copper because of their non-crystalline or amorphous structure [16]. However, recent studies on techniques for extracting manganese have found that silicates can be recovered by treating them in a similar manner to treatment for manganese, owing to the similarity in their metallurgical behavior [17].

It has been demonstrated that a reducing agent is required to extract Mn from MnO_2 in acid media [18,19]. Other studies have obtained good results dissolving MnO_2 with different reducing agents like H_2SO_3 [20], SO_2 [21], wastewater from producing molasses-based alcohol [22], and various iron-based reducing agents [20,23,24]. Iron, which is abundant and inexpensive, has proven to be a good alternative when working with MnO_2 in acid media.
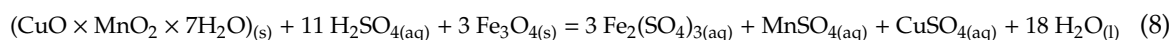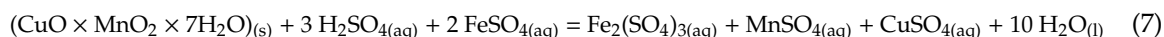
Zakeri et al. [25] obtained an Mn extraction rate of 90% in 20 min at ambient temperature with the addition of ferrous ions to the system, with an Fe^{2+}/MnO_2 molar ratio of 3.0 and H_2SO_4/MnO_2 ratio of 2.0. They proposed the following series of reactions for MnO_2 dissolution:

$$MnO_2 + 4H^+ + 2e^- = Mn^{2+} + 2H_2O \tag{1}$$

$$2Fe^{2+} = 2Fe^{3+} + 2e^- \tag{2}$$

$$MnO_2 + 2Fe^{2+} + 4H^+ = Mn^{2+} + 2Fe^{3+} + 2H_2O \tag{3}$$

Toro et al. [26] leached Mn nodules using tailings with high Fe_3O_4 contents (58.52%) from slag flotation for the recovery of Cu from the Alto Norte Foundry Plant and optimized the working parameters (Fe_2O_3/MnO_2 ratio and H_2SO_4 concentration). They found that for short periods of time (5 to 20 min), the optimal MnO_2/Fe_2O_3 ratio is 1/3, with H_2SO_4 concentration of 0.1 mol/L, giving Mn extraction rates of approximately 70%. The authors proposed the following reactions to dissolve MnO_2 with the addition of iron oxides:

$$Fe_2O_{3(s)} + 3\,H_2SO_{4(aq)} = Fe_2(SO_4)_{3(s)} + 3\,H_2O_{(l)} \tag{4}$$

$$Fe_3O_{4(s)} + 4H_2SO_{4(l)} = FeSO_{4(aq)} + Fe_2(SO_4)_{3(s)} + 4\,H_2O_{(l)} \tag{5}$$

$$2\,FeSO_{4(aq)} + 2\,H_2SO_{4(aq)} + MnO_{2(s)} = Fe_2(SO_4)_{3(s)} + 2\,H_2O_{(l)} + MnSO_{4(aq)} \tag{6}$$

The following reactions are proposed to dissolve manganese from black copper:

$$(CuO \times MnO_2 \times 7H_2O)_{(s)} + 3\,H_2SO_{4(aq)} + 2\,FeSO_{4(aq)} = Fe_2(SO_4)_{3(aq)} + MnSO_{4(aq)} + CuSO_{4(aq)} + 10\,H_2O_{(l)} \quad (7)$$

$$(CuO \times MnO_2 \times 7H_2O)_{(s)} + 11\,H_2SO_{4(aq)} + 3\,Fe_3O_{4(s)} = 3\,Fe_2(SO_4)_{3(aq)} + MnSO_{4(aq)} + CuSO_{4(aq)} + 18\,H_2O_{(l)} \quad (8)$$

Equation (5) gives the reaction of magnetite with sulfuric acid forming ferrous sulfate, which is a good reducing agent for the leaching of MnO_2. This is shown in Equation (6), where Mn^{4+} is reduced to Mn^{2+}. In Equation (7), the solution of manganese from black copper (copper wad) is proposed, using ferrous sulfate expressed in Equation (5). In general, Equation (8) represents the dissolution of manganese with iron oxide as a reducing agent, which demands high concentrations of sulfuric acid to first form $FeSO_4$ from Fe_3O_4 and then continues to dissolve manganese until a manganese sulfate solution is obtained.

In Chile, big copper mining poses new challenges and needs. It seeks to diversify the extractions of other elements (besides the Cu) in order to boost the export of commodities and raise employment. Black copper ores are resources that are generally not incorporated into the extraction circuits or left untreated, whether in stock, leach pads, or waste [27]. These exotic minerals have considerable amounts of Mn (approximately 29%), which represent a commercial appeal. Besides, according to the study conducted by Benavente et al. [27], by dissolving black copper ores in a reducing condition, the decrease in redox potential favors the dissolution of manganese. This would allow the subsequent extraction of the Cu present in black copper, given the potential commercial value of these "wastes".

This work aimed to study the dissolution of MnO_2 from black copper in acid media comparing the use of iron and iron oxide tailings as reducing agents.

2. Methodology

2.1. Black Oxide Samples

Two samples of black copper, obtained from different mines in northern Chile, were used in this investigation. One sample, black copper sample-1 (BCS-1), was from a high-grade vein and was almost 100% pure, while the other, black copper sample-2 (BCS-2), was low-grade and taken from the mine dumpsite. The black oxides ores were ground in a porcelain mortar to sizes ranging from −173 to +147 μm. Chemical composition was determined by inductively coupled plasma atomic emission spectrometry (ICP-AES). Table 1 shows the chemical composition of the samples. A QEMSCAN analysis was applied, which is an electronic scanning microscope that was modified both in hardware and software. This performed the identification and automated quantification of ranges of elementary definitions that can be associated with inorganic solid phases (minerals, alloys, slags, etc.). To determine the mineralogical composition, the samples were mounted on briquettes and polished. The identification, mapping of 2-D distribution, and quantification of inorganic phases, was done by combining the emissions of retro-dispersed electrons (BSE) with a Zeiss EVO series, a Bruker AXS XFlash 4010 detector (Bruker, Billerica, MA, USA) and the iDiscover 5.3.2.501 software (FEI Company, Brisbane, Australia). The QEMSCAN analyses are based on the automated obtaining of EDS spectra (dispersed energy from X-rays) in hundreds of thousands or millions of collected analysis points, each in a time of milliseconds. The classification of mineralogical phases is done by classifying each EDS spectrum in a hierarchical and descending compositional list known as the "SIP List". The BSE image is used to discriminate between resin and graphite in the sample, to specify entries in the SIP list, and to establish thresholds for acceptance or rejection of particles. As a result, pixelated, 2-D and false color images of a specimen or a representative subsample of particles are obtained. Each pixel retains its elementary and BSE brightness information, which allows subsequent offline data processing. Through software, customized filters are generated that allow the quantification of ore and gangue species, mineral release, associations between inorganic phases, and the classification of particles

according to criteria of shape, size, texture, etc. Figure 1 shows the chemical species to black oxides using QEMSCAN.

Table 1. Chemical composition of black oxide samples.

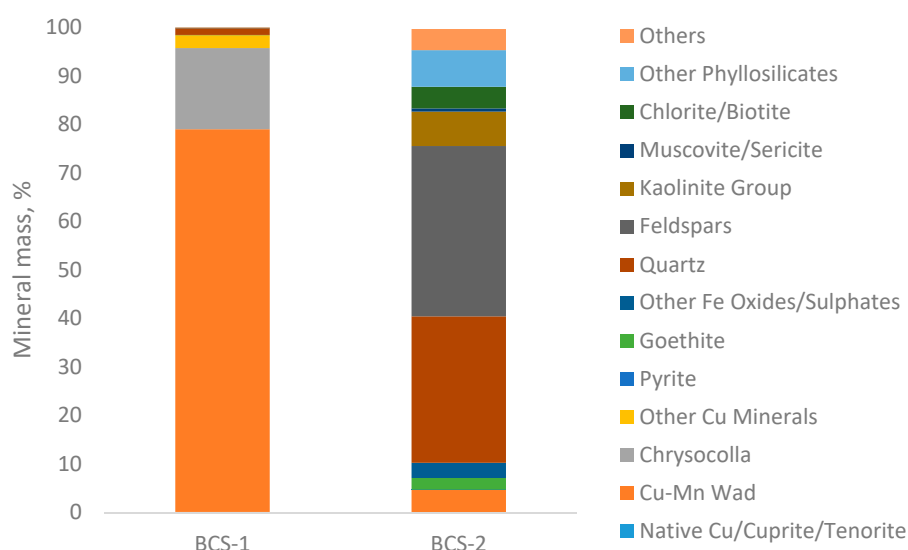| Sample	Mn (%)	Fe (%)
Black Copper Sample-1	22.01	7.92
Black Copper Sample-2	0.51	3.88

Figure 1. Detailed modal mineralogy.

Table 2 shows the mineralogical composition of the black copper samples. Copper wad refers to a subgroup of copper composed of manganese and copper hydroxides, as well as also traces of other elements such as Co, Ca, Fe, Al, Si, and Mg.

Table 2. The mineralogical composition of the black copper samples as determined by QEMSCAN.

Mineral (% Mass)	Black Copper Sample-1	Black Copper Sample-2
Native Cu/Cuprite/Tenorite	0.12	0.00
Cu-Mn Wad	78.90	4.64
Chrysocolla	16.72	0.03
Other Cu Minerals	2.69	0.03
Pyrite	0.00	0.01
Goethite	0.01	2.39
Other Fe Oxides/Sulphates	0.00	3.15
Quartz	1.41	30.20
Feldspars	0.02	35.11
Kaolinite Group	0.01	7.08
Muscovite/Sericite	0.01	0.67
Chlorite/Biotite	0.01	4.45
Montmorillonite	0.00	4.56
Others	0.09	7.35
Total	100	100

2.2. Ferrous Ions

The ferrous ions used for this investigation ($FeSO_4 \times 7H_2O$) were WINKLER brand, with a molecular weight of 278.01 g/mol.

2.3. Iron Oxide Tailings

The iron oxide tailings used were from the Altonorte Smelting Plant. The particle sizes were in a range between −75 to +53 μm. The methods used to determine its chemical and mineralogical composition were the same as those used in black copper ores. Table 3 shows the minerals (and chemical formulas) from QEMSCAN analysis, noting that several iron-containing phases were present from which the Fe content was estimated at 41.9%. As the Fe was mainly in the form of magnetite, the most appropriate method of extraction was the same as that used by Toro et al. [26].

Table 3. Mineralogical composition of tailings, as determined by QEMSCAN.

Mineral	Amount % (*w/w*)
Chalcopyrite/Bornite $(CuFeS_2/Cu_5FeS_4)$	0.47
Tennantite/Tetrahedrite $(Cu_{12}As_4S_{13}/Cu_{12}Sb_4S_{13})$	0.03
Other Cu Minerals	0.63
Cu–Fe Hydroxides	0.94
Pyrite (FeS_2)	0.12
Magnetite (Fe_3O_4)	58.52
Specular Hematite (Fe_2O_3)	0.89
Hematite (Fe_2O_3)	4.47
Ilmenite/Titanite/Rutile $(FeTiO_3/CaTiSiO_5/TiO_2)$	0.04
Siderite $(FeCO_3)$	0.22
Chlorite/Biotite $(Mg)_3(Si)_4O_{10}(OH)_2(Mg)_3(OH)_6/K(Mg)_3AlSi_3O_{10}(OH)_2$	3.13
Other Phyllosilicates	11.61
Fayalite (Fe_2SiO_4)	4.59
Dicalcium Silicate (Ca_2SiO_4)	8.30
Kirschsteinite $(CaFeSiO_4)$	3.40
Forsterite (Mg_2SiO_4)	2.30
Barite $(BaSO_4)$	0.08
Zinc Oxide (ZnO)	0.02
Lead Oxide (PbO)	0.01
Sulfate (SO_4)	0.20
Others	0.03
Total	100.00

2.4. Reagent and Leaching Test

The sulfuric acid used for the leaching tests was grade P.A., with 95–97% purity, a density of 1.84 kg/L, and a molecular weight of 98.80 g/mol. The leaching tests were carried out in a 50 mL glass reactor with a 0.01 solid/liquid ratio. A total of 200 mg of black oxide ore was maintained in suspension with the use of a five-position magnetic stirrer (IKA ROS, CEP 13087-534, Campinas, Brazil) at a speed of 600 rpm. The tests were conducted at a room temperature of 25 °C, while variations were iron additives, particle size, and leaching time. The tests were performed in duplicate and measurements (or analyses) were carried out on 5 mL undiluted samples using atomic absorption spectrometry with a coefficient of variation ≤ 5% and a relative error between 5 to 10%. The measurements of pH and oxidation-reduction potential (ORP) of the leach solutions were made using a pH-ORP meter (HANNA HI-4222 (HANNA instruments, Woonsocket, Rhode Island, USA)). The solution ORP was measured in a combination ORP electrode cell composed of a platinum working electrode and a saturated Ag/AgCl reference electrode.

2.5. The Effect of the Fe/MnO$_2$ Ratio

Other investigations have shown that variables of particle size and stirring speed do not have significant effects when working with a high Fe/MnO$_2$ ratio [26,28]. Given this result, we decided to work with the following parameters: Fe/MnO$_2$ ratios of 1/1, 2/1 and 3/1, a particle size range of −75–+53 μm, a stirring speed of 600 rpm, 1 mol/L sulfuric acid, and room temperature (25 °C).

2.6. The Effect of the Acid Concentration on the System

The present research studied the effect of the sulfuric acid concentration on the system, working with H_2SO_4 concentrations of 0.5, 1, 2, and 3 mol/L under the following operating conditions: Reducing agent/black copper ratio of 1/2, particle size range of $-75 + 53$ μm, stirring speed of 600 rpm, and a temperature of 25 °C.

3. Results

3.1. The Effect of the Fe^{2+}/MnO_2 Ratio

Figure 2a,b show the results for the dissolution of two black copper samples using Fe^{2+} in acid media. As can be seen, better results were achieved with the sample BCS-1, which was due to the high presence of clay in sample BSC-2. It was observed that high Mn extraction rates can be achieved in short periods of time using MnO_2/Fe^{2+} ratios of 1/2 or less, achieving dissolution rates of over 78% in 5 min with sample BCS-1, and 65% in 5 min with sample BCS-2. The results shown in Figure 2a are similar to the 90% recovery obtained by Zakeri et al. [25] in 20 min leaching MnO_2 from manganese nodules with an Fe^{2+}/MnO_2 ratio of 3, and an H_2SO_4/MnO_2 molar ratio of 2/1. A 1/1 Fe^{2+}/MnO_2 ratio resulted in a lower MnO_2 dissolution kinetics, with an extraction of 40% in 5 min with sample A and 31% in 5 min with sample B. In general, Mn dissolution rates were similar with a longer period (30 min). However, the dissolution kinetics were slower for the sample BCS-2.
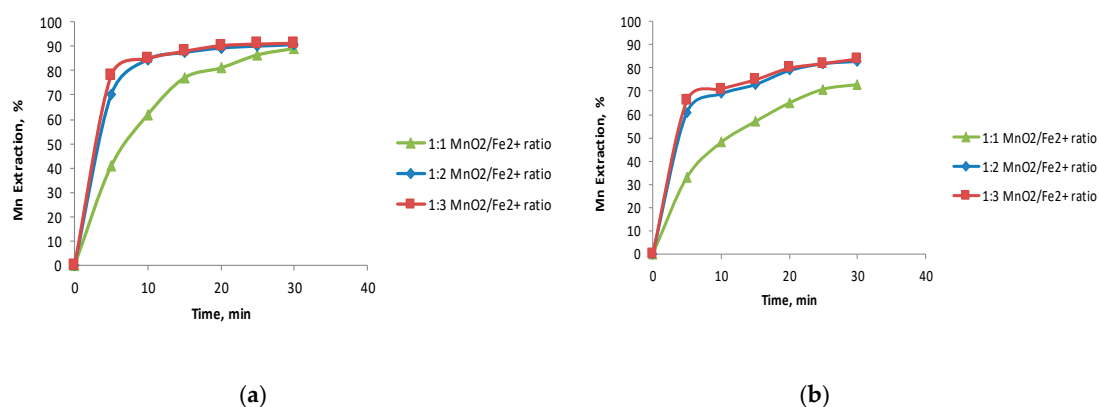

(**a**)   (**b**)

Figure 2. The effect of the Fe^{2+} concentration on MnO_2 dissolution (**a**) Black copper sample-1 (BSC-1); (**b**) Black copper sample-2 (BCS-2), 25 °C, particle size range of $-75–+53$ μm, 1 mol/L H_2SO_4.

3.2. The Effect of the Fe_2O_3/MnO_2 Ratio

Figure 3a,b show Mn dissolution with two black copper samples using Fe_2O_3 in acid media. As in earlier investigations by Toro et al. [26,28], working with an Fe_2O_3/MnO_2 ratio of 2/1 or higher significantly increased MnO_2 dissolution kinetics. There was little difference in the Mn extraction rates working with Fe_2O_3/MnO_2 ratios of either 2/1 or 3/1, while the Mn extraction fell significantly when the quantity of Fe_2O_3 was reduced. Potential and pH levels were respectively in the ranges of -0.5 to 1.3 V and -1.5 to 0.4 in all the tests in this study.
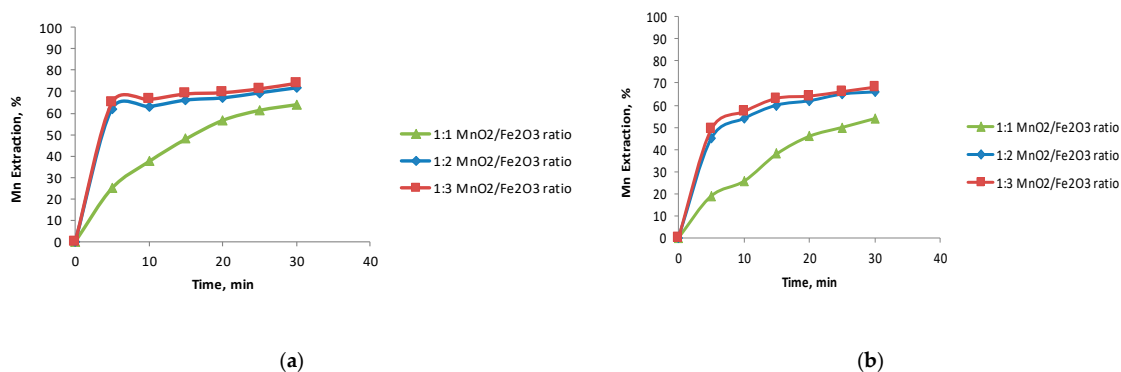
(**a**)

(**b**)

Figure 3. The effect of the iron oxide tailings concentration on MnO_2 dissolution (**a**) BSC-1; (**b**) BSC-2, 25 °C, particle size range of −75–+53 μm, 1 mol/L H_2SO_4.

3.3. The Effect of the H_2SO_4 Concentration

Figure 4 shows the effect of the acid concentration on dissolving Mn dissolution from the two black copper samples with the addition of high concentrations of iron oxides from tailings or ferrous ions. It can be seen from Figure 4a,c that for sample BCS-1, the sulfuric acid concentration was not significant in either case when working with high concentrations of the reducing agent. Differences in the effect of the acid concentration could only be noted with very low concentrations of iron oxide tailings (0.5 mol/L). The above concurs with findings of previous studies by Toro et al. [24,26] on extraction of MnO_2 from manganese nodules. The Mn extraction rate from the BCS-2 sample increased with higher concentrations of H_2SO_4, possibly owing to the high consumption of acid generated by the presence of mineral impurities in this sample, mainly montmorillonite, kaolinite, and chlorite. This is consistent with what was previously found by Helle and Kelm [29], where the leaching of exotic Cu minerals (atacamite, chrysocolla, and malachite) required higher acid consumption by incorporating reactive bargains into the system. This was driven by smectites, mordenite bargain, and the presence of kaolinite, illite, and quartz.
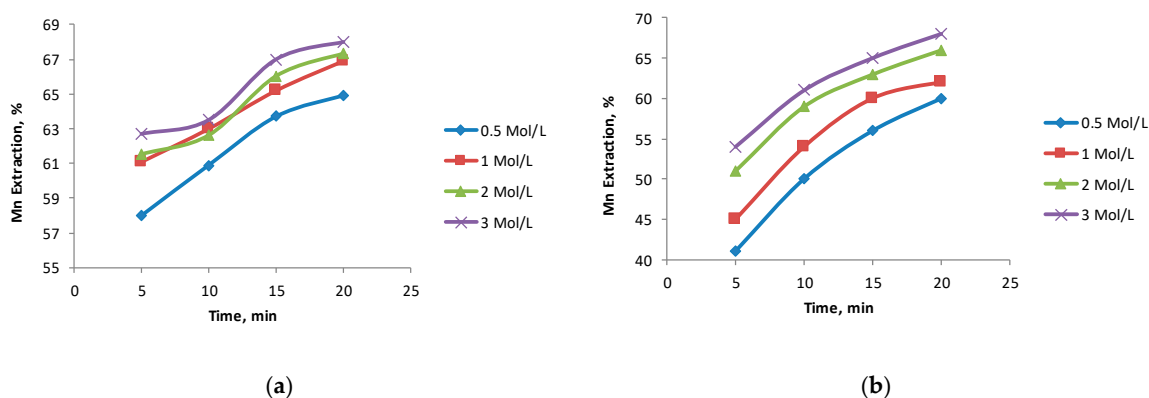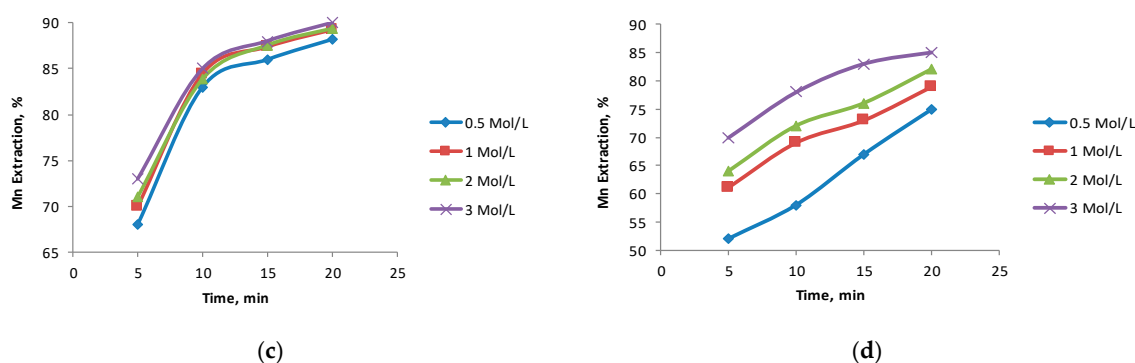

(**a**)

(**b**)

Figure 4. *Cont.*

(**c**)

(**d**)

Figure 4. The effect of the sulfuric acid concentration on the system (**a**) BSCe-1; (**b**) BSC-2, MnO_2/Fe_2O_3 ratio of 1/2; (**c**) BSC-1; (**d**) BSC-2, MnO_2/Fe^{2+} ratio of 1/2.

4. Conclusions

This study presents the results obtained for dissolving Mn from black copper using iron oxides (and specifically magnetite) from tailings and Fe^{2+} as reducing agents in acid media. Both reducing agents yielded good results with the two samples studied. Similar behavior was observed with the two samples in relation to Mn extraction, with the best results obtained in all the experiments with the BCS-1 sample. These encouraging results give new options to extract the Cu present in these exotic minerals, which are considered as industrial waste today. The main findings are the following:

(1) The ferrous ions were a better reducing agent than iron oxides to dissolve MnO_2 in black copper.
(2) The optimal reducing agent/black copper ratio was 2:1 for the studied reducing agents studied.
(3) High concentrations of H_2SO_4 had a positive effect on the dissolution of Mn with the BCS-2 sample owing to the high content of clay (montmorillonite and kaolinite) and gangue (chlorite), which consume significant amounts of acid. The acid concentration was not significant with the BCS-1 sample.
(4) The best results in this study were obtained working with the sample with fewer impurities (BCS-1), with an Fe^{2+}/black copper ratio of 2:1, and 1 mol/L of sulfuric acid.

Despite the good results obtained with BCS-1, BCS-2 was more like the mineralogy found at the industrial scale. It should be noted that although lower Mn extraction rates are obtained using tailings instead of ferrous ions, tailings can be a more attractive additive for leaching black copper because they are an industrial waste with no economic value. Given the above results, future investigations should aim to optimize operational parameters for leaching black copper minerals with high gangue content using industrial waste or wastewater as reducing agents, with the aim of taking this process to the industrial scale.

References

1. Servicio Nacional de Geología y Minería (SERNAGEOMIN). *Anuario de la Minería de Chile*; Servicio Nacional de Geología y Minería: Santiago, Chile, 2018; p. 274.
2. Menzies, A.; Campos, E.; Hernández, V.; Sola, S.; Riquelme, R. Understanding Exotic-Cu Mineralisation Part II: Characterization of 'Black Copper' ore ('Cobre Negro'). In Proceedings of the 13th SGA Biennial Meeting, Nancy, France, 24–27 August 2015; pp. 3–6.
3. U.S. Geological Survey and U.S. Department of the Interior, Mineral. *Commodity Summaries*; U.S. Geological Survey: Reston, Virginia, 2018.
4. Ossandon, C.G.; Freraut, C.R.; Gustafson, L.B.; Lindsay, D.D.; Zentilli, M. Geology of the Chuquicamata Mine: A Progress Report. *Econ. Geol.* **2001**, *96*, 249–270. [CrossRef]
5. Mote, T.I.; Becker, T.A.; Renne, P.; Brimhall, G.H. Chronology of Exotic Mineralization at El Salvador, Chile, by 40Ar/39Ar Dating of Copper Wad and Supergene Alunite. *Econ. Geol.* **2001**, *96*, 351–366. [CrossRef]
6. Cuadra, C.P.; Rojas, S.G. Oxide mineralization at the Radomiro Tomic porphyry copper deposit, Northern Chile. *Econ. Geol.* **2001**, *96*, 387–400.
7. Mora, R.; Artal, J.; Brockway, H.; Martinez, E.; Muhr, R. El Tesoro exotic copper deposit, Antofagasta region, northern Chile. *Econ. Geol. Spec. Publ.* **2004**, *11*, 187–197.
8. Pinget, M.; Dold, B.; Fontboté, L. Exotic mineralization at Chuquicamata, Chile: Focus on the copper wad enigma. In Proceedings of the 10th Swiss Geoscience Meeting, Bern, Switzerland, 16–17 November 2012; pp. 88–89.
9. Kojima, S.; Astudillo, J.; Rojo, J.; Tristá, D.; Hayashi, K.-I. Ore mineralogy, fluid inclusion, and stable isotopic characteristics of stratiform copper deposits in the coastal Cordillera of northern Chile. *Miner. Deposita* **2003**, *38*, 208–216. [CrossRef]
10. Pincheira, M.; Dagnini, A.; Kelm, U.; Helle, S. *Copper Pitch Y Copper Wad: Contraste Entre Las Fases Presentes En Las Cabezas Y En Los Ripios En Pruebas De Mina sur, Chuquicamata*; X Congreso Geológico Chileno: Concepción, Chile, 2003; p. 10.
11. Hellé, S.; Kelm, U.; Barrientos, A.; Rivas, P.; Reghezza, A. Improvement of mineralogical and chemical characterization to predict the acid leaching of geometallurgical units from Mina Sur, Chuquicamata, Chile. *Miner. Eng.* **2005**, *18*, 1334–1336. [CrossRef]
12. García, C.; Garcés, J.P.; Rojas, C.; Zárate, G. Efecto sinérgico del tratamiento de mezcla de minerales conteniendo copper wad y sulfuros secundarios. In Proceedings of the IV International Copper Hydrometallurgy Workshop, Viña del Mar, Chile, 16–18 May 2007.
13. Zambra, J.; Kojima, S.; Espinoza, S.; Definis, A. Angélica Copper Deposit: Exotic Type Mineralization in the Tocopilla Plutonic Complex of the Coastal Cordillera, Northern Chile. *Resour. Geol.* **2007**, *57*, 427–434. [CrossRef]
14. Consejo Minero. *Guía Metodológica sobre Drenaje en la Industria Minera*; Subsecretaría de economía Consejo Nacional de Producción Limpia: Santiago, Chile, 2002.
15. Sequeira, R. A note on the consumption of acid through cation exchange with clay minerals in atmospheric precipitation. *Atmos. Environ. Part. A Gen. Top.* **1991**, *25*, 487–490. [CrossRef]
16. Helle, S.; Pincheira, M.; Jerez, O.; Kelm, U. Sequential extraction to predict the leaching potential of refractory. In Proceedings of the XV Balkan Mineral Processing Congress, Sozopol, Bulgaria, 12–16 June 2013; pp. 109–111.
17. Hernández, M.C.; Benavente, O.; Melo, E.; Núñez, D. Copper leach from black copper minerals. In Proceedings of the 6th International Seminar on Copper Hydrometallurgy, Viña del Mar, Chile, 6–8 July 2011; pp. 1–10.
18. Randhawa, N.S.; Hait, J.; Jana, R.K. A brief overview on manganese nodules processing signifying the detail in the Indian context highlighting the international scenario. *Hydrometallurgy* **2016**, *165*, 166–181. [CrossRef]
19. Saldaña, M.; Toro, N.; Castillo, J.; Hernández, P.; Trigueros, E.; Navarra, A. Development of an Analytical Model for the Extraction of Manganese from Marine Nodules. *Metals* **2019**, *9*, 903. [CrossRef]
20. Kanungo, S. Rate process of the reduction leaching of manganese nodules in dilute HCl in presence of pyrite. *Hydrometallurgy* **1999**, *52*, 313–330. [CrossRef]
21. Kanungo, S.; Das, R. Extraction of metals from manganese nodules of the Indian Ocean by leaching in aqueous solution of sulphur dioxide. *Hydrometallurgy* **1988**, *20*, 135–146. [CrossRef]

22. Su, H.; Liu, H.; Wang, F.; Lu, X.; Wen, Y.-X. Kinetics of Reductive Leaching of Low-grade Pyrolusite with Molasses Alcohol Wastewater in H2SO4. *Chin. J. Chem. Eng.* **2010**, *18*, 730–735. [CrossRef]

23. Bafghi, M.S.; Zakeri, A.; Ghasemi, Z.; Adeli, M. Reductive dissolution of manganese ore in sulfuric acid in the presence of iron metal. *Hydrometallurgy* **2008**, *90*, 207–212. [CrossRef]

24. Toro, N.; Saldaña, M.; Gálvez, E.; Cánovas, M.; Trigueros, E.; Castillo, J.; Hernández, P.C. Optimization of Parameters for the Dissolution of Mn from Manganese Nodules with the Use of Tailings in An Acid Medium. *Minerals* **2019**, *9*, 387. [CrossRef]

25. Zakeri, A.; Bafghi, M.; Shahriari, S. Dissolution Kinetics of Manganese Dioxide Ore in Sulfuric Acid in the Presence of Ferrous Ion. *Iran. J. Mater. Sci. Eng.* **2007**, *4*, 22–27.

26. Toro, N.; Saldaña, M.; Castillo, J.; Higuera, F.; Acosta, R. Leaching of Manganese from Marine Nodules at Room Temperature with the Use of Sulfuric Acid and the Addition of Tailings. *Minerals* **2019**, *9*, 289. [CrossRef]

27. Benavente, O.; Hernández, M.C.; Melo, E.; Núñez, D.; Quezada, V.; Zepeda, Y. Copper Dissolution from Black Copper Ore under Oxidizing and Reducing Conditions. *Metals* **2019**, *9*, 799. [CrossRef]

28. Toro, N.; Herrera, N.; Castillo, J.; Torres, C.M.; Sepúlveda, R. Initial Investigation into the Leaching of Manganese from Nodules at Room Temperature with the Use of Sulfuric Acid and the Addition of Foundry Slag—Part, I. *Minerals* **2018**, *8*, 565. [CrossRef]

29. Helle, S.; Kelm, U. Experimental leaching of atacamite, chrysocolla and malachite: Relationship between copper retention and cation exchange capacity. *Hydrometallurgy* **2005**, *78*, 180–186. [CrossRef]